University of Nottingham
UK | CHINA | MALAYSIA

What are the implications of genetic variation on the control of Japanese encephalitis virus?

John Bish

Thesis submitted to the University of Nottingham for the degree of Doctor of Philosophy, November 2023.

Abstract

Japanese encephalitis virus (JEV) is a flavivirus endemic in southeast Asia, an area home to approximately 3 billion people. Infection with JEV can result in paralysis, epilepsy, and death. Currently JEV is well controlled owing to the introduction of several well-tolerated and highly efficacious vaccines.

JEV exists as five distinct genotypes which comprise a single serotype. All vaccines in use are based on genotype III. In the past twenty years the predominant genotype of JEV isolated in nature, and the cause of most human infections, has shifted from genotype III to genotype I. Research has shown that current vaccines are effective at providing antibody-based protection against a genotype I infection however concern remains over protection against genotype V.

Genotype V is the least similar compared to the other four genotypes of JEV and can deviate at the amino acid level by up to 15%. Owing to its rarity, little work has been performed on the effectiveness of vaccine derived antibodies against genotype V. Also of concern is the potential of recombinant JEV composed of heterologous genotypes. Recombination has been demonstrated experimentally within the flavivirus genus and evidence of its existence in nature has been proposed in a handful of scientific papers.

Pseudotype viruses offer an excellent opportunity to better understand the neutralisation potency of vaccine derived antibodies against the emerging genotype V. However, to date flaviviruses have remained a challenging family of viruses to pseudotype owing to several different reasons. In this thesis I describe the screening of all available JEV envelope sequences to comprehensively determine the presence of recombination in a fraction of these samples as well as the production of pseudotype JEV genotypes I, III and V. These pseudotype viruses were then used to develop a pseudotype virus neutralisation test to screen the effectiveness of vaccine derived antibodies against the different genotypes.

Acknowledgements

To all those who helped me throughout this PhD I give my undivided thanks, however there are a few individuals it is important to mention specifically.

Firstly, thank you to my supervisors Dr Janet Daly, Dr Nicola Rose, and Dr Kevin Gough for selecting me for this project and for all of their guidance and support. Particularly during some of the more challenging moments.

I would also like to thank all of my past and present colleagues at NIBSC for their help and advice, “borrowing” of reagents and equipment and all of the help it took to complete this work. In particular my friends Dr Kami Toon and (future Dr) Federica Marchesin who kept me smiling when things weren’t working in the lab and who kept me company on the many tea breaks it took to complete this work.

I am grateful to my family, who despite not being able to tell you what this thesis is about were always hugely encouraging and supportive that I was making the right choice.

Lastly but most importantly, a huge thank you to my partner Natalie. I could not have achieved any of this without your unwavering support and encouragement through some of the long days (and nights) that were had throughout this PhD. It would be impossible to sum up all your contributions in words.

Table of Contents

List of Figures

List of Tables

Abbreviations

aa	Amino acid
nt	Nucleotide
BBB	Blood brain barrier
BHK-21	Baby hamster kidney-21 cells
C	Capsid
CL	Containment level
CNS	central nervous system
CPE	Cytopathic effect
CRFK	Crandall Rees feline kidney (cells)
DNA	Deoxyribonucleic acid
E	Envelope (gene/ protein)
EEEV	Eastern equine encephalitis virus
ER	Endoplasmic reticulum
FBS	Foetal bovine serum
GFP	Green fluorescent protein
GI-V	Genotype 1-5
HeLa	Henrietta Lacks (cells)
HBV	Hepatitis B Virus
HAVcr-1	Hepatitis A virus cellular receptor 1
HIV	Human immunodeficiency virus
HPV	Human papillomavirus
Huh-7	Human hepatocyte 7 (cells)
IgNAR	Immunoglobulin new antigen receptor
IVV	Inactivated viral vaccine
JEV	Japanese encephalitis virus
JEV-PV	Japanese encephalitis virus pseudotype virus
LIV	Louping Ill virus
LVV	Live viral vaccine
M	Membrane
MLV	Murine leukaemia virus
MVA	Modified Vaccinia virus Ankara
MVV	Murray Valley virus
Nef	Negative factor

NS	Non-structural
NT	Nucleotides
ORF	Open reading frame
PCR	Polymerase chain reaction
PHK	Primary hamster kidney (cells)
PK15	Porcine kidney (cells)
p.i	Post-infection
Pr	Pre-membrane
p.t.	Post-transfection
PV	Pseudotype virus
RdRp	RNA-dependant RNA polymerase
RNA	Ribonucleic acid
RSV	Rous sarcoma virus
SERINC3/ 5	Serine including protease 3 and 5
SLEV	St. Louis encephalitis virus
SNP	Single nucleotide polymorphism
SWA	Sliding window analysis
TIM-1	T-cell immunoglobulin and mucin domain 1
TMD	Transmembrane domain
TBE	Tick-borne encephalitis virus
UTR	Untranslated region
VERO	African green monkey kidney cells
VSV-G	Vesicular stomatitis virus glycoprotein
WEEV	Western equine encephalitis virus
WHO	World Health Organization
WNV	West Nile virus
WT	Wild-Type
YFV	Yellow fever virus

1 Introduction

1.1 Background

Flaviviruses are ubiquitous worldwide with each region home to its own endemic species. In Northern Europe where the climate is too cool for year-round mosquito transmission, the tick is a vector of the predominantly ovine virus louping ill (LIV) and tick-borne encephalitis virus (TBEV). In Australia, Murray Valley virus (MVV) has caused over 20 cases since 2000 (Floridis et al., 2018) and St. Louis encephalitis (SLEV) in North America results in an average of 35 cases per year. Individuals infected with either MVV or SLEV often face a very poor prognosis with 40% of survivors left with life-changing neurological damage. The 2015–2016 Zika virus epidemic demonstrates the potential of this group of viruses to quickly spread around the globe (Plourde & Bloch, 2016).

Japanese encephalitis virus (JEV) is the most common cause of infectious encephalitis worldwide. The World Health Organization (WHO) recognises 24 countries in South-East Asia and the Western Pacific which are endemic for JEV. Over 3 billion people live in these affected areas and are thus at risk of infection. Despite being regarded as a rare tropical disease, cases of JEV and related flavivirus infections are increasing. Studies in rural parts of South East Asia suggest that around 10% of the susceptible population is infected each year (Tsai, 1993) and by adulthood most of the population possess antibodies suggesting previous infection in childhood. There is clear evidence that the range of JEV transmissible areas is increasing also, spreading as far west as Pakistan and Nepal (Partridge, Ghimire, Sedai, Bista, & Banerjee, 2007). There is growing concern that China and India, the most populous nations in the world, are at a growing risk of JEV infection due to rapid population growth and changing agricultural practices (Rajaiah & Kumar, 2022).

Each year, over 60,000 cases of JEV are reported, resulting in 20–30,000 deaths (Campbell et al., 2011), and these figures are believed to be widely under-reported due to a lack of proper diagnostic testing and epidemiological record keeping in most affected countries. One in one thousand cases

present clinical signs and of these, up to 30% can be fatal and among survivors 30–50% are left with permanent neurological or psychological sequelae as a result of the encephalitic infection.

The first documented cases of JEV infection were described in Japan during the 1800s. Described as a “summer encephalitis”, significant outbreaks were originally reported roughly every 10 years, often affecting thousands (T. M. D. Solomon, N.; Kneen, R.; Gainsborough, M.; Vaughn, D.W; & Thi Khanh, V., 2000). Human infection with JEV is almost always the result of a bite from an infected mosquito or nosocomial transmission via contaminated surgical equipment, with most infections being the former. The virus initially infects cells surrounding the feeding site, often keratinocytes and melanocytes. From there the virus spreads into the bloodstream and in rare cases can infect neuronal mast cells crossing the blood brain barrier (BBB) resulting in the characteristic encephalitis.

Despite the large number of infected individuals, the ratio of symptomatic cases is low at around 1:1000 (T. Solomon et al., 2003). In infected individuals JEV presents itself between 4 and 14 days with a variety of possible symptoms including pyrexia, seizures, confusion, slurred or confused speech, tremor and muscle weakness leading to paralysis. Humans are considered dead-end hosts and onward transmission is not observed. Because of the low viraemia in humans, by the time symptoms present, viral copies in the patient are usually far too low to be detected by polymerase chain reaction (PCR). Serological methods are therefore the most common technique used to diagnose infections.

JEV is a member of the family *Flaviviridae*, a large family of viruses containing many medically important pathogens such as dengue, Zika, West Nile and yellow fever viruses (Figure 1). The name *flavi*-virus is derived from the Latin word for yellow, named as such after the prototype member of this genus, yellow fever virus. The virus was first isolated in Nakayama, Japan in 1935 from the brain of a patient with a fatal outcome. As well as phylogenetic classification (Figure 1), JEV is a part of the JEV serocomplex, a group of nine antigenically related flaviviruses, four of which cause human disease resulting

in encephalitic signs. Some of the viruses of this group also cause severe infections in equids. The human pathogens in this group aside from JEV are MVV, West Nile virus (WNV) and SLEV (T. Solomon et al., 2003).

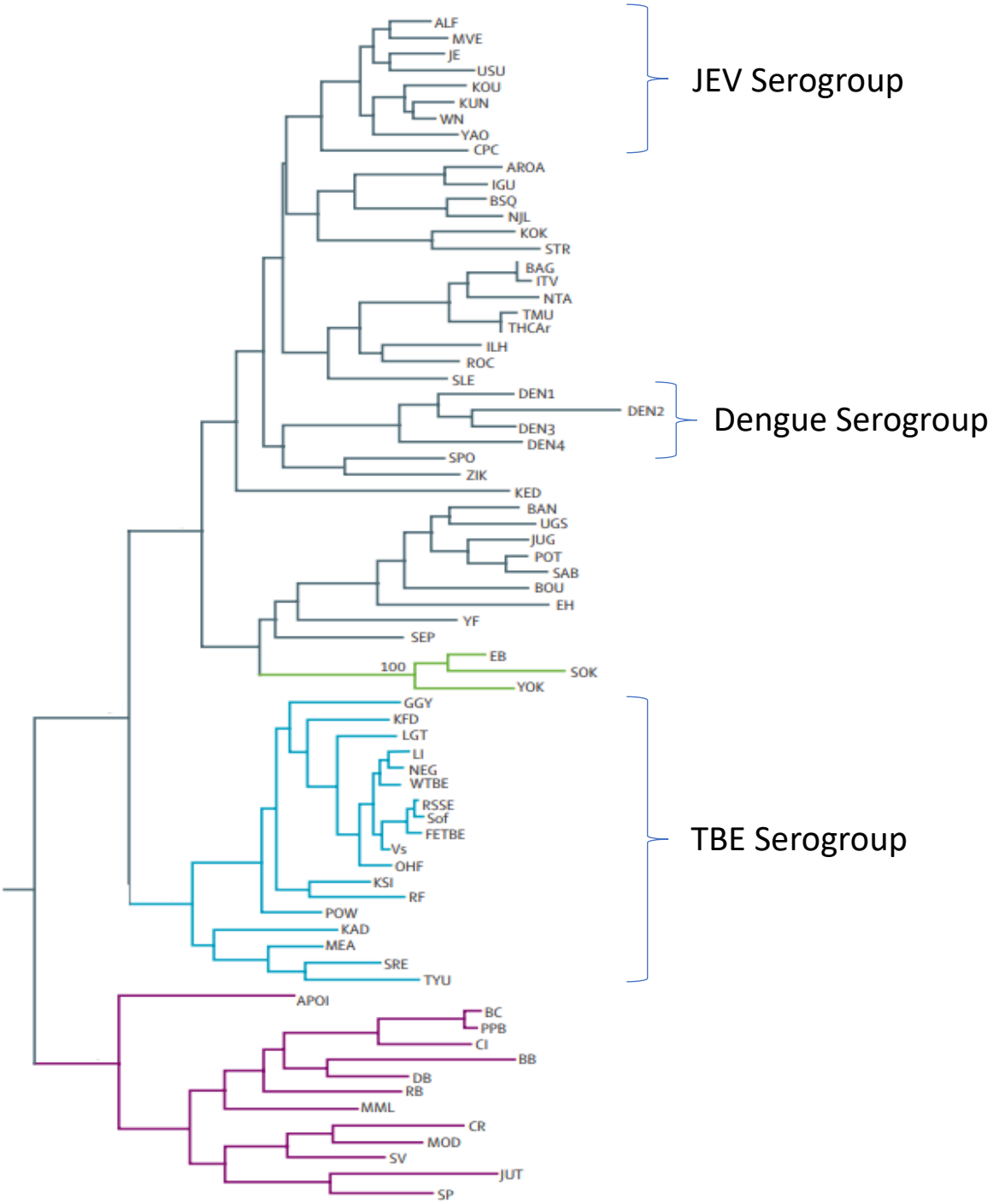

Figure 1.1. Phylogenetic relationships of the envelope proteins of the pathogenic flaviviruses. Envelope protein homology is used to categorise viruses into their corresponding serogroups. Also shown is the primary vector for each group. Grey: mosquito borne. Blue: Tick borne. Green and purple: no known vector however virus has been isolated in Bats and Rodents (Gould & Solomon, 2008)

1.2 Genotypes

Five genotypes of JEV (GI–GV) are defined based on homology of their envelope (E) protein gene. There is 11% nucleic acid and 3% amino acid divergence between them (Han et al., 2014). Recent work has determined that the five genotypes represent the evolution of the virus from its origins in the Indonesia region to its spread westward to India and parts of the Middle East (T. Solomon et al., 2003). Until recently, GIII has been the most common genotype causing of infection and most frequently isolated genotype in both humans and animals. However, since the early 2000s GI has displaced GIII as the dominant genotype. Reasons for this are unclear however theories suggesting that GI replicates more readily in the mosquito vector is the prevailing theory (Amy J Schuh, Ward, Brown, & Barrett, 2014).

Genotype displacement within flaviviruses is not a phenomenon unique to JEV. In North America a more efficiently replicating genotype of WNV replaced the existing circulating strain WNV NY99 (Karna & Bowen, 2019). Genotype displacement is usually the result of differences in replicative efficiency or an increased vector range however this is not always the case as seen in infectious hematopoietic necrosis virus where improved fitness was not observed as a correlate with displacement (Kell, Wargo, & Kurath, 2014). The reason for the displacement of GIII is not yet fully understood. Current theories and evidence are discussed later in this thesis.

1.3 Serotypes

Serotypes are functionally distinct from genotypes. Whereas a genotype is the phylogenetic grouping of an organism, a serotype corresponds to whether different strains of a microorganism can be distinguished by serological assays. Simply, a serotype is defined by whether an infection from one strain results in production of antibodies which efficiently neutralise other strains. In

the case of Zika virus there are two distinct genotypes, the African and Asian lineages. However, these two genotypes comprise only one serotype as infection from either lineage results in a sufficiently strong immune response to prevent reinfection from the other lineage (Dowd et al., 2016).

The question of how many serotypes of JEV exist is still debated. Tsarev, Sanders, Vaughn, and Innis (2000) performed phylogenetic analysis of 92 isolates of JEV using genome heterogeneity as the means of predicting serotype and concluded from the low inter-genotypic diversity that GI–IV would comprise one serotype. This study had a significant (albeit unforeseeable) flaw however in that one of the strains used, the Muar strain, was not categorised as the fifth genotype until 2011 (Mohammed et al., 2011). Tsarev et al. (2000) noted that this strain was distinct from other sequences analysed and did not include it in their comparisons as a published whole genome sequence was not available at the time.

The idea that genotypes I–IV of JEV comprise a single serotype is well supported (Wei et al., 2019) however since the discovery of a fifth genotype much debate regarding where GV fits within the serotype has occurred. GV exhibits significant antigenic variation compared to GI–IV and there is now evidence that GV is poorly neutralised by current generation vaccine derived antibodies (Honjo, Masuda, & Ishikawa, 2019) indicating its unique nature. Recommendations to include inactivated GV or GV E protein subunits to existing vaccines are growing as more is discovered of this new genotype. Whilst it is now evident that GV is divergent when compared to GI–IV, there is currently insufficient evidence to conclude that it is its own serotype. This theory does however warrant further investigation as the impact on vaccination and JEV control would be significant.

1.4 Epidemiology

JEV transmission can be broadly categorised into two types: seasonal and endemic. In the northernmost countries affected such as Thailand, Korea, Japan and the northern regions of Vietnam, the disease is reported as large spikes in cases during summer whilst in the southernmost countries affected such as Indonesia, the Philippines and Malaysia the disease is reported year-

round albeit at a lower level. This was originally believed to be due to differences in infectivity between the populations of circulating viruses in these countries (T. M. D. Solomon, N.; Kneen, R.; Gainsborough, M.; Vaughn, D.W; & Thi Khanh, V., 2000). This idea was supported by the discovery of differing genotype ranges.

Broadly speaking, GI and III are predominantly found in northern areas and genotypes II, IV and V are more common in southern latitudes. Further, whilst average rainfall in these regions is very similar, temperatures can vary drastically throughout the year between northern and southern Asian climates. These factors were believed to limit genotype spread (T. M. D. Solomon, N.; Kneen, R.; Gainsborough, M.; Vaughn, D.W; & Thi Khanh, V., 2000).

However, there are many exceptions to these rules and the true range of each genotype is still being drawn as more surveillance data are gathered. These ranges also constantly changing as a result of environmental (seasonal differences) and human (climate change, urbanisation, deforestation) factors. GV has also now been detected in Korea (Takhampunya et al., 2011) and numerous epidemic outbreaks caused by both GI and GIII are well documented across Asia (Gao et al., 2019). In addition, isolated viruses from epidemics in northern regions and endemics in southern regions of Vietnam have been found to be caused by the same genotype. Therefore, this explanation for the difference in transmission patterns between latitudes is no longer well supported by evidence.

The increase in JEV incidence is therefore likely to be due to a combination of socioeconomic factors involving changing farming practices such as increased industrialisation in affected countries, the expansion of areas used for rice-cultivation, and small-scale animal rearing which has accompanied the rapid population growth seen in Asia since the middle of the 20th century.

1.5 Transmission cycle

JEV transmission is maintained in nature via the vector mosquito species *Culex* (mainly *Culex tritaeniorhynchus*) and host reservoirs of swine and ardeid birds (such as herons). Birds help spread the virus over large distances while swine are regarded as amplifying hosts. Humans are a dead-end host

and human-to-human transmission does not occur. Aside from accidental laboratory exposure, or nosocomial transmission, human infection is always the result of a bite from an infected mosquito. As a result of this transmission cycle, infections are most likely to occur in areas where the vector and amplifying hosts coexist with humans. Because of this, areas where rice and pork cultivation cross-over are hotspots for JEV infection. The virus is highly unstable outside of the host environment and is rapidly inactivated by ultraviolet light, ethanol, or desiccating conditions. These factors limit the spread of JEV to warm, humid environments where sufficiently sized populations of vector and host co-exist.

The impact of demographic factors on virus spread must not be overlooked. Many populations within the Indonesian archipelago are of Islamic faith, one of the tenets of which is the prohibition of consuming pork. Compared to islands where the majority religion is not Islam, such as Bali, rates of JEV infection are significantly lower. This demonstrates the importance of social factors in creating an environment where both vectors and amplifying hosts (swine) are in abundance for successful virus transmission to occur.

The case for the impact of economics on rates of transmission is seen in mainland rural Asia where small-scale pig farms are the majority means of production. In Vietnam, over 80% of national pork production is managed in farms of fewer than 500 animals (D. Zhang, Wang, & Zhou, 2017). This style of farming leads to close contact between humans and pigs, a known risk factor for JEV transmission.

Infection with JEV results in different outcomes depending on the infected organism. As an amplifying host, infections in swine cause a high viraemia with severe outcomes for newborn piglets. Infection can cause reproductive failure in adults manifesting as orchitis (testicular swelling) in males and spontaneous abortion in pregnant sows. In affected areas seroconversion in pig populations can reach 98% (Cha et al., 2015). Mortality in adult pigs is rare, however in newborn piglets, the fatality is close to 100%: a significant economic burden on small-scale rural pig farmers. Adult pigs maintain a long viraemia after the initial infection, which enables transmission to humans in

close contact via the mosquito vector. Pig-to-pig transmission has been observed and suggested as a mechanism for the virus to survive through seasons where the climate is not suitable for mosquito reproduction (Diallo et al., 2018) but it is unknown if this constitutes to maintenance of an infectious reservoir capable of spilling over to human populations.

1.6 Recombination

Recombination between different viral strains and genotypes is widely observed in nature. Recombination occurs through exchange of genetic material as a result of sequence homology. This can result in novel combinations of genes and allows faster adaptation than mutation alone. The most well-documented example of the potential of viral recombination is Western equine encephalitis virus (WEEV). This virus is the result of a co-infection of a competent vector with both Eastern equine encephalitis virus (EEEV) and Sindbis virus (Hahn, Lustig, Strauss, & Strauss, 1988). WEEV maintained the neuronal tropism of EEEV which causes encephalitis and combines it with the antigenic properties of Sindbis virus. The discovery that such a widespread virus was the result of recombination supports concerns that the increased use of multivalent live attenuated vaccines could result in rescue of virulent potential or even generation of novel viruses. The question then arises whether there is a risk of recombination between different genotypes of JEV.

Vaccine design continues to become ever more sophisticated combining many different epitopes and genotypes of a virus into a single product. This has had huge benefits in preventing the spread of many infectious diseases including human papilloma virus (HPV), seasonal influenza, measles, mumps, and rubella. However, with this increased complexity there are also additional complex factors to consider. Recombination between attenuated and wild-type virus is one such concern. It is possible through intermolecular interactions of closely related genomes to result in novel or rescued virulence of attenuated strains.

The existence of multiple genotypes of JEV raises questions regarding the importance of the differences observed between them. As mentioned

previously there is very little amino acid divergence across genotypes I-IV, however the biological relevance of these differences is beginning to gather interest. It has been observed that current GIII based vaccines generate cross-reactive neutralising antibodies against genotypes I, II, and IV. Evidence is growing however, that genotype V is only poorly neutralised in vaccinated individuals (Cao et al., 2016; Honjo et al., 2019) and that infection could result in a more severe disease in naïve populations. A recent study highlighted that amino acid changes in the pre membrane and envelope proteins of GV are responsible for the increased virulence of this genotype observed in mouse models (Tajima et al., 2019). Due to the rare occurrence of GV infection more research and surveillance to monitor human cases is required before conclusions can be made regarding the potential increased infectivity and virulence of this divergent JEV genotype.

1.7 Genotype displacement

It has been repeatedly observed that GI is replacing GIII as the most frequently isolated genotype of JEV (Do, Bui, Hasebe, Morita, & Phan, 2015; Han et al., 2014; A. J. Schuh, Guzman, Tesh, & Barrett, 2013; T. M. D. Solomon, N.; Kneen, R.; Gainsborough, M.; Vaughn, D.W; & Thi Khanh, V., 2000). The exact mechanism of this replacement is still under debate. As the genome difference between GI and GIII is around 1%, research into this displacement may aid overall understanding of lineage displacement for both related and unrelated viruses.

Several explanations have been proposed to explain this shift. One of the more compelling arguments reasons that GI is more efficient at replicating in the mosquito vector than is GIII. Do, Bui, and Phan (2016) performed *in vitro* growth experiments using human (R6), swine (PS) and mosquito (C6/36) cell lines. Their results indicated that GI was indeed more efficient at replicating in both mosquito and porcine cell lines than in human cells. An interesting observation was that this was not the case for GIII, which replicated most efficiently in human cells. GIII was also able to maintain replication in R6 cells for 8 passages whilst GI failed to replicate beyond passage 4. The reverse

was true in PS cells: GI replication was maintained up to passage 8 whilst GIII was undetectable after passage 6.

While this study is interesting, it was limited in the number of different cell lines used and the authors only tested one strain each of GI and GIII. A wider sample of strains and cell lines would be required to provide a more comprehensive answer.

Growth experiments using live vectors and hosts to imitate a natural transmission cycle have progressed these studies further. Karna and Bowen (2019) utilised an existing avian host and mosquito vector species to examine growth kinetics of three GI and three GIII strains. *In vivo* data were collected using Indian runner duck chicks and *Culex quinquefasciatus* mosquitos. Blood samples were taken from infected ducklings daily for 21 days and titrated using a traditional plaque assay. Mosquitos were fed with virus-spiked cattle blood and homogenised at 7- and 14-days post feeding before viral titres were determined by plaque assay.

All six strains of JEV produced comparable growth curves when grown in Vero cells: virus titre peaked 2 days post infection, dropped by day 5, and rose again by day 8. This pattern was not observed in the *in vivo* data. Both JEV genotypes demonstrated equivalent growth in infected runner ducks. Differences were observed however, in the mosquito populations: GI-infected mosquitos exhibited a higher titre of JEV than those infected with GIII. Together, these results support previous work suggesting that GI is more efficient at replicating in the mosquito vector to the detriment of replicative potential in the host.

These data raise the question that whilst GI has replaced GIII as the most frequently isolated strain, will this displacement result in fewer or less severe human cases due to its diminished ability to replicate in human cells? This may be the case in some countries. Han, Adams, Fang, Liu, and Rayner (2015) collated hospital records and sequenced isolates from established JEV infections and noted that a statistically significant drop in reported /verified human cases occurred in areas where GIII had been displaced by GI. This

observation warrants further research on the impact of continued vaccination with a heterologous genotype.

1.8 Viral entry

The key receptor which facilitates JEV entry into the cell is unknown, however, numerous studies have been performed identifying various attachment receptors and cellular factors which strongly correlate with entry into the cell.

One class of molecules with strong evidence for involvement with JEV cell entry is the heparan sulphate proteoglycans (HPSGs and glycosaminoglycans (GAGs). These cell surface proteins are responsible for non-specific, charge-based attraction of JEV particles to the cell surface. They do not internalise the viral particle however their absence does result in a reduced viral load. This class of molecules is widely associated with the initial attachment of many groups of viruses (Kalia, Chandra, Rahman, Sehgal, & Jameel, 2009; O'Donnell & Shukla, 2008).

Another protein strongly correlated with JEV entry into the cell is T-cell immunoglobulin and mucin domain 1/TIM-1 (also known as Hepatitis A virus cellular receptor 1/ HAVcr-1). TIM-1 exists as three variants (TIM-1, -3 and -4). These variants are presented independently on subclasses of T-cells and antigen presenting cells and are heavily involved in T-cell and antigen-presenting cell activation and suppression. TIM-1 was demonstrated to be an important factor mediating JEV entry by Niu et al. (2018). Knockdown of TIM-1 in A549 cells impaired JEV entry. Further studies by Niu et al. showed that JEV could still attach to the cell surface indicating that TIM-1 was likely not a binding factor but facilitated entry into the cell as part of a downstream process.

One protein which has growing evidence as its role as a binding factor is CD4. In studies performed by Q. Wang et al. (2023). Despite the study being performed using porcine cell line PK15 the group demonstrated that CD4 knockdown drastically reduced JEV attachment to the cell surface. Further work is certainly required to ascertain the full series of events leading from viral attachment to cell entry.

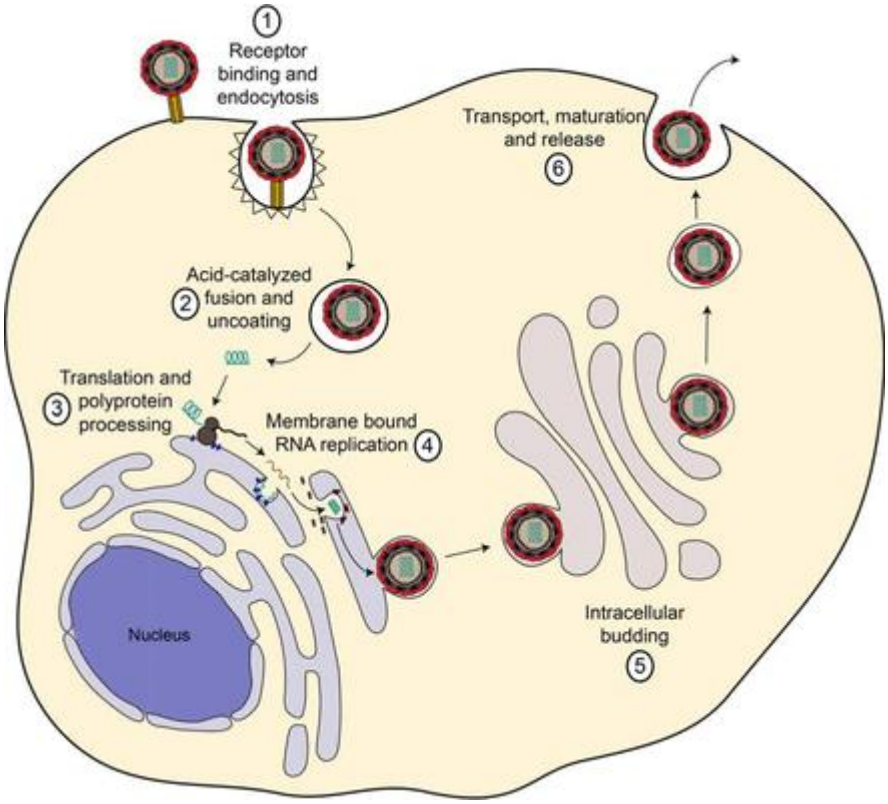

Figure 1.2 The pathway of flavivirus infection within the cell. 1. Virus receptor binding initiates endocytosis. 2. The acidic environment of the endosome causes membrane fusion and release of viral RNA. 3. Viral polyprotein is synthesised at the ER and through self-cleavage the viral proteins are released. 4. The RNA genome is replicated within the ER and transported to the assembling capsid. 5. Immature virions are released from the ER and move to the Golgi, post translational modifications prepare the virion for egress. An exosome buds from the Golgi, pH dependent conformational changes mature the envelope protein. 6. The exosome fuses with the plasma membrane and mature virus is released from the cell (adapted from (Gerold, Bruening, Weigel, & Pietschmann, 2017)).

Once bound to one or several entry receptors, clathrin-dependent endocytosis brings the virion into the cell within a lipid bound vesicle. The low pH within the endosome causes conformational change of the E protein which results in merging of the viral envelope and the endosome membrane. The viral RNA is now free from the inner capsid and is released into the cell cytoplasm where it is translated into a single large polyprotein at the ER comprising three structural and seven non-structural proteins. The polyprotein is cleaved through a combination of host and viral proteases and virion assembly begins as the immature virus is transported from the ER to the Golgi. Maturation continues as the virion is passed through the Golgi network until furin-

mediated cleavage causes rearrangement of the membrane and E protein and form the mature structure of the virus particle (Yun & Lee, 2018).

1.9 JEV genome

JEV, like other members of the *Flaviviridae* family, is a positive sense, single-stranded RNA genome. The viral genome is approximately 11 Kb and comprises 3 structural and 7 non-structural (NS) genes organised in a single open reading frame (ORF) read in the following order: capsid (C), pre-membrane (PrM), envelope (E), NS1, NS2a, NS2b, NS3, NS4a, NS4b and NS5. As well as the large polyprotein the viral genome also contains highly conserved 5′ and 3′ untranslated terminal regions (UTRs) at the ends of its genome. These terminal regions form complex secondary structures involved in translation initiation and regulation.

1.9.1 Untranslated regions (UTRs)

The 5′ UTR is around 100 nucleotides (nt) while the 3′ UTR is 500–700 nt in length. These two regions form complex tertiary structures based on their nucleotide sequence. These structures are vital for genome cyclization which is essential for viral replication to occur as well as evading innate host immune features such as exoribonucleases (Ng, Soto-Acosta, Bradrick, Garcia-Blanco, & Ooi, 2017).

It has been known since early research in the 1980s (Hahn et al., 1987) that complementary regions exist in the 5′ and 3′ UTRs of flaviviruses. These regions are required to form the circular genome which initiates replication (Khromykh, Meka, Guyatt, & Westaway, 2001; Villordo & Gamarnik, 2009). Disruption of this complementarity is detrimental to the efficiency of viral replication and leads to an increased rate of clearance of the viral genome by the host.

It has been demonstrated with other flaviviruses, notably dengue virus, that a balance between linear and circular forms of the genome are essential for maintaining a cycle of viral replication (Villordo, Alvarez, & Gamarnik, 2010).

Due to their necessity in viral replication both UTRs have recently been viewed as potential drug targets. Short peptide-conjugated oligomers called

morpholinos have been designed to bind to specific circularisation-enabling sequences in the UTRs resulting in stearic hinderance of the normal interaction of these regions (Panda, Alagarasu, & Parashar, 2021). The idea of interrupting genome circularisation has been explored further with the use of small interfering RNA (siRNAs). Pacca et al. (2009) demonstrated as much as 97% reduction in yellow fever virus titres when infected cells were treated with siRNAs designed to target UTRs as well as other parts of the YFV genome.

The use of siRNAs is an attractive prospect as an antiviral however until issues surrounding biological half-life and cell entry are developed further these methods will remain research tools.

1.9.2 Capsid

The first viral protein in the JEV ORF is the capsid. This small 15 kDa protein forms the inner component of the virion that encapsulates the RNA genome. The protein is overall highly positively charged (Chambers, 1990). Conserved amongst flaviviruses capsid proteins are a hydrophobic C-terminal region preceded by a hydrophilic stretch of amino acids and a central hydrophobic region (Mandl, Heinz, & Kunz, 1988). The JEV capsid has a quadra-helical structure and forms antiparallel homodimers via interactions with homologous helical subunits of α1-α1, α2-α2 and α4-α4. The α4-α4 interaction results in a coiled structure. While it is possible this structure could facilitate RNA binding, comparisons with other nucleic acid binding domains indicate that such a coiled structure would in fact prevent binding (Poonsiri, Wright, Solomon, & Antonyuk, 2019). Thus, the mechanism of RNA association with the capsid remains to be elucidated.

1.9.3 Pre-membrane (PrM)

PrM is often described as two separate proteins as it assumes distinct functions throughout the replication cycle. The immature precursor PrM is trafficked through the secretory pathway where cleavage by viral proteases results in maturation into the structural form M. The conjugated precursor is a small, 19 kDa glycoprotein which is primarily responsible for chaperoning of the E protein along the secretory pathway and affording protection from the

acidic vesicle environment which left unshielded would result in permanent conformational changes to the envelop protein structure, impeding its function.

The Pr segment contains 6 highly conserved cysteine residues responsible for forming disulphide bridges which maintain the protein's tertiary structure as a seven stranded beta-barrel (Nowak & Wengler, 1987). A highly conserved N-terminal glycosylation site is also critical for proper virus maturation and pathogenesis (Kim et al., 2008). Post-cleavage, Pr remains in contact with the fusion loop of the envelope protein in order to prevent premature binding to receptors within the internal surface of the infected cell membrane (I.-M. Yu et al., 2009).

The mature M protein is a small 8 kDa proteolytic fragment formed by cleavage of PrM (Smit, Moesker, Rodenhuis-Zybert, & Wilschut, 2011). M contains two transmembrane (TM) helices which anchor it into the host derived membrane. These TM regions were previously only considered as structural components however recent work has identified putative ER retention signals within their amino acid sequence (Ciczora, Callens, Seron, Rouille, & Dubuisson, 2010) indicating they have a secondary purpose closely related to the primary function of the PrM protein. Ensuring proper transportation of the E to the site of maturation and post-translational modifications.

1.9.4 Envelope (E) protein

The JEV E protein is responsible for many important biological functions including cell entry via attachment to receptors and is the major factor affecting cell tropism and host range (Tani, Morikawa, & Matsuura, 2011). This glycoprotein is a 50 kDa type I membrane protein (type I proteins span the cell membrane once) with 12 conserved cysteine residues which form essential disulphide bonds (Nowak & Wengler, 1987). Like all flavivirus proteins, the E is synthesised in the ER and moves through the secretory pathway achieving different maturation states dependent on the pH of the cellular compartment it is in. To prevent premature cell membrane fusion

during the maturation, process the E protein must be continuously shielded: this is achieved through capping by its chaperone protein, PrM.

The E protein is divided into three domains; these domains are not split equally or arranged in sequential order. Domain one (DI) consists of 127 residues, 1–51, 135–193 and 283–299. Domain two (DII) consists of 172 residues, 52–134 and 194–282. Domain three (DIII) is the site of receptor binding responsible for viral entry and comprises the final 100 residues, 300-399 (Tang, Ogawa, Eshita, Aono, & Makino, 2010).

In terms of function, each domain has a distinct purpose within the overall protein structure. Domain I is a beta-barrel located between domains I and III, domain II is an elongated dimerization region and contains the fusion loop necessary for receptor mediated-endocytosis at its distal end (S. Mukhopadhyay, Kuhn, & Rossmann, 2005) and is also in contact with domain III of the homologous subunit. Domain III is believed to be the major target for both human and mouse neutralising antibodies (Fernandez et al., 2018) and maintains association with domain I of the homologous subunit.

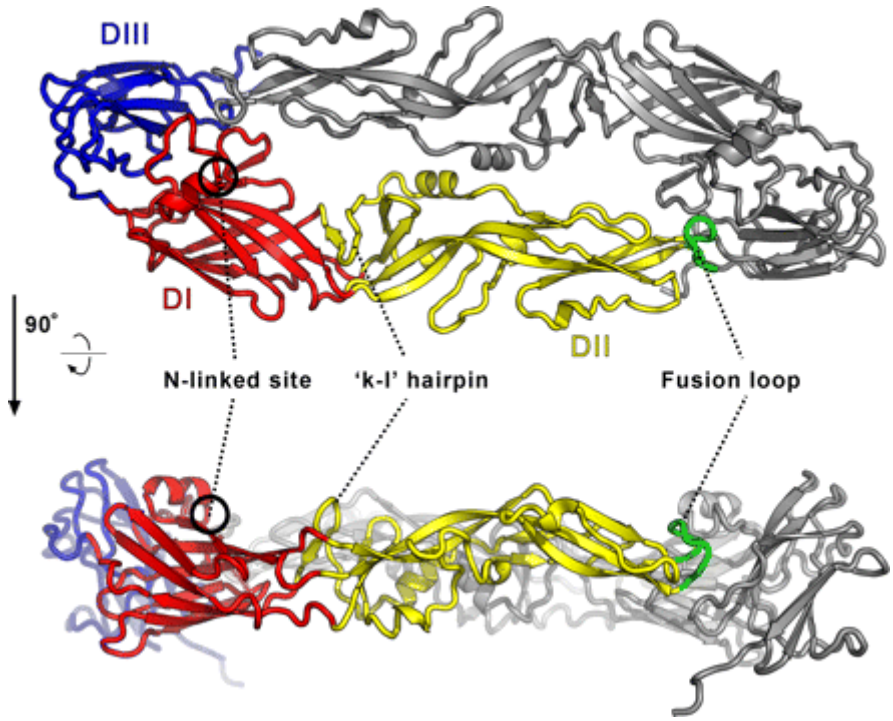

Figure 1.3 Crystal structure of the Japanese encephalitis virus envelope protein highlighting the fusion loop location in the proteins quaternary structure (Luca, AbiMansour, Nelson, & Fremont, 2012).

The mature E protein forms head to tail homodimers that are held in place flat against the virion surface by M (Rey, Heinz, Mandl, Kunz, & Harrison, 1995). Each E protein homodimer is also part of a larger organisation comprising three dimers arranged in parallel “rafts”. Thirty of these rafts comprise the complete viral envelope.

JEV E proteins self-assemble into a dimeric herringbone lattice on the viral surface. The crystal structure of JEV has been resolved to a high atomic detail (Luca et al., 2012) and the physical structures and differences of the virion surface can now be studied in greater detail than ever before. Specific structural features appear to make the JEV envelope unique among flaviviruses.

As mentioned, the monomeric E protein forms an antiparallel homodimer in the mature virion. This dimer is stabilised through various contacts in DII. The DII interface in JEV is unusually small compared to that of other flaviviruses and also lacks residues shown to be important epitopes for neutralising antibody binding (Luca et al., 2012). Other unique features of the JEV

envelope include a far more available surface area with around half as much of the protein exposed as compared to other related viruses.

The E dimers of JEV, TBEV and to an extent dengue virus, all possess open pores on the inside edge of the dimer interface. The function of this open structure is not fully understood and appears unrelated to pathogenicity or host range as evidenced by the varying viruses which contain this feature.

The dimeric E protein complex forms an antiparallel hairpin which when compared to other flavivirus envelope dimers has the smallest area of contact between the monomeric subunits. Luca et al. (2012) compared the area between the subunits for several different flaviviruses and discovered that the exposed area between the subunits of the JEV E protein was the largest observed. As a comparison the buried surface area within the dengue virus E protein ranged from 1590 to 1930 angstroms (Å) (depending on dengue virus serotype), whereas the buried surface area in JEV is roughly half of this, at only 843 Å. This open area between subunits forms two solvent channels whose function is still unknown. TBEV, a close relative of JEV, also contains these central channels between subunits although they are smaller.

The fusion loop of JEV is particularly small compared to other flaviviruses and located internally during the trimeric stage of maturation. It is only when the protein converts into the dimeric conformation and PrM is shed that the internal fusion loop is exposed. This sequence of events prevents premature membrane fusion.

1.9.5 Non-structural (NS) protein 1 (NS1)

The functions of many of the JEV non-structural proteins are generally poorly understood. Much of the knowledge which exists has been inferred from research with similar related viruses such as HCV and dengue virus.

NS1 has a function related to RNA replication but its specific purpose is still unknown. Knockout studies have determined that reduction or removal of NS1 greatly reduces the rate of RNA replication but does not ablate it completely, suggesting an accessory role to the viral polymerase. NS1 is a small (46 kDa) hydrophobic protein which when released extracellularly forms trimeric

hexagonal structures which accumulate in the liver, potentially enhancing viral susceptibility (Alcon-LePoder et al., 2005).

1.9.6 Non-structural protein 2 (NS2)

This NS protein is processed into two proteins, NS2a and NS2b. NS2 is a cysteine protease required to cleave the NS2/3 junction. Other functions have been suggested including downregulation of host transcription therefore increasing resources available for virion production (in experiments using HCV) (Dumoulin et al., 2003)) and interaction/ stabilisation of other non-structural proteins.

1.9.7 Non-structural protein 3 (NS3)

NS3 is a multifunctional protein with both protease and RNA helicase activity. It is well-characterised and crystal structures of this protein have been resolved for many flaviviruses including JEV (Yamashita et al., 2008). The JEV NS3 structure is typical of flaviviruses with few differences when compared to YFV or WNV (Yamashita et al., 2008).

1.9.8 Non-structural protein 4 (NS4)

The smallest JEV protein is NS4 at only 54 kDa. Within the cell NS4 forms a complex with NS3 to become a part of the membrane-bound replication factory. NS4 is known to be membrane-bound, however the arrangement of this protein in its free state has not been resolved. Others suggest its function is related to membrane permeabilization, citing increased intracellular cytopathic effects when upregulated (Chang et al., 1999). The true function of NS4 is likely to be a combination of all these effects.

1.9.9 Non-structural protein 5 (NS5)

NS5 is processed into two proteins, NS5a and NS5b. NS5a is a phosphoprotein which along with NS5b forms part of the flavivirus replication complex and is involved in the regulation of the other NS proteins production. Removal of NS5a from the replication complex is detrimental to viral replication.

NS5b is the RNA dependent RNA polymerase (RdRp) responsible for viral genome replication. As would be expected RdRp is highly conserved among JEV genotypes with little variation amongst the *flavivirus* family. Mutations to

this protein often result in severely impaired or complete failure of viral replication.

1.10 Vaccines

Whilst there is currently no effective treatment for JEV infection, several highly efficacious vaccines exist and are the current best strategy to prevent infection; their use has drastically reduced the number of cases in endemic countries. However as other genotypes, particularly GV, appear to be emerging and species of vector competent mosquitos increase their range due to climate change, the efficacy of these vaccines against emergent/ divergent genotypes must be considered. Table 1 highlights the types of vaccines available; the list of products is not exhaustive.

Table 1.1 Categories of vaccine and JEV vaccine products. categories.

Type	Source of antigen	Example product
Inactivated	Vero-cell culture	IXIARO
	Mouse-brain derived	National manufacturer (China)
Live attenuated	Attenuated strain	SA14-14-2
Live recombinant (chimeric)	YFV 17D attenuated strain core and JEV SA14-14-2 envelope	IMOJEV

The first vaccines available for JEV were crude, inactivated brain homogenate preparations sourced from infected neonatal mice. The Nakayama strain is used by most manufacturers for mouse brain-derived vaccines, however in Japan the strain used is Beijing-1. The use of mouse brain-derived vaccine is being gradually phased out and replaced by cell culture-derived versions due to safety concerns and the ease of manufacturing scale-up due to the demand for large volumes for national vaccination campaigns.

The other type of inactivated vaccine originates from cell culture-derived virus. One such vaccine uses the P3 strain, which is grown in the BHK21 cell line

and inactivated by formalin. An inactivated vaccine derived from the attenuated SA14-14-2 strain grown in Vero cells is also in use.

More recently developed vaccines utilise a live-attenuated strain. The most widely used is SA14-14-2 which was developed after 100 passages in primary hamster kidney (PHK) cells. The progenitor strain SA14 was isolated from a pool of *Culex pipiens* larvae in China (Y. Yu, 2013) and was first licensed for use in China in 1989. Despite being the most widely used JEV vaccine, the precise mechanism of attenuation is still unclear in the SA14-14-2 strain. This is the result of the complex and time-consuming way it was developed. Iterative passages in a variety of cell lines by different laboratories over a period of many years resulted in numerous SNPs and deletions of relatively large parts of the genome. Various groups have attempted to determine which specific changes have resulted in the reduced virulence now seen in this strain.

The E gene has been the target of much of this work as it is the target of neutralising antibodies deemed to provide protection. Chimeric JEV vaccine contains the SA14-14-2 E gene. Insertion of the E gene from the Nakayama strain rescues neurovirulence. The difference between the E protein of these two strains is only 10 amino acids. Four of these residues are predicted virulence determinants (Gromowski, Firestone, & Whitehead, 2015). Combinations of amino acid reversions to wild type (WT) yielded the most virulent virus. Single WT substitutions were not sufficient to restore virulence in the attenuated vaccine. Further work by Zheng et al. (2018) discovered that one of most important SNPs responsible for attenuation is Glu138Lys. This change represents an acid to base mutation. It is not fully understood, however, how this change reduces virulence of the SA-14-14-2 strain. Further work performed by the group found similar effects of attenuation if other acidic residues are mutated to an alkaline residue. An acidic amino acid at position 47 of the E gene reduced neurovirulence suggesting that acidity/ alkalinity is a vital component of neurovirulence in JEV. One theory on why this is the case is that positively charged, acidic residues result in a higher affinity to the negatively charged cell surface glycoproteins. This increased affinity to cell

membranes perhaps results in a lower chance of spread into the brain and CNS from replication sites in other areas of the body.

Aside from attempts to better understand the mechanism of SA-14-4-2 attenuation, some groups have now suggested that with the advent of more advanced molecular biology technologies it is possible to rationally design an improved version of this widely used vaccine strain (Gromowski et al., 2015).

All currently approved vaccines for JEV are based on GIII. This decision made sense when most of these products were developed, as GIII was the most commonly isolated genotype and most frequent cause of infections. However, as mentioned previously, GI has now displaced GIII. This raises questions regarding vaccine efficacy towards heterologous genotypes and whether a multivalent vaccine may now be most suitable to control JEV infection. Further, if heterologous genotypes in live vaccines are the next phase in JEV vaccination then the risks of recombination between genotypes must be assessed before these products are released to market.

1.11 Host immune response

As previously mentioned, domain III of the E protein is widely regarded as the site of the various neutralising antibody epitopes which result in protection. The specific sites which contribute to the generation of neutralising antibodies have not been finalised, it is highly likely there is not one “neutralising epitope” and in fact protection is generated by developing antibodies to a variety of epitopes on the envelope protein. Wu et al. (2003), through the use of extensive site-directed mutagenesis studies on wild-type JEV (WT-JEV), reported that mutations at residues 306, 331, 333 and 386-390 of the envelope protein gene result in escape from neutralising antibody binding. This is not unexpected as within this region lay important positions related to the tertiary structure of the E protein: positions 304 and 335 are highly conserved cysteine residues.

That these sites are recognised as being important for neutralising antibody recognition is supported by Lin and Wu (2005) who determined that Ser331

and Asp332 are functional neutralisation sites. These residues are highly conserved in GI-IV. However, in GV they are substituted by Thr331 and Asp332. This adds further support to the evidence that GV is divergent from the other genotypes and that this may constitute it belonging to its own serotype.

Despite the plethora of individual amino acids suggested as forming critical neutralising epitopes there is strong evidence that S331 is vital for antibody recognition. Lin and Wu (2003) performed mutational studies on S331 showing that changing this residue to A, L, Q, K, R or E results in a reduced affinity with the neutralising monoclonal antibody (mAb) E3.3. More work is required to fully identify the neutralising epitopes of the JEV E protein however the advancement in structural knowledge of this protein and research utilising pseudotype viruses and reverse genetics systems will surely provide new information.

1.12 Research tools

Because of the hazard posed to human and animal health, JEV research requires high biocontainment facilities, a feature that many establishments do not possess. Therefore, to continue to study the entry mechanisms and immune response to this virus, many groups utilise viral pseudotypes. Pseudotype viruses contain the Core of one virus and the Envelope protein(s) of another. Common systems to generate pseudotypes involve the use of the retrovirus, murine leukaemia virus (MLV), the lentivirus, human immunodeficiency virus (HIV) or vesicular stomatitis virus (VSV) Cores.

The potential for the development of pseudotype viruses was first noted as a result of research into Rous Sarcoma Virus (RSV). RSV fails to bud from infected cells without a “helper virus”. A number of released virus particles were observed to possess the viral core and genome of RSV but the outer envelope proteins of the helper virus. It was later discovered that all retroviruses have this ability to incorporate host cell membrane proteins on their outer surface, in many cases this is a deliberate attempt to evade the

host immune systems demonstrated in HIV by the incorporation of host T-cell proteins to avoid detection.

Once this feature was discovered researchers began attempting to graft viral envelope proteins of interest onto retroviral cores. The use of pseudotypes has many advantages over working with the wild-type virus, including removing the requirement for high biocontainment and the associated cost of maintaining such a facility as well as removing the risk to personnel of working with highly infectious, highly pathogenic viruses which are highly hazardous to human and/or animal health.

As envelope proteins are critical for facilitating viral cell entry and are frequently the site of the host neutralising antibody response, the ability to research this component of viral structure at lower containment levels has advantages for a wide variety of viruses.

Pseudotype viruses have uses beyond basic research including potential as a vaccine candidate and use in diagnostic platforms. A pseudotype neutralisation test for highly pathogenic influenza is routinely used to avoid the necessity for high containment laboratories and the current generation human papillomavirus vaccine is based on recombinant HPV subtype virus like particles (VLPs).

To create a VSV-pseudotype virus (VSV-PV) the VSV-glycoprotein (VSV-G) gene, which encodes for the envelope, is replaced by a reporter gene such as *luc* or *GFP*. This is combined with a plasmid encoding for the desired viral envelope. In addition to this the viral nucleoprotein (N), phosphoprotein (P) and polymerase protein (L) must be co-transfected into the producer cell line. The recombinant VSV (rVSV) genome is transcribed by the RNA polymerase T7. This can be introduced by either the addition of a T7-encoding helper virus such as modified vaccinia Ankara-T7 (MVA) or Fowlpox-T7, or by the use of constitutively expressing cells. Due to the complexity and time-consuming nature of this work, the rVSV is often purchased commercially. Once delivered a simple transfection of a producer cell line with a plasmid containing the envelope of interest followed by transduction of the rVSV is sufficient to generate a VSV-PV in most cases.

HIV and MLV core systems both utilise a three-plasmid transfection method to generate the respective pseudotype viruses. The two-plasmid system was the first developed and combined the HIV/MLV capsid and packaging signal in the same plasmid. The three-plasmid system was developed to remove the risk of generating a replication competent virus. The three plasmids contain the core, packaging signal with reporter gene and envelope gene of interest. These are transfected simultaneously into a producer cell line at specified amounts which must be optimised beforehand. The resulting media should contain pseudotype particles with the envelope protein of interest. The topic of pseudotype optimisation and production is a lengthy subject although some excellent reviews exist (King et al., 2016).

As well as the three-plasmid lentiviral system, a third generation 4-plasmid system is also now widely used. This differs from the aforementioned system via the addition of another plasmid splitting the packaging system (GAG, POL, REV) across two plasmids, further improving safety by reducing the risk of recombination even further.

Several groups report having produced JEV pseudotypes, however, attempts to replicate these data have been widely unsuccessful. This may be due to otherwise undescribed factors affecting pseudotype success or poor/ misleading experimental design by the original authors.

Lee et al. (2009) compared the titre of JEV pseudotype produced from a variety of cell lines (summarised in Table 2).

Table 1.2 Titres of JEV pseudotype produced in a range of cell lines. Data are reported in infectious units/ml.

	Producer Cell							
JEV strain	Vero	BHK-21	HeLa	CRFK	PK15	HEK-293T	MDBK	HOS
Nakayama prM/E	$1.90*10^4$	$7.46*10^3$	$4.08*10^3$	$9.74*10^4$	$1.33*10^3$	$1.14*10^2$	$2.08*10^2$	0
Nakayama E	$4.25*10^4$	$7.58*10^3$	$4.12*10^3$	$1.20*10^3$	$1.09*10^3$	$1.32*10^2$	$2.11*10^2$	0
Beijing I prM/E	$4.12*10^4$	$7.76*10^3$	$4.35*10^3$	$1.02*10^5$	$1.82*10^3$	$2.04*10^2$	$2.08*10^2$	0

Beijing I E	$4.83*10^4$	$7.91*10^3$	$4.29*10^3$	$1.36*10^5$	$2.90*10^3$	$2.05*10^2$	$2.23*10^2$	0

Unexpectedly E gene alone resulted in higher titres than prM/E transfected together in all host cells. Beijing-I transfection produced higher titres than Nakayama strain genes though the reasons for this are not immediately clear. The Nakayama and Beijing-I strains are 97.9% identical at the nucleotide level and 96.6% identical in their amino acid sequence. Sixteen amino acid differences exist between their prM, and E genes and it is likely one or more of these mutants is less efficiently translated or has a toxic effect on the producer cell line which results in a reduced titre of the produced pseudotype.

CRFK and Vero cells appear to be the most efficient target for a JEV pseudotype. However, the lack of controls means that a direct comparison to other pseudotype systems is not possible. Compared to other pseudotypes such as VSV-G on a retroviral core or rabies virus envelope on a VSV core which result in titres of 10^8-10^{10}, then these would be considered low. Flavivirus pseudotypes are generally low titre however without any controls it cannot be ascertained if these are real results or background incorporation of naked cores into the target cells.

It has been suggested that problems with pseudotyping flaviviruses are the result in an incompatibility between the life cycles of the various viral cores used and the natural infectious cycle of the flavivirus. As mentioned previously, the flavivirus envelope buds from the ER in a rapid process which is believed to bring the capsid and PrME complex together forming immature virions. These immature virions mature in the acidic environment of the endosome before being released at the cell surface. Many pseudotype system cores bud from the plasma membrane therefore never coming into proximity with the envelope protein.

This theory is supported experimentally. Studies utilising flow cytometry showed often a negligible (<5%) amount of produced envelope displayed on the cell surface. To circumvent this problem, groups are investigating ways to increase export of envelope proteins to the cell surface in order to form complete pseudotypes with the respective core used.

Flaviviruses are unique among viruses in possessing a double transmembrane anchor in their envelope protein (Fritz et al., 2011). This may contribute to the strong affinity of the PrME complex to the ER. Nishimura & Balch (1997) identified a specific amino acid sequence which facilitates selective export from the ER. This diacidic signal comprises an aspartame residue followed by any amino acid and then glutamate (D-X-E). This signal was first noted in VSV-G protein but has since been recorded in many other proteins that undergo migration from the ER to the plasma membrane.

Due to the problematic nature of flavivirus pseudotyping other methods have been employed to investigate the effect of envelope protein modifications including reverse genetics systems involving rescue of live virus from one or more plasmids. Reverse genetics is achieved by chemically synthesising the viral genome either as a single stretch of DNA or several oligomers. These oligomers are then ligated together if required (due to length restrictions of DNA synthesis) and transfected into a producer cell where the various viral proteins are translated, and viral particles self-assemble. This method has the advantage of being able to investigate the effect of changes on any part of the viral genome and is routinely used. However, as viable virus is produced this work necessitates the use of high containment laboratories which are expensive to run and must utilise highly trained personnel. This method of work is also very labour intensive and high throughput studies are challenging.

As mentioned, the incompatibility between the JEV and core system life cycle is believed to be the major limiting factor affecting JEV pseudotyping success. It has been hypothesised that increasing the amount of envelope protein exported to the cell surface will result in association between envelope and capsid which will result in the formation of functional pseudotype particles. Numerous methods have been employed to achieve this including increasing production of the envelope protein and complex modifications to the transmembrane domains of JEV which act as retention signals (Ciczora et al., 2010).

Modification of the TM membrane dom4.7ains may result in a new issue, research into the entry mechanism of JEV strongly supports the idea that the envelope transmembrane regions function as a crucial “hinge” allowing the membrane-envelope protein complex to unfold and attach to the putative receptor on the cell surface (Fritz et al., 2011). Modification of these regions or replacing them with the transmembrane domains of other viruses (as has been suggested) may critically impair viral entry into the cell. It is important to bear in mind therefore that simply increasing the amount of envelope protein reaching the plasma membrane must be balanced with retaining wild-type functionality. Without this any downstream processes lack validity.

Recently, Kretschmer et al. (2020) developed a Zika virus pseudotype delivery system to treat glioblastoma. Zika virus has a high affinity for glial cells and its envelope protein serves as an effective and novel “targeting system” to deliver nucleic acids coding for anti-tumour factors and other pro-apoptotic proteins to glial cancer cells. The crucial discovery was that the addition of the HIV protein negative regulatory factor (Nef) to the Capsid-encoding plasmid resulted in a significant increase in the production of pseudotype virus. The reason for this relates to a newly discovered function of Nef in that it downregulates the membrane serine incorporator 3 and 5 proteins (SERINC3 and 5). These host proteins inhibit HIV infectivity and may prevent release of pseudotype particles from the producer cells. Further research utilising *nef*+ plasmids may finally solve the flavivirus pseudotyping issue.

1.13 Aims

The research presented in this thesis aims to establish a reliable method of generating pseudotype JEV in order to compare the neutralising potency of vaccine-mediated antibodies against the emerging genotype 5. This will enable the development of a pseudotype neutralisation assay as well as screening of a nanobody phage library in order to isolate neutralising epitopes on the JEV E protein. As well as this a comprehensive bioinformatic analysis will be performed to determine whether recombination is a common or rare occurrence within and between genotypes of JEV.

2 Materials and Methods

2.1 Cell Culture

2.1.1 Cell lines

Retroviral, lentiviral and dengue replicon-based pseudotypes were grown using transfected HEK-293T cells aside from specific experiments where other cells were assessed for their potential as producers or reporters.

Pseudotype virus was titrated on BHK and Vero cells depending on the downstream application.

HEK-293T, BHK21, Huh7, LLC-MK2, Vero (E6) and CRFK cell lines were kindly provided by colleagues at NIBSC.

HEK cells were used as producer cells for all transfections as well as reporters in some neutralisation assays. BHK, CRFK and Vero cells were used as reporters in neutralisation assays.

NEB 5-α competent *E. coli* (NEB catalogue number C2987H) were used for propagation of all plasmids. Manufacturers' protocols were followed for general usage.

2.1.2 Growth Media and Incubation Conditions

During routine passage and growth, mammalian cell lines were grown in Dulbecco's minimum essential media, Glutamax™ (catalogue number 10566016) supplemented with 10% foetal bovine serum (FBS), 1% penicillin/ streptomycin (10,000 units/ml. Catalogue number 15140122) and 1% non-essential amino acids (100x. Catalogue number 11140050). This is referred to as M10 in this thesis.

For infection assays (titration, neutralisation assays etc) cells were grown in Dulbecco's minimum essential media, Glutamax™ (catalogue number 10566016), 1% penicillin/ streptomycin (10,000 units/ml. Catalogue number 15140122) and 1% non-essential amino acids (100x. Catalogue number 11140050). This is referred to as M0 in this thesis.

Bacterial cells were produced in LB Broth made by NIBSC scientific support services according to the following procedure: 10g tryptone, (Fisher LP0042), 8g NaCl (Fisher S/3160/65) and 5g yeast extract (LP0021) was added into 1L ultrapure water. If required, pH was adjusted to 7.5 using 2M NaOH. The fully dissolved solution was autoclaved at 121˚C for 15 minutes. The sterilized LB broth could be stored at RT for up to 1 year.

LB Agar was made by NIBSC scientific support services according to the following SOP: 1.5% total volume agar (Sigma A6686) was added to unsterilised LB broth solution. The solution was allowed to dissolve fully and subsequently autoclaved at 121˚C for 15 minutes. Sterilized LB agar can be stored at RT for up to 1 year.

Terrific broth was made via reconstitution from dry powder purchased from Sigma Aldrich (Cat# 22711022).

All cell lines were maintained at 37˚C, 5% CO_2 in a humidified HERA cell incubator.

Room temperature in the laboratories used was approximately 21˚C.

2.1.3 Passaging and counting cells

2.1.3.1 Countess method

Cell counting was performed by mixing a trypsinised cell suspension 1:1 volume ratio with 0.4% trypan blue solution (Thermo Fisher catalogue number 15250061), adding 10µl to each side of a Countess™ cell counting chamber slide (ThermoFisher catalogue number C10228) and inserting into a Countess™ automatic cell counter. The average value of live cells between the two sides of the counting chamber was used to calculate cell count. The cell suspension was then diluted/ aliquoted according to the required number of cells for the downstream task. The formula used to calculate the volume of cells to add from a master stock was as follows:

(Final cell number/ cell count) * volume required.

2.1.3.2 Haemocytometer method

If the countess cell counter was unavailable, a manual counting method was used. Trypsinised cell suspension was mixed 1:4 (vol/vol) with trypan blue

(*e.g.*, 100µl cell suspension to 400 µl trypan blue). Then 100µl of this cell/trypan blue mixture was applied to a haemocytometer and viewed under a light microscope at 10X objective magnification. Live (unstained) cells were counted in each of the four large corner squares of the haemocytometer (Cambridge Bioscience, UK) and the average count from each large square was multiplied by 10,000 and then 5 (to account for the initial trypan blue dilution).

2.1.4 Long-term cell storage

Cryogenically preserved stocks were produced at the lowest passage to ensure a low passage number was available throughout the project. Earlier passages were resuscitated when cells began to change morphology or behaviour within assays: this was monitored throughout all experiments.

Stocks were generated by growing 3xT75s of the required cell line for the appropriate length of time for the cell line. Cells were washed with 2ml trypsin, this was then discarded and then a further 2ml of trypsin was used to remove the cells from the flask surface, the mixture was collected into 50ml falcon tubes and centrifuged at 10,000rpm for 10 minutes. Pellets were then combined and resuspend the pellets into 1ml freeze media. This was followed by immediate storage in a ≦-70°C freezer inside a Mr. Frosty freezing container (ThermoFisher cat no. 5100-0001) for 24 hours. After 24 hours vials were moved to storage in the vapour phase of liquid nitrogen (LN_2) until required.

Freeze media was prepared by making a 90% FBS, 10% DMSO solution.

Frozen cells were resuscitated by rapid thawing and immediate addition to pre-warmed M10 in an appropriate size cell culture flask.

2.2 Molecular Biology

2.2.1 Restriction enzyme digests

When required, restriction sites were introduced into terminal primer ends, plasmids and other DNA fragments by overlap extension PCR. The corresponding restriction enzyme was purchased from NEB (USA) and manufacturers recommendations were followed for digests. Where possible,

HF® enzymes were purchased for the advantage of universal rCutSmart® buffers and high-speed protocols. All restriction enzymes and their associated buffer(s) were stored at -20˚C and exposed to RT for as short a time as possible when used.

2.2.2 Primer design and reconstitution

Primers were designed to have a T_m of between 60-64 ˚C. Primers were synthesised by Eurofins (UK) and reconstituted to 100nM using nuclease-free water.

2.2.3 PCR

A standard set of thermocycling conditions was used for each PCR carried out. The annealing temperature was modified depending on the melting temperature (T_m) of the primers used in the respective reaction. These conditions were:

Forward/Reverse primers: 1µl each	95˚C	30 s	
2x Taq master mix (NEB, UK): 25µl	95˚C	30 s	x30 cycles
DNA: <1000ng/ reaction	*X˚C*	*X s*	
Water: to 50µl	68˚C	1.5 min	
	68˚C	5 min	
	4˚C		

Overlap extension PCR was performed by including a 5-nucleotide poly-A region at the 5′ end followed by the restriction site of interest and then at least 10 nucleotides complementary to the target sequence at the 3′ end of the oligonucleotide.

5′ AAAAAGAATTCGCTCTAGTAGTA **3′**

Figure 2.1. Example restriction site introduction primer

2.2.4 Agarose gel electrophoresis

In order to confirm the identity of amplified, restriction digested, and ligated DNA fragments and plasmids agarose gel electrophoresis was used. A 1%

agarose gel was cast by combining 50ml TAE buffer with 0.5g UltraPure™ Agarose (ThermoFisher catalogue number 16500100). This mixture was swirled to distribute agarose powder and then heated in a microwave until all powder had visibly melted. The solution was left to cool until no longer hot to touch then 1/10000 of the total gel volume of SybrSafe DNA gel stain (ThermoFisher catalogue number S33102) was added, mixed gently and then the molten agarose was poured into an appropriately sized gel mould, a gel comb was placed in the molten agarose then left to solidify at room temperature. Once solid the gel was submerged in TAE and the comb was carefully removed. A DNA ladder was added into the leftmost well and samples were subsequently added in the remaining wells. The gel was subjected to an electric current to separate DNA according to fragment size.

2.2.5 Purification and quantification of nucleic acids

All plasmid purification was performed using Qiagen mini, midi and maxi-prep kits (following manufacturer's instructions) depending on the quantity of plasmid required for the downstream task. Extracted plasmid DNA was eluted from the Qiagen column(s) using either nuclease-free water or TE buffer if the downstream tasks required cloning and/or sequencing. The final plasmid concentration was quantified using a Nanodrop spectrophotometer and stored at ≦-20˚C until use. When using the Qiagen maxi-prep kit, the eluted plasmid DNA was left overnight at +4 ˚C to allow the larger quantity of nucleic acid to fully dissolve into the solvent before quantification via Nanodrop.

2.2.6 Gel extraction

Gel extraction was utilised for the purification of specific fragments of DNA yielded by restriction endonuclease treatment. Samples were electrophoresed through a 1% agarose gel at 110v, 400mA for 45 minutes to 1 hour depending on gel size or until good separation of fragments visible by ladder migration. The gel was visually inspected under a blue-light transilluminator, to minimise damage to the DNA, and the band of interest was carefully excised from the gel using a clean scalpel taking care to trim as much excess agarose from the sample as possible.

The extracted sample was weighed and then solubilised and eluted using a Qiagen gel extraction kit.

2.2.7 Transformation of competent bacteria

When new plasmids were required to be amplified into working stocks or old libraries of plasmid were to be refreshed, chemically competent *E. coli* NEB 5-α were thawed on ice until all ice crystals had disappeared (approximately 5 minutes). A 1-5ul volume of plasmid DNA (containing 1pg–100ng DNA) was added into the cell mixture and mixed by gently flicking the tube 4-5 times since vortex mixing may cause shearing damage of the fragile cell membrane. The cell-plasmid mixture was incubated on ice for 30 minutes and then subjected to a heat shock of 42˚C for 30 seconds to permeabilize the cell membrane and allow entry of the plasmid DNA into the cytoplasm. The cell mixture was placed back on ice for a further 5 minutes.

Pipette 950µl SOC media into the cell mixture and incubate at 37˚C, 225RPM for 60 minutes. During this step, ampicillin selection plates (50µg/ml) were pre-warmed to 37˚C. This ensured the cells did not endure a second heat shock and dried any surface condensation on the selection agar which may have prevented defined colonies from growing.

After 60 minutes, appropriate fold dilutions of the cell mixture were performed and pipetted directly onto the selection agar. The mixture was spread using a cell spreader and the plates were incubated upside down at 37 ˚C overnight.

The next day, colonies were counted and compared to a control lacking an antibiotic resistance gene.

2.3 Pseudotype virus manufacture

2.3.1 Nomenclature

Harvested pseudovirus was labelled with the abbreviation for the pseudotyped envelope followed by the batch number (if multiple batches were made in that round) and the date harvested. For example, the first batch of JEV-PV harvested on 16 May 2021 would be designated JE1 16.5.21.

2.3.2 Transfection reagents

Different pseudotype systems were used in the attempt to generate JE-PV. Some of these systems are optimised for use with unique transfection reagents. All the transfection reagents used in this chapter are listed below along with their associated pseudotype system.

Table 2.1. Summary of transfection reagents used for each pseudotyping system.

Transfection reagent	**Pseudotype virus core**
PEI – branched (polyethylenimine)*	Dengue replicon/ rVSV
Fugene-6	HIV/ MLV
Polyfect	

*PEI was diluted to a final concentration of 1mg/ml (408727-Sigma, UK)

2.4 Serology and Immunological assays

2.4.1 Determining TCID50 and IU/ml

The Spearman-Kärber method was used to determine TCID50. Triplicate sample values were deemed either “positive” or “negative” at each dilution point based on whether they were higher than 3-times the standard deviation of the background relative luminescent units (RLU). Measured as Vero cells only. The TCID50/ml value was then converted into infectious units/ml (IU) through multiplying it by 0.69 (the Poisson distribution).

Once calculated, IU/ml was used to determine the quantity of PV added to neutralisation assays.

2.4.2 Pseudotype titration

In order to quantify the relative concentration of pseudotype virus particles, a titration assay was performed. Output was measured in RLU using a luminometer. An undiluted volume of PV was added to the first well of rows A-C on a 96-well plate. A total of 9 sequential dilutions of 1:10 were performed in each row to achieve a dilution range of neat, 1:10-2560. Media was removed from the cell monolayer and the diluted PV was added to each respective well. The 96-well plate was returned to the incubator for 4-5 hours, after which the PV dilutions were removed and replaced with fresh M10. The cells were incubated for a further 3 days.

On the third day post infection, cells were lysed by adding 100 µl of the Nano-glo substrate, incubated at RT for 3 minutes then 90µl of the lysate was transferred to a white-bottomed 96-well plate and read at default settings in a luminometer.

2.4.3 Pseudotype neutralisation

Functionality of pseudotype viruses was tested via a neutralisation assay using convalescent sera or neutralising antibodies resulting from infection on which the wild-type virus the pseudotype was based.

Sample dilution and plate layout was similar to the titration assay.

An appropriate dilution range was selected based on the titre of the batch of pseudotype virus used. Prior to dilution the TCID50 and IU/ml of each pseudotype virus batch was calculated from the results of the titration assay. The assay parameters were then adjusted to ensure that a standardised quantity of pseudotype virus was added to each well. This varied throughout the development process until a value of 300IU was elucidated as the optimum quantity which provided enough targets for the neutralising sera/ plasma or antibodies without saturating the assay.

2.4.3.1 Plasma and sera

Human anti-JE plasma and negative control plasma, both freeze-dried, were sourced from the NIBSC catalogue (product number 02/182 and 02/184, respectively). The anti-JE plasma was the pooled plasma obtained from six recipients of the Biken (inactivated Nakayama-National Institute of Health strain) vaccine. The negative control plasma is the pooled pre-bleed material from the same six recipients.

The instructions for use state that the anti-plasma may be strain specific to the Nakayama strain and therefore a specific unitage was not assigned.

2.5 Phage display general materials

Tris buffered saline (1L)

6g tris base was mixed with 8.75g NaCl in 800ml dH20 and adjusted to pH 7.5. Made up to 1L in water.

5xM9 salts (500ml)

32g $Na_2HPO_4.7H_2O$ **or** 21.35g $Na_2HPO.2H_2O$ **or** 15g Na_2HPO_4 (anhydrous) – otherwise called disodium hydrogen orthophosphate anhydrous was mixed with 7.5g KH_2PO_4 potassium phosphate monobasic (sigma p9791 – 500g) – (otherwise called potassium dihydrogen orthophosphate), 2.5g NH_4Cl ammonium chloride (fisher A/3880/s3), 1.25g NaCl and 500ml dH_2O. Mix thoroughly and autoclave.

Min agar (100ml)

1.5g agar powder was mixed with 78ml H_2O, 25ml 5x M9 salts, 1.6ml 25% glucose, 100ul MgCl2 (20% w/v or 2.1M, sterile filtered) and 50ul thiamine hydrochloride (10mg/ml, sterile filtered). The mixture was then autoclaved.

2YT / 2YT agar (500ml)

8g tryptone was mixed with, 5g yeast, 2.5g NaCl and 500ml dH_20. 7.5g of agar was added per 500ml. The mixture was then autoclaved.

Elution buffers

Tris neutralising buffer: Tris 1M pH7.4 – 60.57g tris base was mixed with 350ml dH20. The pH adjusted to 7.4 and sterilised.

Glycine eluting buffer: Glycine 0.1M pH2.2 – 0.75g glycine was added to 100ml water. The pH was adjusted to 2.2 and sterilised.

3 Phylogenetic analysis of Japanese encephalitis virus envelope gene sequences

3.1 Aim

The work within this chapter examined publicly available JEV E gene sequences for evidence of recombination and categorised these sequences into their respective genotypes. The objectives were to:

1) Create a database of all publicly available JEV E gene sequences.
2) Screen these sequences for evidence of recombination using a sliding window analysis, which in turn allowed for genotyping.
3) Compare and contrast these data in the context of geographical and historical differences.

3.2 Introduction

As previously discussed in 1.6 it has been demonstrated that recombination within flaviviruses is possible and has occurred in nature (Carney, Daly, Nisalak, & Solomon, 2012). There is debate on the potential of recombination between live viral vaccines and wild-type JEV, which may result in the generation of novel genome combinations which could reduce vaccine effectiveness or increase virulence. As well as this, the notable sequence divergence of genotype V (GV) when compared to GI–IV is of particular interest, in particular as some studies have suggested that GV infection may result in poorer clinical outcomes as a result of increased neurotropism (de Wispelaere, Frenkiel, & Despres, 2015). However, the rarity of GV circulation and lack of sequencing performed at the time of infection has resulted in this being difficult to confirm.

3.2.1 Techniques to study recombination

The displacement of genotype III by genotype I has been well documented since whole genome sequencing of JEV isolates has become more commonplace in affected countries (Erlanger, Weiss, Keiser, Utzinger, & Wiedenmayer, 2009; Nabeshima et al., 2009; Nitatpattana et al., 2008; Pan et al., 2011; Saito, Taira, Itokazu, & Mori, 2007; H. Y. Wang et al., 2007). A comprehensive analysis of the

sequencing and meta data available for this was performed using a variety of tools. The purpose of this work was to investigate reports of recombination in JEV and establish whether existing recombinants represent a rare event or recombination is more commonplace than previously thought. There are several methods available to investigate recombination from sequence data. The method chosen for this work was a sliding window analysis, also known as bootscanning (Salminen, Carr, Burke, & McCUTCHAN, 1995).

The sliding window analysis is a distance-based method of recombination detection. This method was selected as it is generally fast, and the phylogeny of the sample sequence does not need to be known. Other methods include site-by-site compatibility and analysis of nucleotide substitution distributions when compared to a parent sequence.

3.2.2 Genotype distribution and recombination

Genotype distribution is not the same across the endemic countries. Different theories have been put forward to explain the reasons for this, including different competencies between certain genotype/ host combinations as is the case for WNV (Kilpatrick, Meola, Moudy, & Kramer, 2008) or reproductive advantage in the vector and/or amplifying host (Xiao et al., 2018).

For recombination to be detected, multiple genotypes must co-circulate within an ecosystem. Performing genotyping on all available JEV E gene sequences will allow a fuller understanding of which countries are more/ less at risk of recombination if it is found to be an underreported phenomenon across JEV genotypes.

It is understood that different parts of the JEV genome are prone to differing selection pressures such as the 5′ and 3′ terminal repeat regions (Liu, Zhang, Niu, & Liang, 2021) which are relatively volatile compared to the largely stable NS5 gene which codes for the RNA dependent RNA polymerase, a critical viral protein. These selection pressures also act within genes as different areas of a protein are subject to varying levels of attention by the host immune system (receptor binding domains, self-cleavage sites *etc*).

The scope of this thesis is focussed on investigating differences within the PrME genes of JEV. The reasoning for this was that the E gene is the region on which genotypic characterisation is based and the structural proteins are the most

important for studying viral entry as well as the fact that neutralising antibodies raised against the E protein are the primary correlate of protection for vaccine mediated immunity.

3.3 Methods

3.3.1 JEV genome metadata

Metadata for JEV genome sequences were downloaded from the NCBI and EMBL databases into Microsoft Excel and categorised by accession number, base count, collection date, country of origin, strain description, genotype (if available), date first publicly available and host. Only sequences containing full length E gene were included for analysis.

3.3.2 Phylogenetic analysis

Genotypic characterisation of suitable sequences was performed by phylogenetic alignment in Geneious® (version 2020.03) using the neighbour joining method coupled with the Tamura-Nei substitution model (Tamura, Nei. 1993) against known reference sequences representing each genotype. Phylogenetic trees were constructed using 500 bootstraps then transcribed manually to the database of JEV sequence information derived from EMBL and the NCBI.

3.3.3 Sliding window analysis

To analyse sequences for evidence of recombination, a similarity plot was generated using sliding window analysis (SWA). This technique was first described by Salminen et al. (1995), the SWA generates multiple phylogenetic trees based on a short stretch of nucleotides that is moved along the sequence by a defined value each iteration. In this case, each phylogenetic tree was created from a sequence length of 300 nucleotides (nt) and shifted by 150 nt each iteration. For the 1500 nt JEV E protein this resulted in nine phylogenetic trees per sequence. A sequence can be identified as recombinant if it changes position (genotype) between trees.

Recombinant sequences were initially detected manually using Geneious software (version 11.7) and were later confirmed using SimPlot (version 3.5.1), an automated SWA software tool. Simplot displays which reference sequence the input sequence is most closely related to using overlapping lines.

Table 3.1 Reference sequences used for phylogenetic grouping.

Genotype	Strain	Accession Number	Year of Isolation	Country of Origin
GI	Ishikawa	AB051292	1998	Japan
GII	FU	AF217620	2000	Australia
GIII	Nakayama	AB920348	1935	Japan
GIV	JKT6468	AY184212	2002	Indonesia
GV	Muar	HM596272	1952	Japan

3.4 Results

3.4.1 Phylogenetic and genotypic characterisation

Of the 1262 JEV genome sequences acquired from both databases, 778 were suitable for genotypic characterisation. The remaining 484 sequences were too fragmented to generate concurrent phylogenetic trees or did not contain or were missing E gene sequence. Using the metadata gathered from the NCBI and EMBL databases genotypic characterisation of all JEV genome sequences which contained the full-length E gene sequence was performed (data correct as of July 2020) and used to create Table 3.2.

Table 3.2 Spread of JEV genotypes across endemic areas highlights non-homogeneity in their distribution.

Country	GI	GII	GIII	GIV	GV	Total
Australia	3	2	-	-	-	5
Cambodia	12	-	-	-	-	12
China	205	-	191	-	1	397
India	5	-	33	1	-	39
Indonesia	-	8	1	1	-	10
Japan	27	-	18	-	-	45
Laos	1	-	-	-	-	1
Malaysia	-	2	1	-	1	4
Philippines	-		2	-	-	2
Singapore	1	5	-	-	1	7
South Korea	31	1	17	-	9	58
Sri Lanka	1	-	-	-	-	1
Taiwan	78	-	50	-	-	128
Thailand	25	-	1	-	-	26
Vietnam	23	-	15	-	-	38
	412	18	329	2	12	773

Genotyping of the 484 suitable JEV E gene sequences highlighted the distribution of the five genotypes is not homologous throughout endemic countries and despite the well documented shift in prevalence from most cases being caused by GIII to now being caused by GI, this is not the case in every country sampled. In India for example GIII is still the prominent genotype found in surveillance efforts.

There has been a significant increase in sequences deposited in publicly available databases since the early 2000s. This reached a peak of almost 100 sequences a year being submitted to databases such as EMBL between 2010–2014. Figure 3.1 highlights the recency bias of sequences deposited in online databases from the early adoption of next generation sequencing in the early 2000s to 2019. Sequences

are also deposited intermittently with large numbers being submitted directly after outbreaks.

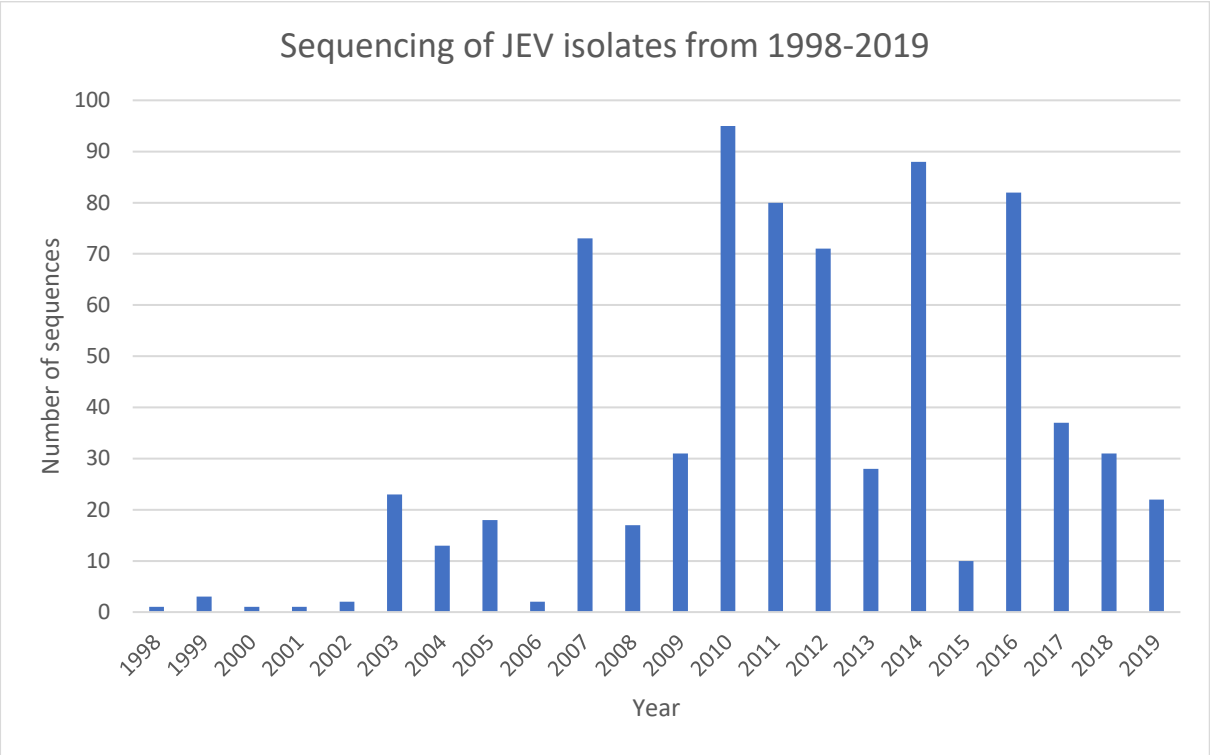

Figure 3.1 Sequencing frequency of JEV isolates highlights the rapid increase in sequencing from 2000 onwards.

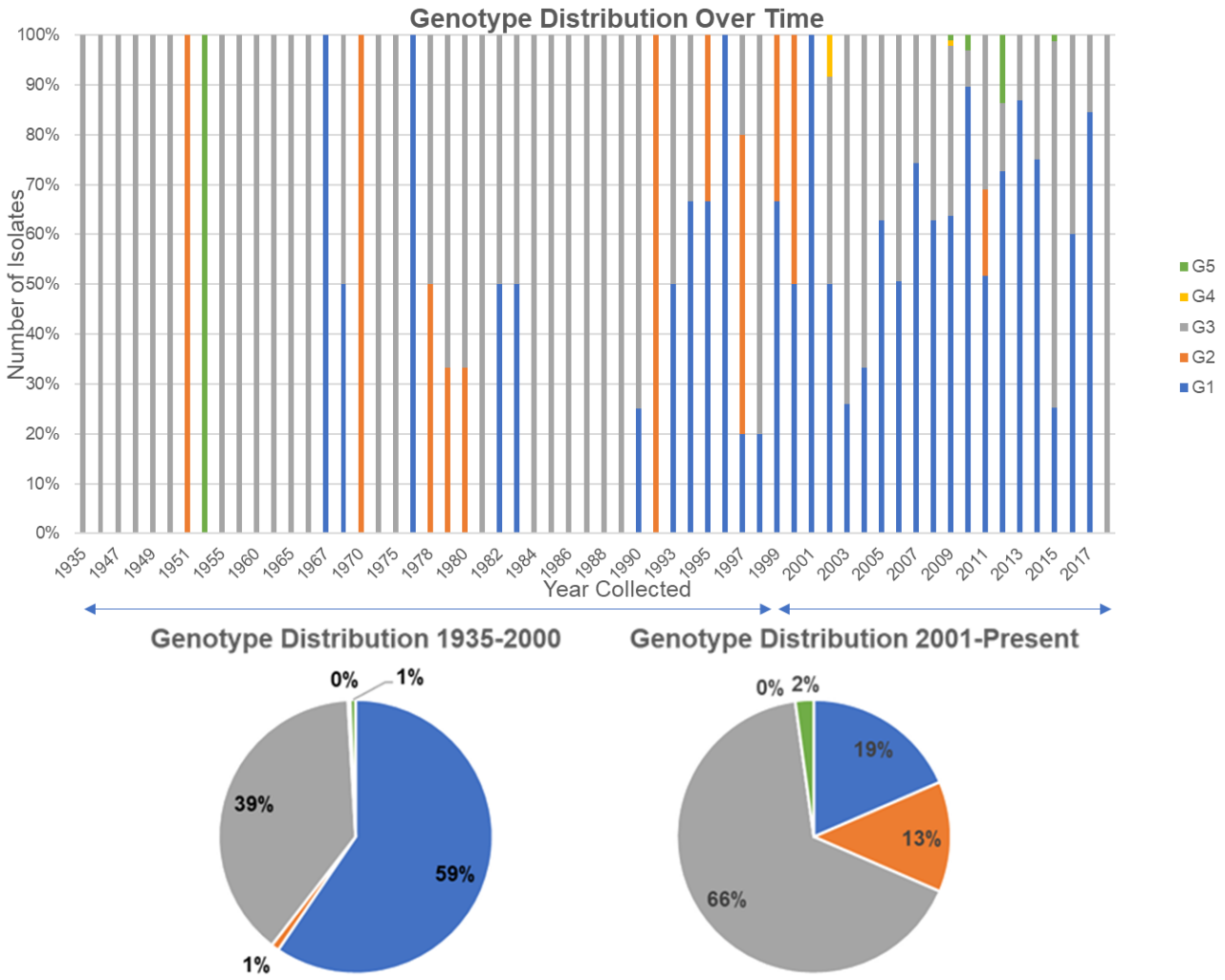

Figure 3.2 Distribution of genotypes I-V from 1935 to 2017 shows a displacement of genotype III by genotype I beginning in the early 1990s.

Using the genotyped E gene sequences, the distribution over time of the five genotypes from the earliest recorded sequence (1935) to the present day was analysed. The well documented genotypic shift from GIII to GI is shown in Figure 3.2. Whilst the increase in GV appears modest, this 1% increase globally is the result of an 550% increase in South Korea which is the country from which the most sequenced samples of GV have been available starting in 2010 when GV was first detected in the country, to 2020 when the last isolate used in this thesis was sequenced. Utilising a SWA using Geneious followed by analysis in SimPlot and performing these methods across the entire curated JEV database, 4 recombinants were identified from the sample set of 778 sequences giving a recombination rate of 0.5%.

Table 3.3. Sources of JEV isolates demonstrates a bias to mosquito sampling.

Host	**Isolate count**	**Percentage of total**
Mosquito	683	65.1
Human	224	11.8
Swine	124	21.4
Bat	6	0.2
Horse	6	0.6
Mouse	2	0.1
Midge	2	0.6
Sheep	1	0.1
Seal	1	0.2
	1049	

*34 separate mosquito species are listed as hosts in the extracted data. These have been summarised as mosquito species for brevity.

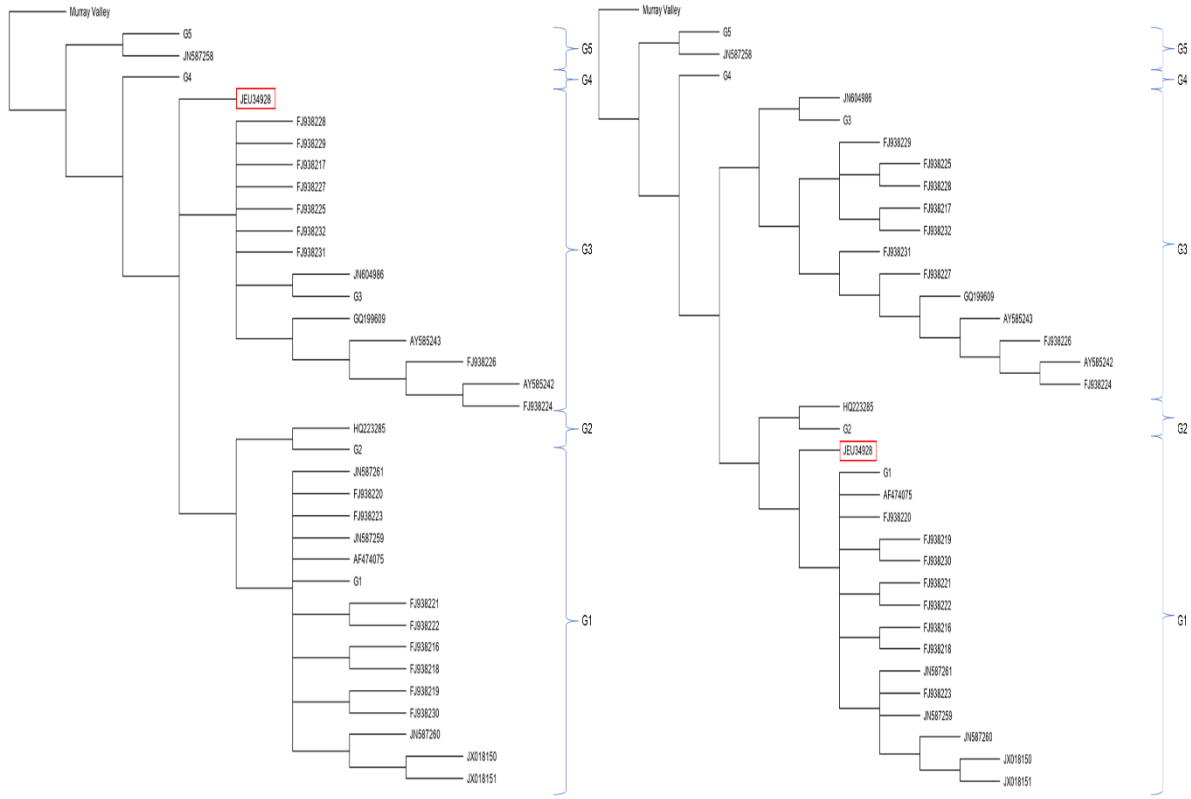

Figure 3.3. Phylogenetic swap of JEU34928 between GIII and GI visible through comparison of two phylogenetic trees generated using a SWA method.

An example output from one such SWA is shown in Figure 3.3. Sequence JEU34928 (highlighted in red) is classified as GIII in the SWA phylogenetic tree on the left. This sequence changes to being more closely related to other GI sequences in the tree on the right. After further analysis in SimPlot it can be seen that this change occurs close to nucleotide position 580 (Figure 3.4). Therefore, JEU34928 can be said to be the product of a recombination event at an unknown point in time between GI and GIII in a co-infected host. Isolate JEU34928 is a putative recombinant of GIII and GI. It was isolated from a mosquito collected in South Korea in 2016. The recombination break point is located around position 600 of the envelope gene. Data are plotted as percentage similarity against consensus reference genotypes and nucleotide position.

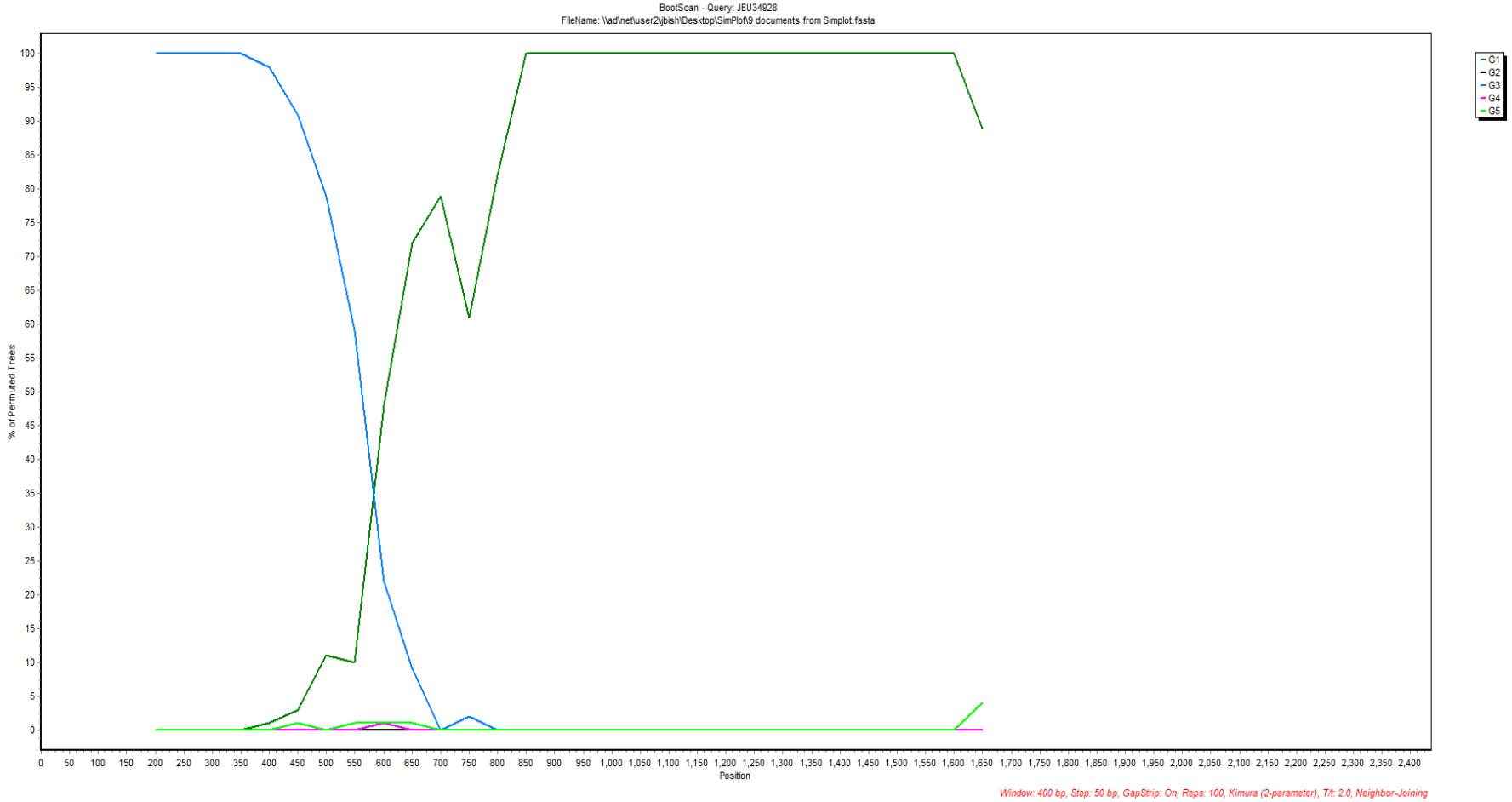

Figure 3.4. Simplot output of JEU34928 displaying recombination breakpoint at position 600 between GIII and GI using a window size of 300nt shifting 130nt from the 5' to 3' end of the JE-E gene. Data are plotted as percentage similarity against consensus reference genotypes and nucleotide position

Isolate JEU034928 is a putative recombinant of GI and GIII (Figure 3.4). The recombination break point is located around position 550 of the envelope gene. Data are plotted as percentage similarity against consensus reference genotypes and nucleotide position.

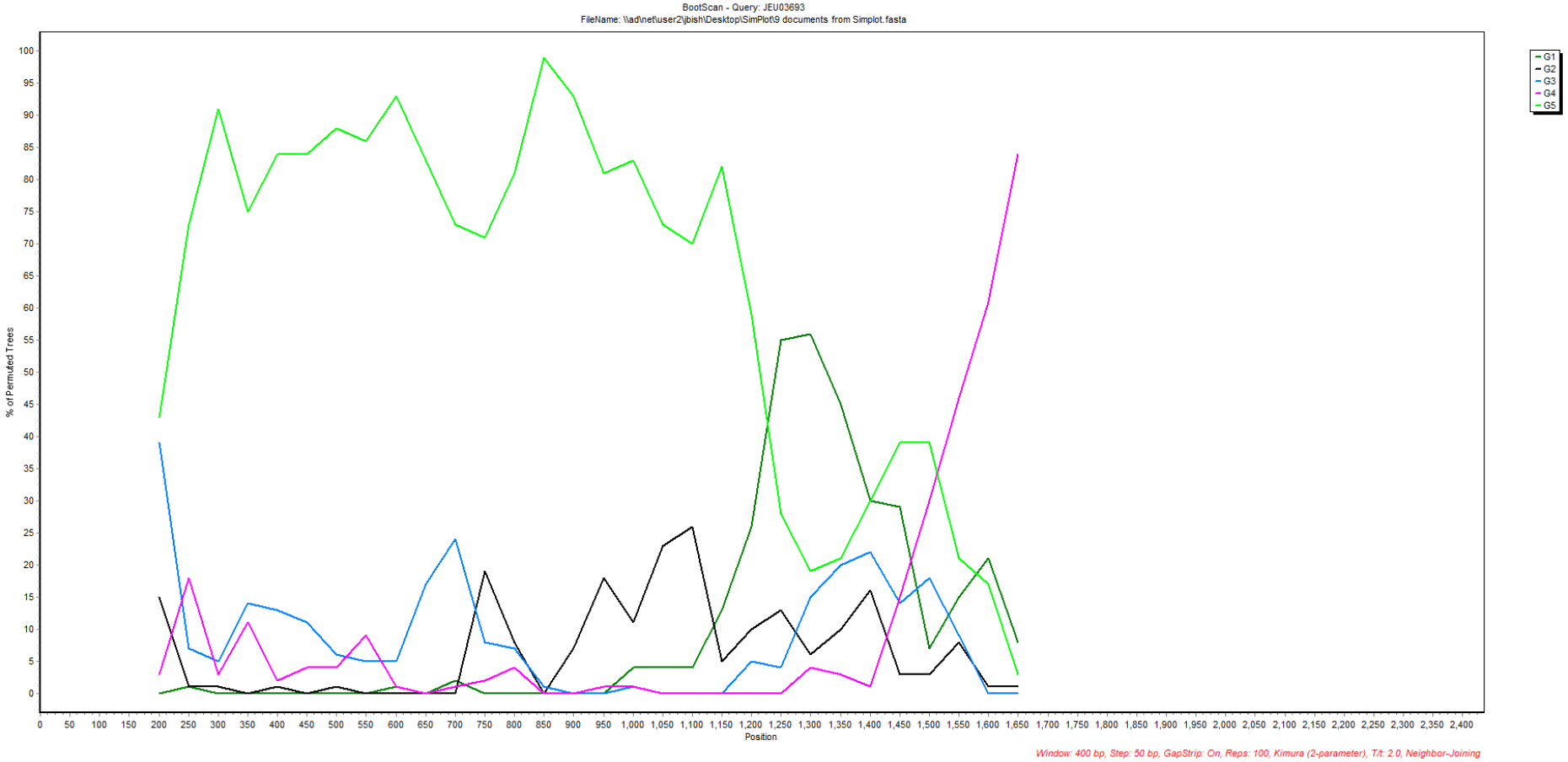

Figure 3.5. Simplot output of JEU03693 displaying recombination breakpoint around position 1250 between GII and GIII using a window size of 300nt shifting 130nt from the 5' to 3' end of the JE-E gene. Low percentage homology to genotypes 4, 2 and 5 were detected within the envelope gene region (0-1500nt). Data are plotted as percentage similarity against consensus reference genotypes and nucleotide position

Isolate JEU03693 is a putative recombinant of GI and GIII (Figure 3.5). The recombination break point is located around position 700 of the envelope gene. Data are plotted as percentage similarity against consensus reference genotypes and nucleotide position.

Sequencing data for this isolate was poor, resulting in a high background compatibility with the other three genotypes. There appears to be a homology to G4 from position 1400 however this was not reflected when overlapping phylogenetic trees were made from this region.

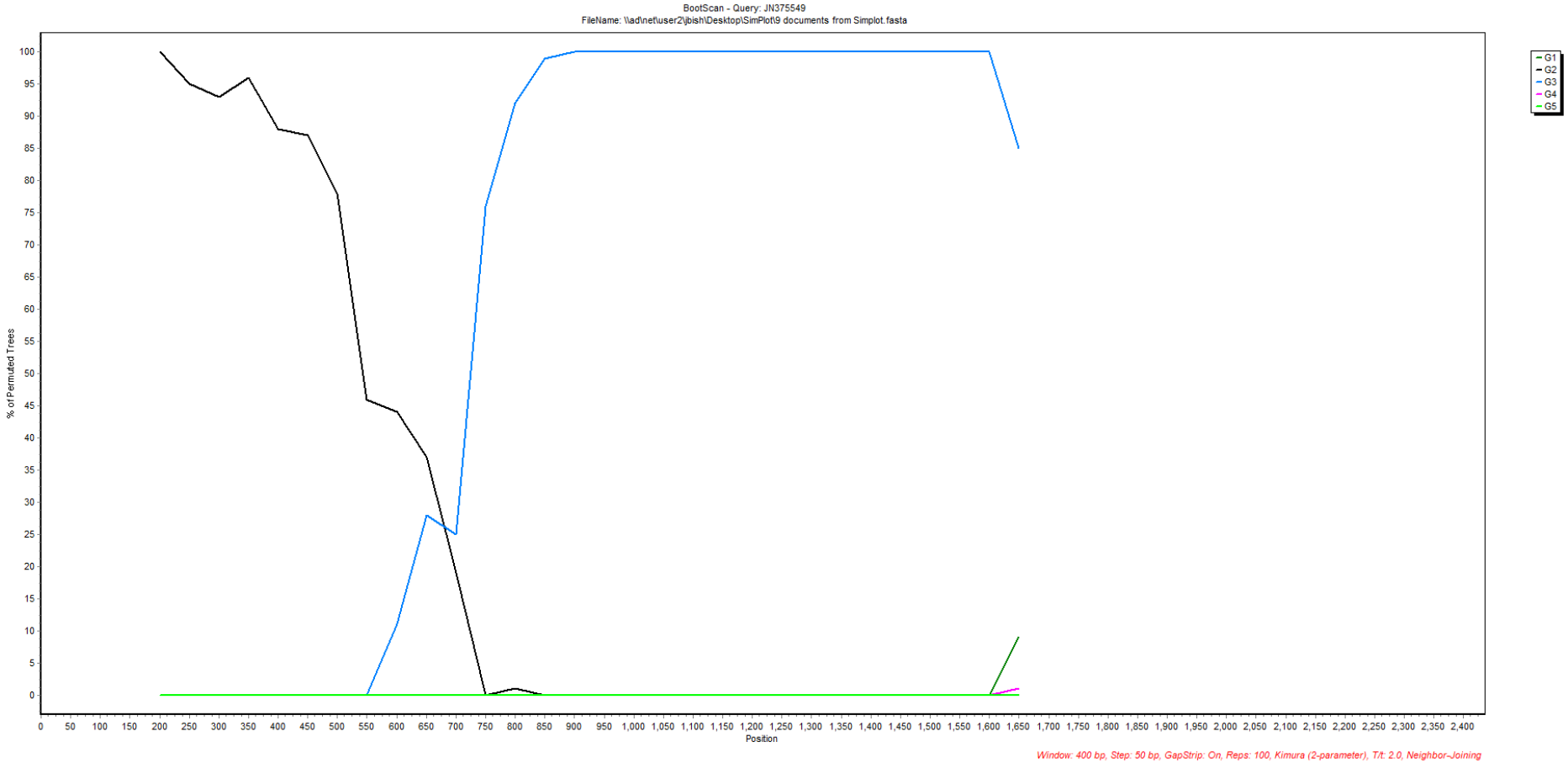

Figure 3.6. Simplot output of JN375549 displaying recombination breakpoint between GII and GIII around position 700 using a window size of 300nt shifting 130nt from the 5' to 3' end of the JE-E gene. Data are plotted as percentage similarity against consensus reference genotypes and nucleotide position

Isolate JN375549 was collected in 1979 from a mosquito in Indonesia; it is a recombinant between GII and GIII (Figure 3.6). The recombination break point is located around position 700 of the envelope gene. Data are plotted as percentage similarity against consensus reference genotypes and nucleotide position. Two isolates of JEV are documented as originating from Indonesia in

1979, one contains insufficient E gene sequence to genotype accurately, and the other isolate was characterised as GII. There are 12 genotyped isolates from Indonesia to date consisting of genotypes II, III and one genotype IV.

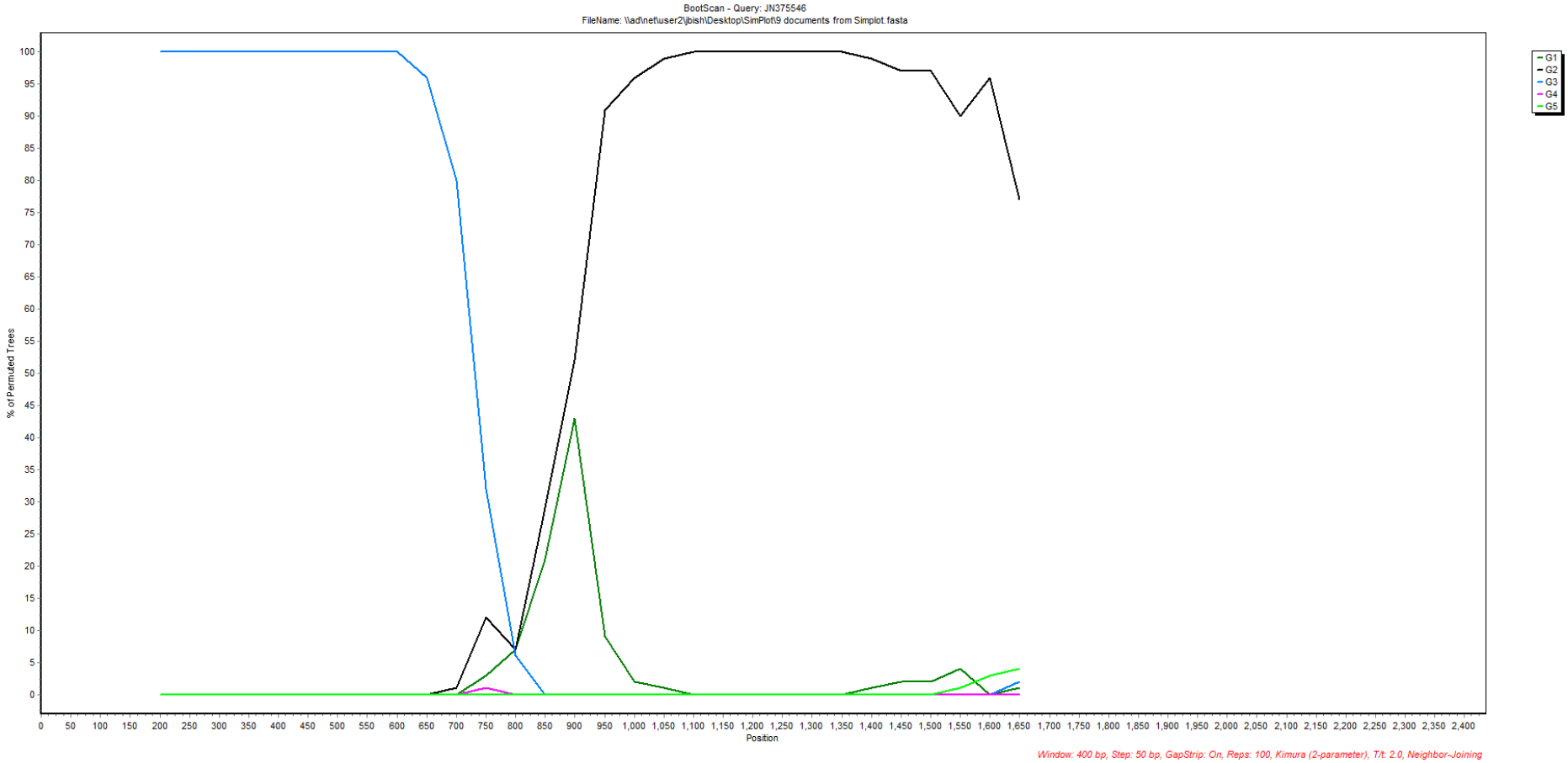

Figure 3.7. Simplot output of JN375546 displaying recombination event between GIII and GII around position 800 of the envelope gene using a window size of 300nt shifting 130nt from the 5' to 3' end of the JE-E gene. Data are plotted as percentage similarity against consensus reference genotypes and nucleotide position

Isolate JN375546 was collected in 2011 from a mosquito in Indonesia (Figure 3.7). It is the result of a recombination between GIII and GII. The recombination break point is located around position 800. A maximum of 45% homology to the reference genotype III sequence was detected at position 900, this was disregarded as an artifact resulting from poor sequencing data.

The details of the four recombinant sequences identified are summarised in Table 3.4.

Table 3.4. Recombinants detected through SWA and SimPlot screening.

Accession number	Origin	Collection Date	Lineage	Approximate site of recombination (nucleotide number)	Isolation host
JN375549	Indonesia	1979	GII-GIII	700	Mosquito
JEU03693	Thailand	1982	GI-GIII	1200	Mosquito
JN375546	Indonesia	2011	GIII-GII	800	Mosquito
JEU34928	S. Korea	2016	GI-GIII	400	Mosquito

3.5 Discussion

The presence of mixed populations of JEV genotypes in endemic countries raises the risk of recombination and potential vaccine escape. This has been previously reported to have occurred by separate groups (Carney et al., 2012; Twiddy & Holmes, 2003). This work involved the genotyping of all publicly available sequences in order to better understand the distribution of genotypes and therefore the potential for future recombination events to occur and to use this newly genotyped database to analyse for evidence of recombination that has occurred in sequences deposited since the previously reported recombinants were identified.

A neighbour-joining method was used to generate phylogenetic trees which were then used as part of a sliding window analysis to detect evidence of recombination across JEV genotypes. The accuracy of this method is limited to the size “window” used to screen the sequences. Too large and it will miss breakpoints, too small and many false positives will appear. The neighbour joining method was selected for its speed and relatively low computational requirements, other methods such as

maximum likelihood analysis are more accurate however have a longer analysis time, given the number of sequences analysed simultaneously neighbour joining was selected for convenience.

Four recombinant sequences were identified in this analysis, two are distinct from the previously reported recombinant JEV sequences noted by Twiddy and Holmes in 2003. These samples were collected over a wide time period from 1979 to 2016 and disparate geographic locations (Indonesia, Thailand, and South Korea). All recombinants described were isolated from mosquitos, which is unsurprising given that most sequences analysed in this work were also sourced from mosquito pools. Mosquito populations are the most widely screened for JEV surveillance (Table 3.3). Human cases are rarely detected early enough in the viraemic stage of infection for live virus to be isolated. The presence of human-infecting recombinants is therefore extremely challenging to detect.

A common feature of large-scale sequencing efforts, not only limited to the samples analysed in this work, is that surveillance and screening of viral diseases is restricted to nations with advanced healthcare systems. This is seen by the disproportionate number of samples isolated in China, a country which has one of the lowest numbers of JEV cases of affected countries thanks to a robust childhood vaccination programme. This adds to the importance of funding surveillance efforts in less economically developed countries to not only reduce the burden of disease, but also to fully understand a distribution and evolution of viruses as they spread regardless of borders.

Despite the bias of samples to countries with developed sequencing programmes, this does not skew the overall distribution of genotypes across the region. The proportion of each genotype found and sequenced in each country follows the general pattern of G1 being the most prevalent with GIII second. If the data had presented one nation with a particularly distinct and differing distribution of genotypes this may have had implications for the recombination analysis, however this could have been mitigated by either omitting the data from that nation if believed that the reason for the differing distribution was due to inaccurate data, or the data was not a significant portion of the total number of sequences.

In addition to the disproportionate number of sequences gathered in a small number of the sample nations is that most sequences were gathered from mosquitos. Mosquito pools are easy to access and provide a high chance of success of detection. These are valid targets for surveillance efforts as mosquitos are a sentinel organism in which to study how the virus is spreading throughout a country, however, this can lead to incorrect information about the ability of a virus to infect humans. It has been suggested by numerous groups that the shift in majority genotype from GIII to GI may be due to an ability to an ability to outcompete other genotypes through increased reproduction rate in the bird vector rather than an improved ability to infect humans or swine (Hameed et al., 2021)

One of the considerations when using a SWA as a means of detecting recombination is the potential impact of sequencing errors. Many of the isolates used in this analysis were from 1970-2000 when Sanger sequencing was the only option available in the regions studied.

Sanger sequencing requires concatamerization of multiple short reads, and errors in the assembly of these concatemers may artificially produce a “recombinant” sequence when it may be that a sample which contained two (or more) distinct genotypes. These problems can be addressed if the virus in question can be grown and sequenced again as confirmation of the original data. However, this is often not possible, and these issues must be considered when the final data is viewed.

Early-generation polymerases which had a reduced proof-reading ability also produce errors at a higher rate than samples sequenced using modern reagents which may result in misleading phylogenetic trees. Even simple errors such as mislabelling of samples can be almost impossible to detect and will provide false results when reviewing historical sequence data.

Viruses are rarely cloned before sequencing and the presence of contaminants were discounted as a negligible proportion of the sample; however, this can result in heterologous genomes being incorrectly attributed to the target virus. When performing phylogenetic analysis on a sample such as this, it would attribute the two different viruses as a recombination event when it was the result of incorrect concatamerization of the original genomes in a sample where perhaps multiple separate genotypes were present. This is much more likely to be the case in a

mosquito sample as they can feed on multiple hosts which all may harbour a different genotype of JEV.

Of the four detected recombinants, all involved a GIII parental lineage. This is most likely a result of GIII comprising a majority of the circulating virus when these isolates were collected. It is not currently known whether GI and/or GIII possess unique features which make recombination more likely than other genotypes, the fact that new recombinants have not been detected post 2015 puts forward the interesting question that in countries where GI has been displaced GIII, is GI less likely to recombine? Recent research into Zika virus recombination between the African and Asian lineages *in vitro* conclude that recombinants were more likely to form 5′ African to 3′ Asian with breakpoints in broadly similar regions. The recombination events were also likely the result of RNA polymerase switching template as opposed to homologous recombination (Dermendjieva, Donald, Kohl, & Evans, 2020, 2022). These types of *in vitro* experiments performed on the different JEV genotypes would be invaluable to understanding the effects of recombination within JEV.

Recombination breakpoints were not clustered around any specific area of the E gene. All of the detected recombinants were isolated from human cases or swine. There appears to be no geographical or chronological clustering of recombinants with cases ranging from the early 1980s up until 2016.

All recombinants described were isolated from mosquitos. Isolates were collected over a wide time period from 1979 to 2016 and disparate geographic locations (Indonesia, Thailand, and South Korea). Most sequences analysed in this work were also sourced from mosquito pools.

It has been mentioned that when analysing historical sequence data the possibility of errors in sequencing or labelling can have an adverse effect on the reliability of any detected recombinants. One such event is the possibility of strand swapping during PCR of a sample which contains two separate genotypes. In this event, a false positive recombination event may be detected. This could be interrogated by performing new PCR amplification of all samples tested. However, given the limitations of time and resources this was not possible. Many of the original samples have also since been destroyed. As such, the possibility that all of the detected recombination events are experimental artefact cannot be excluded.

Homology to other genotypes which were not recombinant highlight one of the difficulties in detecting recombination events. As discussed previously, genotypes I-IV share 91% nucleotide homology (based on reference sequences) therefore a certain degree of homology across phylogenetic trees is inevitable even in the absence of a recombination event. This is counteracted by reducing the size of the region of the genome aligned for phylogenetic analysis however when sequences are highly related this may still result in false positives.

The difficulty in detecting recombinants from historical sequence data has been described, however another limitation of recombination analysis is that a SWA only detects heterologous recombinants. Homologous recombinants, which may be more common in RNA viruses, are more challenging to detect; the detection of homologous recombinants would suggest that recombination is not as rare an event as currently thought.

These results support data obtained from other studies investigating recombination amongst flaviviruses and JEV (Carney et al., 2012); Han et al. (2014); (Taucher, Berger, & Mandl, 2010; Twiddy & Holmes, 2003). That recombination within the E gene of JEV is possible and has occurred multiple times in the past and likely continues to occur in the present day. However, the rate of recombination is low and likely does not present a significant risk to current vaccine strategies. Despite this, continued study and monitoring of virus populations is recommended as the possibility of a rare recombinant with the divergent GV could result in a virus which may escape current vaccine protection.

Only E gene sequences were analysed; a repeat experiment screening the whole genome of JEV sequences may detect additional recombinants. As discussed earlier, a wider analysis of the JEV genome would be of limited use for the aims of this project, namely, assessing genetic variation on the impact of vaccine since protection against JEV is mediated largely by a robust neutralising antibody response that targets the envelope protein of the virus.

Worth noting also is that these methods cannot determine when a potential recombination event occurred only that a virus is the result of such an event. This limits the scope of the conclusions which can be drawn. How stable is such a recombinant? Was a recombinant the result of one rare event in the past or are

recombination events occurring in certain regions under certain conditions? Future experiments will hopefully address these and other questions.

Future work in this area could also investigate the differences within genotypes of JEV. Recent studies investigating Dengue have highlighted that intergenotypic differences can have a significant effect on the potency of neutralising antibodies. If this is true for JEV also, it would be a crucial area of study for vaccine mediated immunity (Brien et al., 2010; Gallichotte et al., 2018; Wahala et al., 2010).

3.6 Conclusion

Analysis of sequences in this work corroborate the well documented genotype shift that has happened in many endemic countries. Phylogenetic analysis performed in this chapter detected four putative recombinants representing isolates from disparate geographic locations and time periods. Recombination amongst other flaviviruses including JEV has been observed previously however, this work represents the largest targeted analysis of the E gene for evidence of recombination to date using publicly available sequences.

Given the low number of putative recombinants detected in relation to the sample size and the level of uncertainty whether these are genuine recombination events, it is unlikely that recombination between live viral vaccines and wild type JEV may result in reversion of attenuation. Furthermore, the risk of a recombination event between genotypes I–IV and genotype V presenting a risk to current vaccination efforts is likely to be minimal.

4 Production of Japanese Encephalitis Virus Pseudotypes

4.1 Aims

The aim of the work presented in this chapter was to generate JEV E pseudotyped virus to perform neutralisation tests with; this was attempted through several different lines of inquiry.

1. Determine whether JEV pseudotypes with sufficient titre could be generated using existing methodologies.

2. Determine whether the addition of Nef enabled JEV pseudotypes with sufficient titre to be generated.

3. Use the published DENV replicon system to generate JEV E pseudotypes.

4.2 Introduction

4.2.1 Pseudotypes

As discussed previously in 1.12, pseudotype viruses are replication-deficient chimeric viruses comprising the core of one virus and the envelope protein(s) of another. Pseudotype viruses are a valuable tool in order to study highly pathogenic viruses such as JEV where expensive biocontainment facilities are required to manipulate the wild-type virus.

4.2.2 Flavivirus pseudotypes

Despite their impact on human health and the breadth of research performed to improve treatments and diagnostic tests for them, flaviviruses remain an elusive target to pseudotype. Several accounts exist in literature which claim to have generated flavivirus pseudotypes, including yellow fever virus (Mercier-Delarue et al., 2017), Zika virus (Kretschmer et al., 2020) and JEV (Lee et al., 2009; Lee et al., 2014; Tani et al., 2010). However, these results are often poorly referenced citing chains of previous work with few specific details, and as a result many have not been replicated outside of the original group. Indeed, the lack of commercially available diagnostic assays utilising flavivirus pseudotypes supports the conclusion that these

results are difficult to replicate at scale and that the *Flaviviridae* remain a challenging family of viruses to pseudotype (Ruiz-Jimenez et al., 2021).

Several reasons have been proposed to explain this:

1) The absence of an interaction mechanism in the pseudotype system being used that is present in the wild-type virus and is crucial for virion assembly and maturation. For example, there is evidence of an interaction between the trans-membrane domains of the E protein and the viral capsid being necessary to form mature virions in flaviviruses (Blazevic, Rouha, Bradt, Heinz, & Stiasny, 2016). The research performed by Blazevic et al. (2016) involved replacing the double-membrane anchor of TBE with that of JEV. This resulted in a larger proportion of capsid-only subviral particles secreted from infected cells. This is in addition to the known role the E protein TMDs play in virion maturation triggered by the acidic pH environment of the Golgi body.
2) The assembly of capsid and protein is a result of random interaction and existing methods have been unable to produce quantities of envelope protein sufficient to interact with the capsid. In theory this can be resolved by increasing the amount of E produced in transfected cells. This has been tested by numerous groups via the incorporation of stronger promoters, high-copy number plasmids and cell lines engineered to produce large quantities of recombinant proteins and has yet to yield any significant increase to pseudotype titres. Increasing the ratio of envelope-coding plasmid in transfection had a very limited effect on downstream pseudotype production in work performed by Ruiz-Jimenez et al. (2021), suggesting that whilst there may be some merit to this argument, this is not the sole reason for failure to produce flavivirus pseudotypes.
3) Differences in intracellular location between the heterologous capsid and envelope result in unfavourable conditions for virion assembly as a result of the differing replication cycles between the original capsid virus and the envelope virus. Flaviviruses bud from the ER, as opposed to the three most common capsids (HIV, MLV, VSV) used for pseudotyping which bud from the cell membrane. The endosomal sorting complexes required for transport (ESCRT) are crucial intracellular organelles which perform membrane remodelling, specifically scission during mitosis, vesicle formation and

exogenous protein transport. The last of these is often coopted by viruses to enable them to bud from their host cell, enveloping themselves in host membrane. In terms of the application of the pathway to the production of pseudotype viruses, it is this system which many believe is the primary reason for the difficulty in generating pseudotype flaviviruses with lentiviral and rhabdoviral systems (Schmidt & Teis, 2012). This theory is the most widely accepted and has received the largest share of research attention in efforts to produce flavivirus pseudotypes. In order to better align the localisation of the pseudotype components within the producer cell, recombinant envelope(s) containing cleavable signal peptides designed to transport the E protein to the plasma membrane have been introduced leading to a higher titre of pseudotype virus (Liu et al., 2017) Unfortunately these studies did not include neutralisation of any produced pseudotype therefore their functional usefulness cannot be assessed. Other methods designed to bring the heterologous capsid and envelope together include mixing envelope and capsid outside of cell culture (Tijani et al., 2018) and adding the C-terminal tail of the heterologous capsid to the E protein resulting in some limited success.

4.2.3 Existing pseudotyping methods

Since the widespread adoption of pseudotyping as a technique, a variety of viral capsids have been found to be broadly compatible with various protein envelopes from a range of virus families. The most widely used of these are the HIV, MLV and rVSV capsids and are referred to as “cores”. These cores and the methods associated with their use are referred to as “pseudotype systems”. Several groups have published work claiming to have utilised one or more of these systems to successfully pseudotype JEV (de Wispelaere, Ricklin, et al., 2015; Lee et al., 2009), however, these results have often failed to be replicated outside of the original lab or group. A comprehensive comparison of these capsids has not been performed in the same body of work, therefore in this chapter I initially evaluated the capacity of these three common cores to pseudotype JEV envelope protein to better understand why they fail to produce JEV pseudotypes and gain insight into modifications that could be made to increase the likelihood of success.

There are benefits to using existing pseudotyping methods when attempting to pseudotype a new or challenging virus as opposed to attempting to develop a new

core system. Protocols and reagents have undergone several iterations to optimise the specific conditions required to successfully pseudotype a heterologous capsid and envelope together. As well as the numerous ways it is possible to alter the transfection procedure and variables surrounding cell culture (choice of cell line, growth media, number of days before harvest, *etc*). Optimisation of pseudotyping processes can be broadly categorised into those which alter the capsid and those which introduce changes into the envelope protein.

The commonly used capsids in pseudotyping have been optimised over decades of work by multiple groups, therefore the capacity to introduce changes to this component of the system is limited. However, some attempts have been made to alter this part of the process as it would result in the fewest changes to the envelope protein maintaining close to wild-type function.

4.2.4 HIV nef

A recently discovered function of the HIV accessory protein Nef was that it is involved with the cytoplasmic delivery of the HIV genome (Yoshiko Usami, Wu, and Göttlinger (2015). When applied to the production of pseudotype viruses it was theorised that the inclusion of *nef* in the transfer plasmid would improve the binding and entry of an associated envelope protein to the target cell line. Y. Usami, Wu, and Gottlinger (2015) concluded that Nef increased the infectivity of HIV virions by preventing transmembrane protein binding therefore allowing more virions to enter the cell in a clathrin-dependent manner.

Kretschmer et al. (2020) designed a retrovirus based Zika virus pseudotype for the specific targeting of glioblastoma cells in order to deliver chemotherapy drugs to treat glioblastoma. The group attempted this by utilising two retroviral packaging plasmids, psPAX2, which is deficient in *nef*, and pNL Luc AM, which is *nef*+. Luciferase activity from pseudotypes packaged using psPAX2 was several orders of magnitude lower than those packaged using pNL Luc AM. Based on this insight, it was theorised that the addition of *nef* to a retrovirus based pseudotype system may increase the infectivity of any resulting virus.

4.2.5 Dengue replicon

A promising solution was proposed in the efforts to pseudotype flaviviruses with work published by(Matsuda et al., 2018). The group successfully pseudotyped the PrME proteins of DENV 1–4, JEV, WNV, YFV and TBEV using heterologous flavivirus capsids. This method utilises a replicon plasmid containing the entire genome of DENV1 minus PrME and the capsid, which are provided on two separate plasmids. As a result, the intracellular processing of the envelope protein and capsid are almost identical as they share a common family lineage. This appeared to be a very successful and scalable technique to rapidly produce flavivirus pseudotypes.

The DENV replicon is based on an earlier methodology which the group used to create a JEV replicon (Suzuki et al., 2014) as a proof of concept. To generate the non-structural gene replicon, the genome from the Nakayama strain was first extracted and reverse transcribed to generate cDNA and then amplified into dsDNA where a T7 RNA promoter and Hepatitis D virus ribozyme (to cleave the translated RNA) was added to the 5′ and 3′ ends of the linearised dsDNA. To excise the structural genes from the genome, *Bsp*T1 restriction sites were added between nucleotides 17 and 18 within the capsid coding region and before the terminal transmembrane domain 90 nucleotides within the envelope coding gene which resulted in 5 aa capsid and 30 aa envelope remnants once the fragments were ligated. To reduce sequence homology between these short fragments and the full-length capsid and envelope which would be present on other plasmids during transfection, 21 distinct nucleotide mutations were introduced which included changes to conserved cyclization sequences critical for successful replication (Khromykh et al., 2001).

In the same way the three-plasmid system has increased the safety of pseudotyping with HIV cores, this method allows the dengue replicon plasmid and associated flavivirus envelope-only plasmid to be manipulated at CL 1 with no risk of homologous recombination of the plasmids.

4.3 Methods

4.3.1 Representative sequences

Reference sequences were chosen to represent genotypes I, III and V based on the criteria of:

- Sequencing accuracy and confidence in published data
- Prevalence in the literature and other studies
- Chronologically recent isolates

Genotypes II and IV were not produced due to their similarity to genotypes I and III and low prevalence.

Table 4.1. JEV reference strains for each corresponding genotype

Genotype	Strain name	Accession number	Year sequenced
I	Ishikawa	AB051292	2001
III	Nakayama	EF571853	2007
V	XZ0934	JF915894	2011

Reference sequences used to pseudotype JEV genotypes I, III and V acquired from GenBank. These sequences would be used to generate the pseudotype virus in later experiments. GI-Ishikawa was selected as it is the most commonly isolated example of its type, GIII-Nakayama is the basis of the inactivated BIKEN vaccine whose efficacy will be investigated in later chapters and GV-XZ0934 is the most recent example of genotype 5 isolated.

DNA fragments coding for the prM and E genes of a representative sequence for the JEV genotypes I, III and V were downloaded from GenBank (NCBI) and synthesised by GeneWiz (Takeley, UK). The DNA fragments were delivered lyophilised and subsequently reconstituted with nuclease-free, sterile water to a final concentration of 100 ng/µl.

Restriction sites coding for the enzymes *Eco*RI and *Xho*I were incorporated to the 5′ and 3′ multiple cloning sites using overlap extension PCR within the pCAGGS transfer plasmid (2.2.1)

These were subcloned into a pCAGGS plasmid vector using the same restriction sites (Figure 4.1) An analytical digest was performed using unique restriction sites for each insert to confirm that the insert had been successfully cloned into the vector.

4.3.2 Plasmids

Expression plasmids pCAGGS (Figure 4.1), pCFCR (Figure 4.2) and pCMVi (Figure 4.3) were kindly provided by colleagues within the MHRA as well as the JEV-E protein-containing plasmid pCAGGS-Vacstrain JEVM_E (SA14-14-2).

Plasmids for the dengue replicon pseudotyping system (Figure 4.4 and Figure 4.5) were kindly provided by Professor Suzuki (National Institute of Infectious Diseases, Tokyo, Japan).

The plasmid pSCNef1 was sourced from the Centre for AIDS Reagents (CFAR) at NIBSC alternative to the plasmid pNL Luc AM is a *nef*+ expression plasmid with the nef gene controlled by a metallothionine promoter. Through the addition of metal chlorides to the cell culture, *nef* can be transiently expressed.

The JE envelope gene utilised in the lentiviral pseudotype experiments was cloned from the attenuated vaccine strain SA14-14-2 into the pCAGGs vector. This is a high copy number plasmid which also contains an ampicillin resistance gene for selection. Upstream of the envelope gene is a CAG promoter which consists of the cytomegalovirus enhancer and a chicken beta-actin promoter (A). This promoter causes high levels of expression within mammalian cells. Immediately downstream of the envelope gene is a rabbit beta-globin poly adenylation signal to ensure proper mRNA capping. The origin of replication is SV40 from the simian virus 40. This origin enables plasmid replication in any cells which possess the SV40 antigen which includes many mammalian cell lines and can therefore be used to generate stable cell lines.

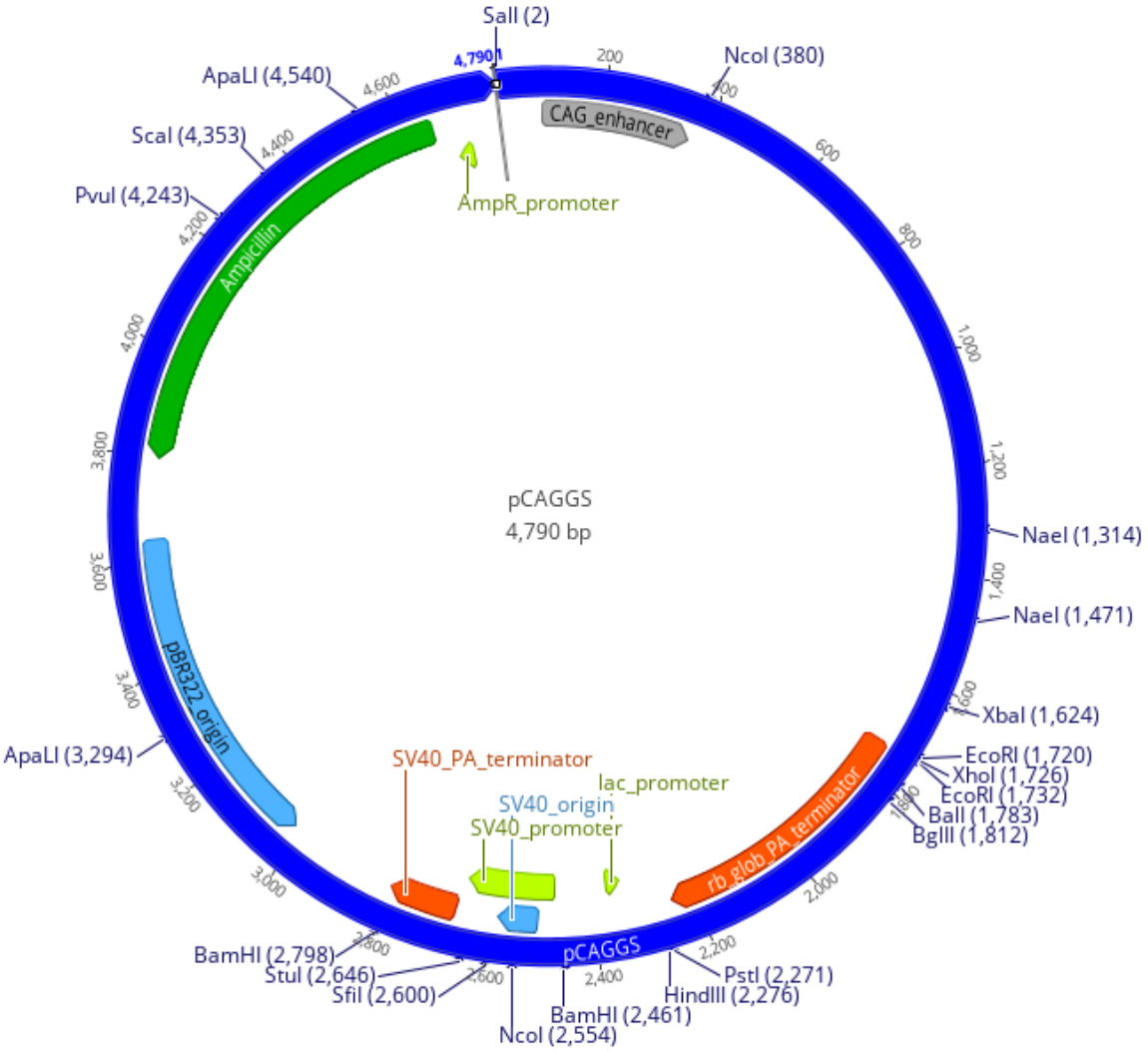

Figure 4.1. Full-length plasmid map for pCAGGS transfer vector (accession number LT727518.5) highlighting the multiple cloning sites used for inserting of genes of interest and ampicillin resistance gene.

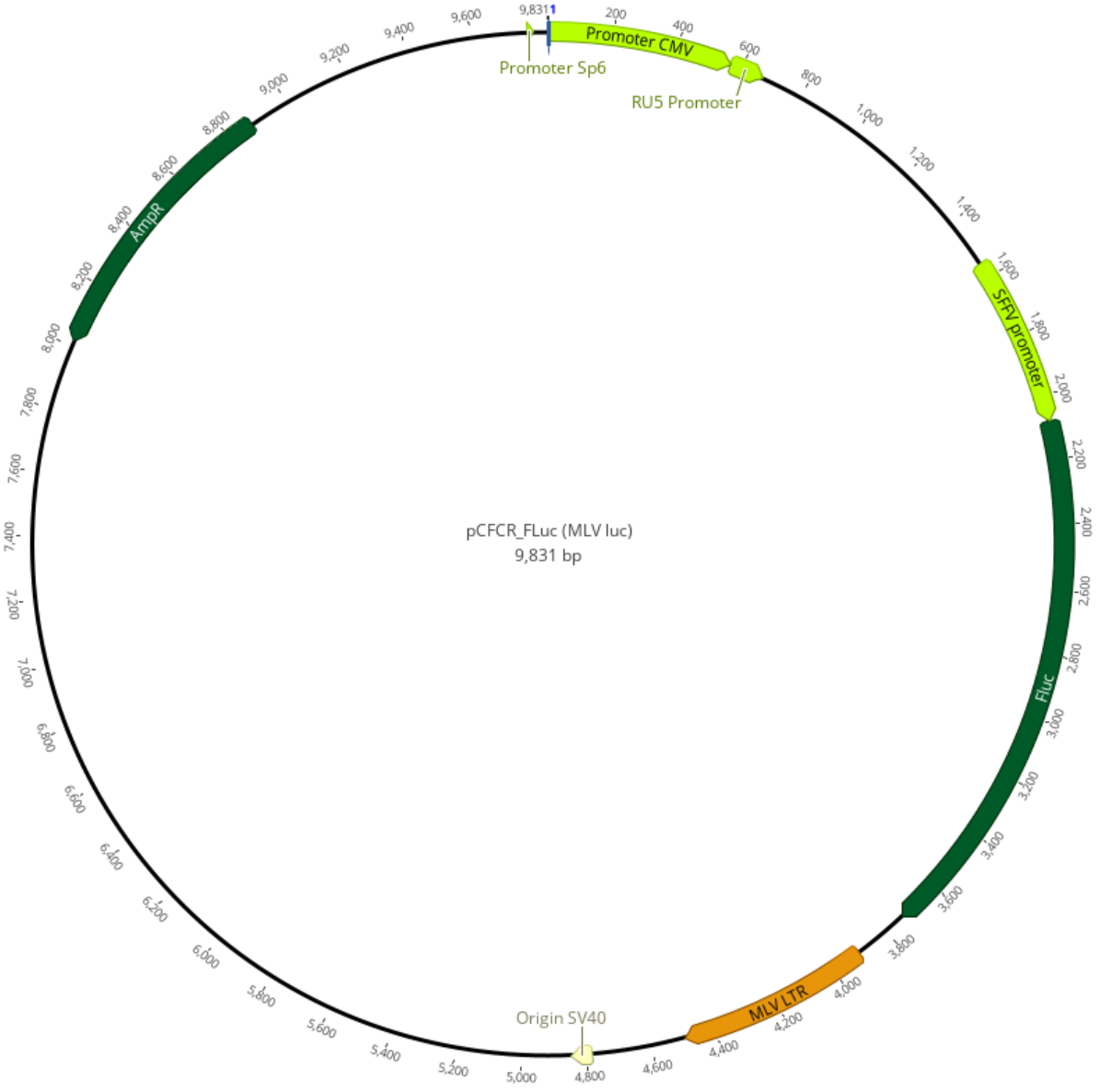

Figure 4.2. Full-length plasmid map for pCFCR, MLV reporter with ampicillin resistance gene, MLV LTR and luminescent reporter gene to determine correct assembly of MLV pseudotype virus.

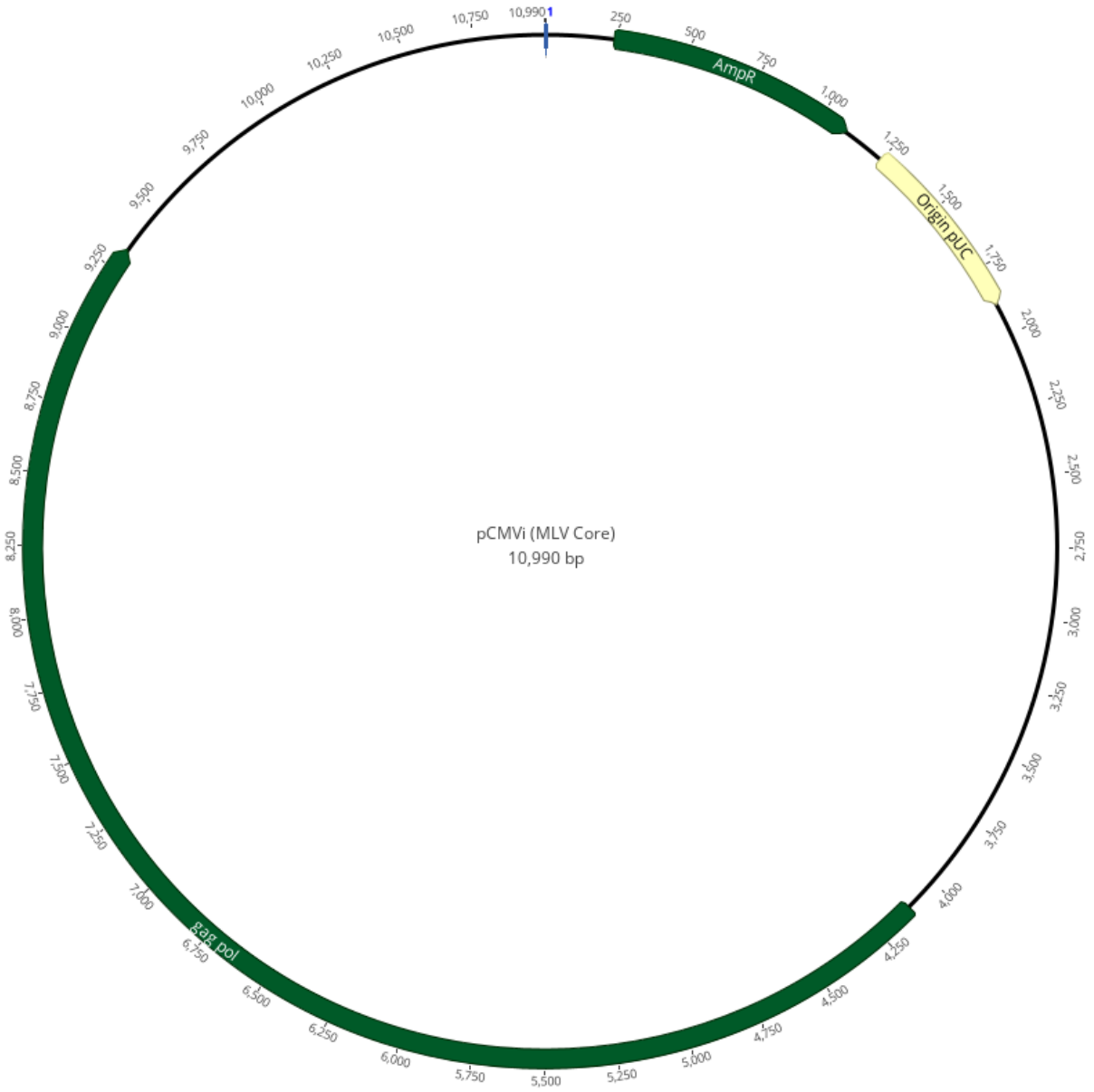

Figure 4.3. Full-length plasmid map for pCMVi (MLV core) containing gag-pol of MLV and an ampicillin resistance gene.

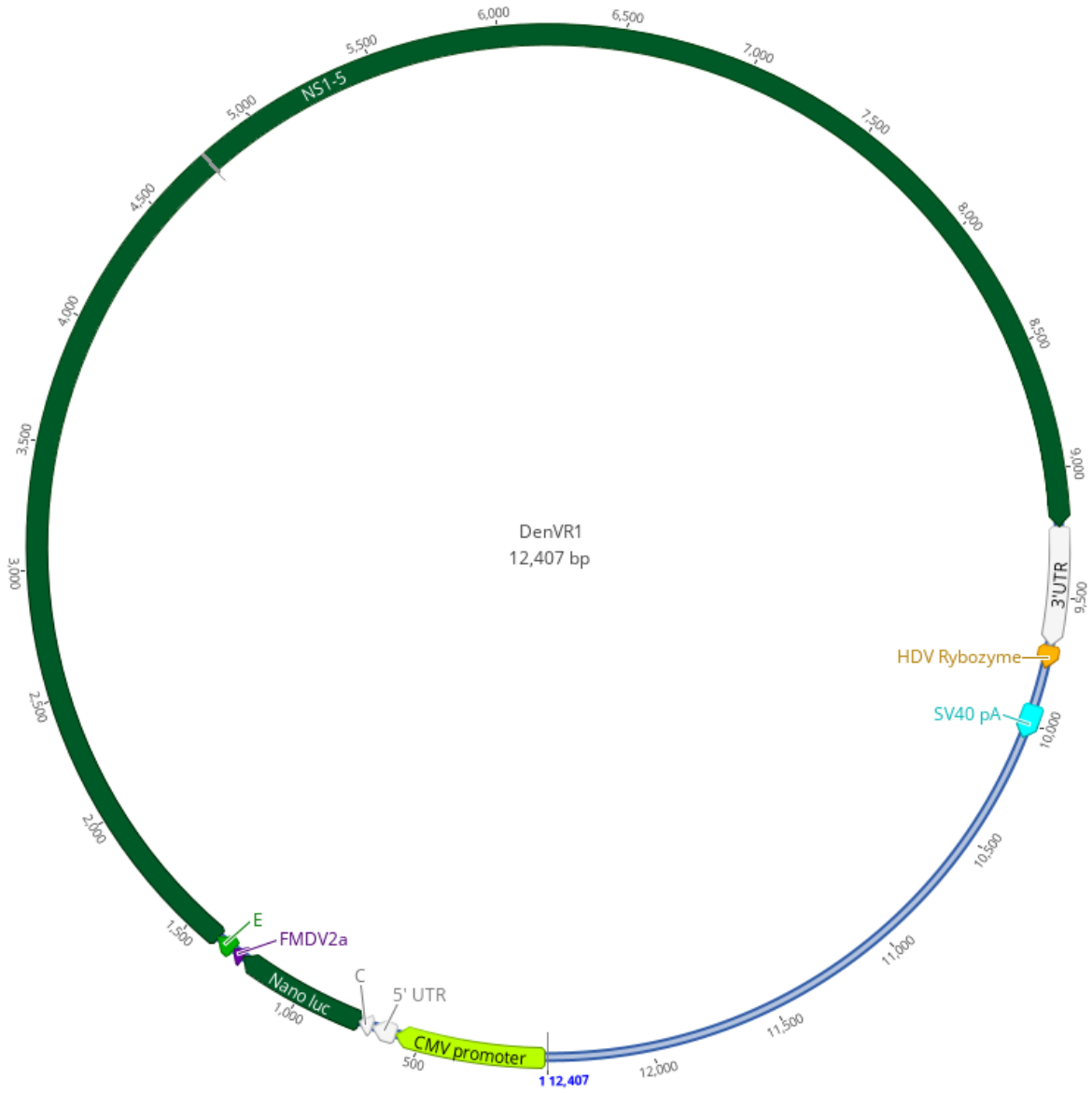

Figure 4.4. Full-length plasmid map for dengue replicon plasmid (DENVR1) containing the non-structural genes of dengue virus 1 as well as a reporter gene encoding for nano-luciferase.

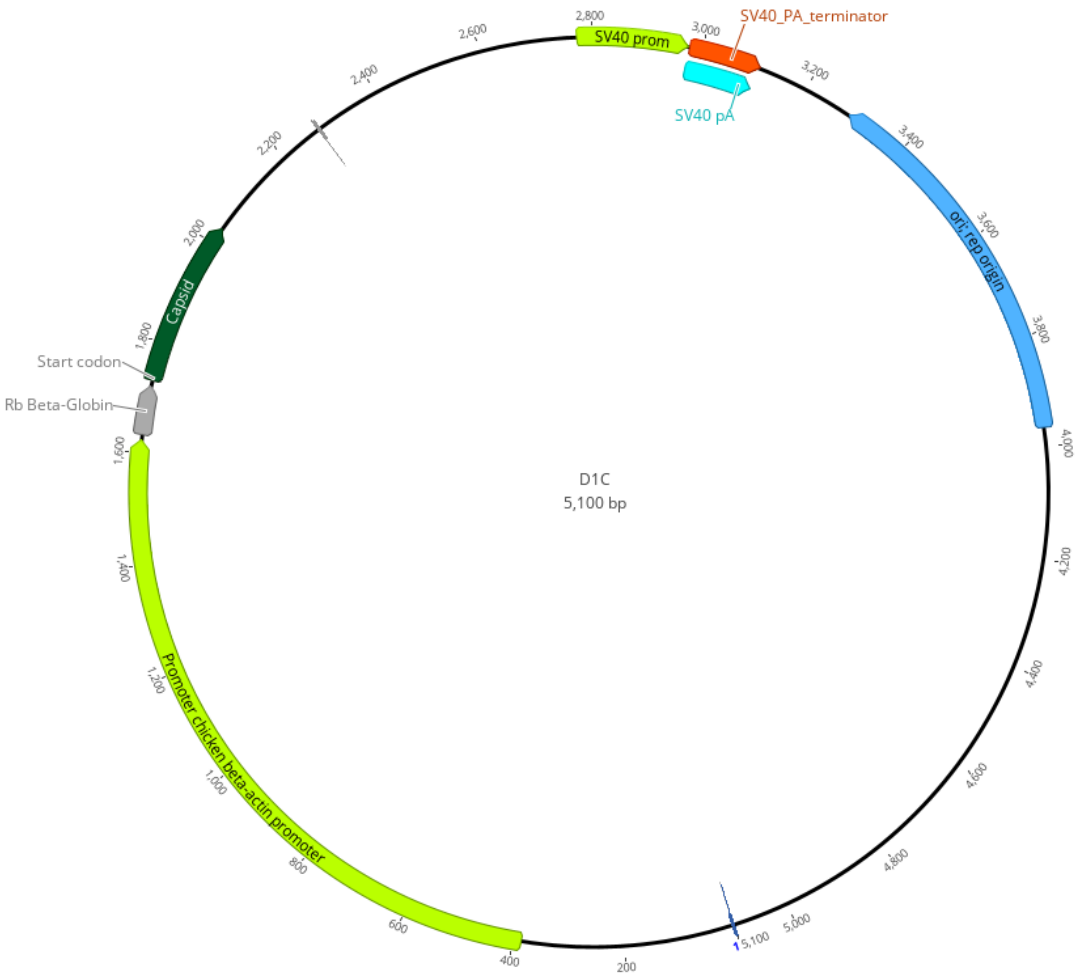

Figure 4.5. Full-length plasmid map of D1C containing structural genes, minus PrME, of dengue virus 1.

Note All plasmid maps were generated using Geneious software (version 11.7).

pSCNef1 was originally made by cloning the nef gene into the MCS within pcDNA3 between the *Bam*HI and *Apa*I restriction sites. A plasmid map is not available (Cooke et al., 1997).

4.3.3 Pseudotyping methods

4.3.3.1 Retroviral and lentiviral capsids

Both the HIV and MLV pseudotype systems were produced in HEK293T cells via Fugene-6 transfection. This was performed by seeding $4x10^6$ HEK293T cells onto a 10 cm Nunc™ (Thermo Fisher, UK) cell-culture dish and allowing to become confluent overnight at 37˚C, 5% CO_2. The next day in a sterile 1.5ml Eppendorf tube; 1 µg envelope plasmid, 1 µg gag-pol plasmid and 1.5 ug reporter gene plasmid were combined. This was then made up to a final volume of 15 µl with sterile TE buffer. In a separate tube, 100 µl OptiMEM and 6 µl of Fugene-6 (this was removed from the fridge as late as possible to reduce degradation of transfection reagent at RT) were added. The plasmid mixture was added to the OptiMEM-Fugene mixture (not the other way around) and mixed by gently flicking the microfuge tube followed by a 30 second centrifugation in a tabletop centrifuge at 9000rpm. This was then incubated for 15 minutes at RT. During this time, the media on the HEK293T cells was replaced to remove any dead cells or floating debris to ensure a more efficient transfection (dead cells may take up plasmid reducing the amount available to live cells). After 15 minutes had elapsed, the plasmid-OptiMEM-Fugene mixture was added slowly, dropwise onto the cell monolayer and mixed by rocking the plate gently back and forth then front to back. The lid was placed on the dish was placed in an incubator for 48 hours at 37˚C, 5% CO_2. After 48 hours, the cell supernatant was collected and passed through a 0.45µm filter. The filtered supernatant was stored at +4˚C until use.

4.3.3.2 rVSV

The rVSV pseudotyping method required $1x10^6$ HEK-293T cells to be seeded on a 10 cm Nunc™ (Thermo Fisher, UK) cell-culture dish and left to become confluent overnight at 37˚C, 5% CO_2. The next day, two 1.5ml Eppendorf tubes, one containing 200 µl OMEM + 60 µl/ 1mg/ml PEI transfection reagent were prepared. In the other tube 200 µl OMEM + 12 µg of plasmid containing the desired envelope

were added. The transfection mixture was added to the DNA mixture and mixed by gently flicking then incubated at RT for 20 minutes. During this incubation the spent media on the cell monolayer was replaced with 8 ml M10. After the incubation was complete the mixture was added dropwise directly onto the cell monolayer, rocked gently side-to side, and incubated overnight at 37˚C, 5% CO_2. The next day a mixture of 5 ml M10 + 0.5 MOI (multiplicity of Infection) of amplified rVSV stocks was prepared ($6x10^6$ cells/plate requires $3x10^6$ IU of rVSV to equate 0.5 MOI). Once prepared, the media was removed from the cells and the M10-rVSV mixture was added and then incubated at 37˚C, 5% CO_2 for 1 hour. After incubation, the media was removed and cells gently washed with 3 ml, sterile 1x PBS taking care not to dislodge any cells from the plate. After washing, 8 ml M10 were added and the cells were incubated at 37˚C, 5% CO_2 overnight. The next day the cell supernatant was collected and passed through a 0.45 µm filter. The filtered supernatant was stored at +4˚C until use.

4.3.3.3 Dengue replicon system

When utilising DenVR1/ D1C to pseudotype; $4x10^6$ HEK-293T cells were plated onto a 10 cm Nunc™ (Thermo Fisher, UK) cell-culture dish and left to grow overnight at 37˚C, 5% CO_2. The next day 2.5 µg DENVR1, 1.25 µg D1C and 1.25 µg PrME plasmid were combined in an Eppendorf tube and 1ml of OptiMEM was added to each plasmid mixture followed by 25 µl (1 mg/ml) PEI and left at room temperature for 15 minutes.

Meanwhile, spent media on the cells was replaced to remove any dead, floating cells which may reduce the transfection efficiency. After 15 minutes, the plasmid/OptiMEM/PEI mixture was added slowly, dropwise directly onto the cell monolayer. The mixture was mixed into the media by gentle hand-rocking and then incubated at 37˚C, 5% CO_2 for 5–6 hours and then the media was replaced with 10 ml M10 and incubated for 2 days. After 2 days post-transfection replace media with 13 ml M10 +10 mM HEPES buffer. Three days post-transfection the supernatant was collected and filtered through a 0.2 µm filter into a 15 ml falcon tube. The filtered supernatant was stored at +4˚C until use.

4.3.4 Nef

As discussed in section 4.2.4, the addition of a plasmid containing *nef* resulted in increased infectivity of a Zika virus pseudotype. Unfortunately, the first generation pNL Luc AM plasmid was not able to be used at NIBSC due to safety concerns involving the risk of recombination with the HIV core plasmid which may result in infectious HIV being produced. Therefore, an alternative source of *nef* was found utilising the Centre for AIDS Reagents (CFAR) repository based at NIBSC. The plasmid pSCNef51 contains *nef* under the control of a metallothionine promoter. The plasmid provides low level expression of *nef* that can be enhanced by exposure of transfected cells to micromolar concentrations of metal chloride.

Zinc chloride ($ZnCl_2$) was used to activate the metallothionine promoter present in pSCNef51 due to its availability, cost and improved safety profile when compared to other metal chlorides such as caesium or lithium.

In order to determine the concentration of $ZnCl_2$ to sufficiently activate the *nef* gene, three different Zinc Chloride concentrations were tested. $ZnCl_2$ diluted in M10 was added at 0, 12.5 and 50 µM 2 days p.t onto a JE-PV transfection. The JEV PV was then harvested and titrated.

4.3.5 Experimental controls

Each pseudotyping system utilises a specific control envelope. These are envelopes which are known to pseudotype readily onto the corresponding core system. For HIV and MVL this is the VSV envelope. When rVSV is used to pseudotype, the rabies viral envelope is used as a control. The DenVR1 core system does not have another envelope which it can readily pseudotype, confirmation of JEV-PV is performed using a specific monoclonal anti-JEV-E antibody in a western blot or neutralisation assay.

All pseudotype systems tested in this thesis also required the use of a suitable negative control. The purpose of this is to measure the background entry of envelope-free (sometimes called “bald”, or “naked”) particles into the reporter cell line. This occurs at a low level for all pseudotypes. This negative control was unique to each pseudotype system but is based on a shared principle. The capsid of each pseudotype was transfected along with a reporter gene into a producer cell line and the resulting supernatant was collected. The product(s) of this transfection would be

envelope-free particles containing a reporter gene. In this way it was possible to establish a baseline of cell entry which all pseudotypes must reasonably exceed (arbitrarily decided as several log) in order to be considered successful and functional.

4.3.6 Quantifying PV titre

PV titrations were performed on a confluent cell layer of $1x10^4$ Vero cells seeded in clear Nunc™ 96-well plates the day prior. Dilutions were prepared in a 2 ml, 96-deep well plate to generate a volume sufficient for triplicate dilutions with minimal manipulation, reducing the error of performing multiple dilutions.

Dilutions of neat, 1:10 and doubling dilutions to 2560 were prepared by adding 400 µl neat PV to the first well, 585 µl M0 to the second well and 325 µl M0 to the subsequent 8 wells. Then, 65 µl of neat PV was taken from the first well into the second, mixed thoroughly by pipetting up and down and then a 325 µl serial dilution was performed for all subsequent wells to achieve the final dilution series.

Once complete, 100 µl of each dilution were added to the respective well(s) of the titration plate and incubated at 37˚C, 5% CO_2 for 4–5 hours before being replaced with fresh M10 and the plate incubated at 37˚C, 5% CO_2 for 3 days.

A cell-only control consisting of a minimum of 3 wells was included on each plate to calculate background RLU.

After 3 days the spent media was removed and replaced with a 1:1 mixture of NanoGlo® buffer: Opti-MEM + 1% NanoGlo® substrate. This was left on the cell monolayer for 3–5 minutes and then transferred to a clean, white-bottomed 96-well plate and read using a luminometer (Promega, GM2000).

Average triplicate RLU values of each dilution were used to determine the TCID50 and then IU/ml of each batch of PV (see section 2.4.1)

4.3.7 Western blot to confirm JE-E protein production in HEK-293T cells.

JE-E protein samples for use in western blot were collected by adding 1 ml lysis buffer (Abcam, UK-ab152163) directly onto the cell monolayer and rocking for 1 minute. The lysed cells were collected and stored at -20˚C until use.

A precast Bis-Tris gel (NuPAGE, ThermoFisher UK) was removed from its packaging, and the white tape at the bottom of the gel was peeled away. The plastic comb protecting the wells was then carefully removed. The gel was placed facing inwards into the electrophoresis tank (Bio-Rad, UK) and was locked into place using the levered support brace. A total of 1 litre of MOPS running buffer (50 ml 20xMOPS + 950ml dH2O) was prepared. To this, 500 µl of antioxidant was added to 200 ml MOPS buffer, and the mixture was poured into the inner compartment of the gel tank.

The samples were then denatured at 70˚C for 10 minutes and were then vortexed for several seconds. A master mix containing LDS buffer (NuPAGE, ThermoFisher UK), reducing agent (NuPAGE, ThermoFisher UK), and PBS (NIBSC) was prepared. Fifteen microliters of the master mix were added to 15 µl of each sample in a clean Eppendorf tube, and the mixture was thoroughly mixed by pipetting. The mixed samples were pipetted into the remaining well(s) of a precast SDS-PAGE gel, and the lid was placed on the gel tank.

The samples were electrophoresed through the gel for 50 minutes at 200V. While the gel was running, 1 litre of 1xTGS buffer was prepared from a 10X stock using distilled water. Once the gel run had finished, it was carefully removed from the plastic casing, and the raised edge at the bottom of the gel, as well as the combs at the top, were removed. The gel was then placed carefully in a tray of 1XTGS buffer to keep it wet. One piece of nitrocellulose and two pieces of 3MM paper were cut, large enough to cover the gel, and were wet using TGS buffer and used to assemble the gel transfer stack as shown in Figure 4.6

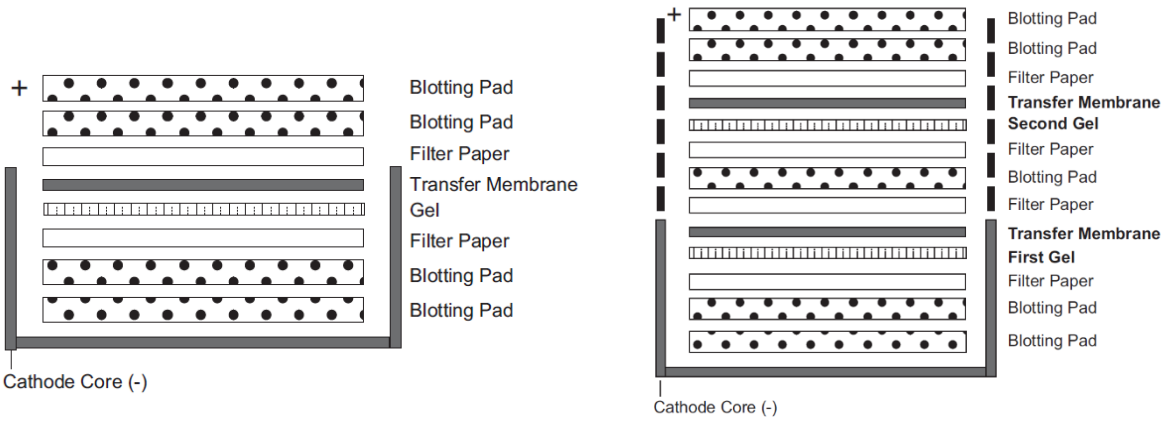

Figure 4.6. Western blot transfer stack assembly

Once assembled, the transfer stack was placed in the transfer chamber, closed, and placed in the gel tank. The inner compartment was filled with 1XTGS buffer, and the outer compartment was filled two-thirds full of 1XTGS buffer. The lid was placed on the gel tank, and the transfer was run at 30V for 1 hour and 15 minutes.

Five percent blocking buffer (100ml PBS-A, 5g milk powder, 200 µl TWEEN-20) was prepared. Once the transfer was complete, the nitrocellulose membrane was removed and placed in the blocking buffer for 1 hour at room temperature, with gentle rocking. To detect the proteins transferred onto the nitrocellulose membrane, the primary antibody was diluted according to the manufacturer's recommendations in blocking buffer and was placed on a rocking shaker for 1 hour at room temperature. The primary antibody solution was poured off, and the membrane was washed three times for 5 minutes each with PBS-A/ 0.5% TWEEN-20. The secondary antibody was diluted according to the manufacturer's recommendations in blocking buffer and was placed on a shaker for 1 hour at room temperature. Meanwhile, the ECL solution was taken out of the fridge and allowed to warm to room temperature. The secondary antibody solution was poured off, and the membrane was washed three times for 5 minutes each with PBS-A/ 0.5% TWEEN-20. The pre-mixed ECL solution was added directly on top of the membrane, and the membrane was incubated in the dark for 5 minutes. The membrane was imaged using the Syngene digital imager to detect the proteins.

4.3.8 Signal peptides

Within an insert coding for the envelope gene for the Nakayama strain of JEV, amino acid positions 801-803 were changed from RDR to ALA. This was achieved by site directed mutagenesis (see section 2.2) using appropriately designed primers.

4.3.9 Flow cytometry

Cells transfected with plasmids expressing JE-E (Nakayama) with modified ER retention signals were harvested after 48 hours then fixed and stained either intracellularly or extracellularly with a mouse, anti-JEV antibody (ab41671; Abcam, Cambridge, UK). Cell fixing and staining was performed using a BD perm/fix kit (BD Biosciences, UK, 554714) using the manufacturer's instructions.

Fixed cells were counted using a BD FACSCanto 2 (BD Biosciences, USA) and data were transformed in FlowJo software (Version 10.6.2). Cells were first gated by live vs dead and then background antibody binding was removed by overlaying a control population of cells which had not been transfected with either of the JEV E plasmids over a population which had been transfected. The remaining population was counted as positively transduced expressors of JEV E protein with either signal peptide.

4.3.10 Electron microscopy

Twenty microlitres of JEV-PV (GIII) produced utilising the dengue replicon pseudotype system were provided to Dr. Maclellan-Gibson who performed the sample preparation and imaging. JE-PV was applied to plasma-cleaned, carbon formvar EM grids for one minute, before two, one-minute washes with 50 µl droplets of dH_2O and then one-minute staining with 2% aqueous uranyl acetate was performed. Excess stain was removed then grids were allowed to airdry. Grids were imaged in a JEM2100 transmission electron microscope using a Gatan ultrascan 4K camera. Images were taken at 50,000 times magnification.

4.4 Results

4.4.1 Cloning JEV envelopes of genotypes I, III and V into transfer vector

Ten Ishikawa envelope gene (GI) purified DNA minipreps were digested with *Cla*I which would result in a 150 bp and 6.5 kb band if the cloning was successful. Samples 1, 4, 6, 9 and 10 presented bands of the predicted sizes indicating the correct insertion of the Ishikawa PrME sequence into the pCAGGS plasmid. The

miniprep with the highest DNA concentration was taken forward for use in GI-PV production.

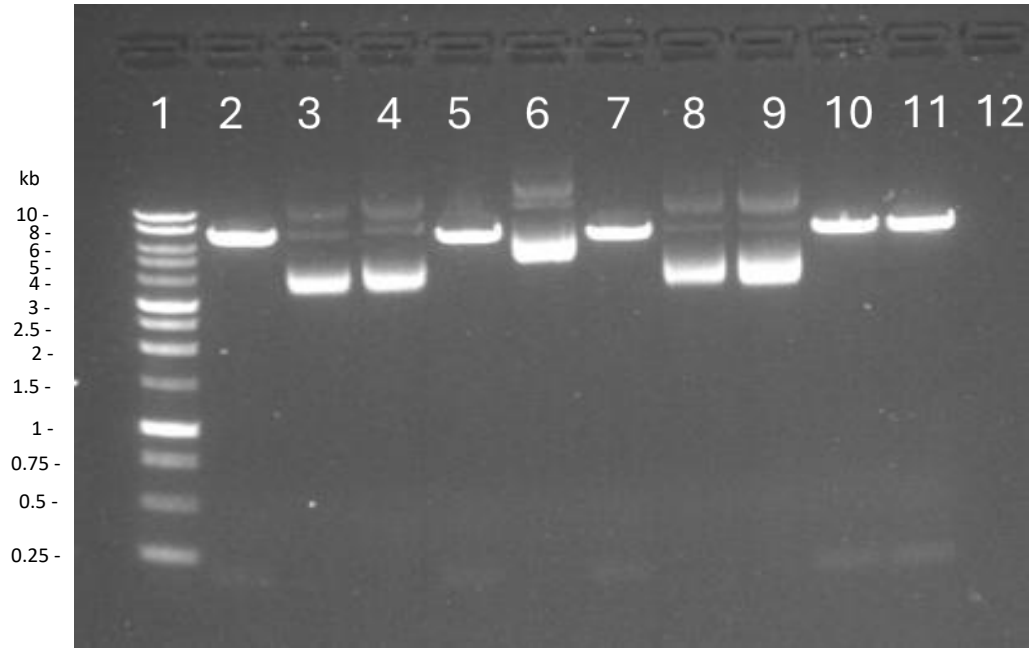

Figure 4.7. Analytical digest of Ishikawa envelope gene minipreps cloned into pCAGGS using ClaI. Lane 1: 1kb ladder (Promega); lanes 2–12: Ishikawa E gene plasmid miniprep samples 1–10.

Seven Nakayama envelope gene (GIII) purified DNA minipreps were digested with *EcoRI* and *Xho*I which according to the plasmid map would result in a of 4.7 and 2 kb band if the cloning was successful. The observed bands for sample 6 correspond with the predicted cut sites.

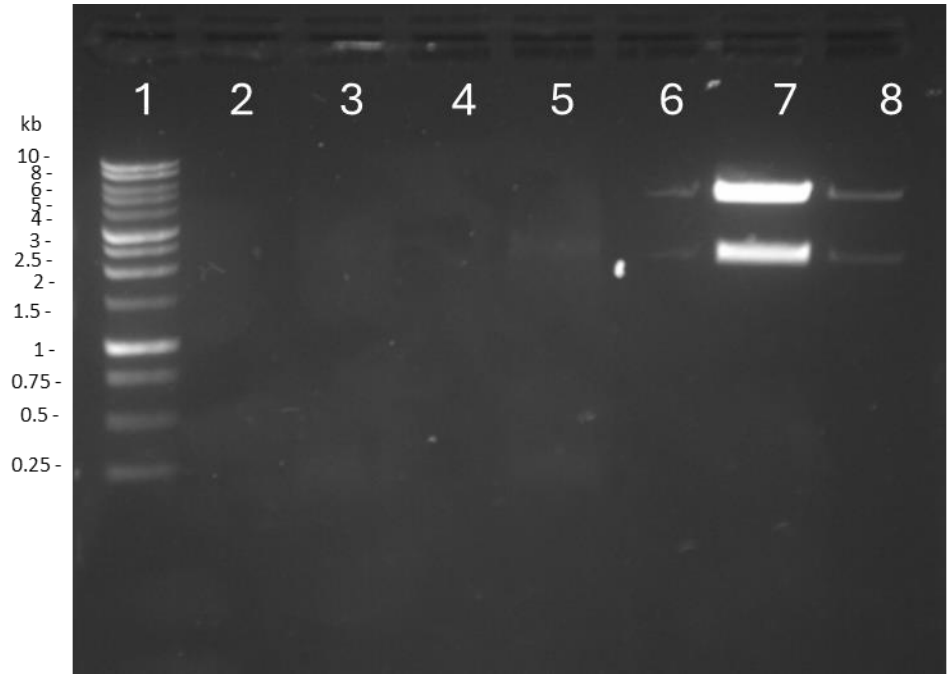

Figure 4.8. Analytical digest of Nakayama strain cloned into pCAGGS using EcoRI and XhoI. Lane 1: 1kb ladder (Promega); lanes 2–8: Nakayama E gene plasmid minipreps 1–8.

Nine XZ0934 envelope gene (GV) purified DNA minipreps were digested with *Cla*I which would result in a 1.5 kb and 6 kb band if the insert was correctly incorporated. Samples 1–7, 9 and 10 presented bands of the predicted sizes indicating the correct insertion of the XZ0934 PrME sequence into the pCAGGS plasmid and were taken forward for use in GV-PV production.

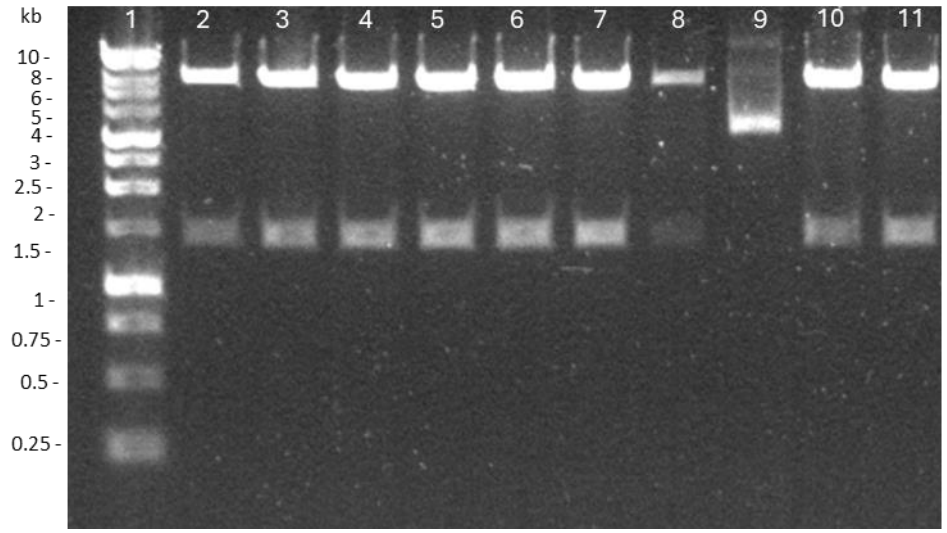

Figure 4.9. Analytical digest of XZ0934 samples cloned into pCAGGS using PvuII and XhoI.

Lane 1: 1kb ladder (Promega); lanes 2–11: XZ0934 E gene plasmid minipreps 1–10.

4.4.2 Traditional pseudotyping systems are unable to produce high titre JE-pseudovirus.

In order to comprehensively assess the potential for existing pseudotyping systems to produce functional JE-PVs, multi-plasmid co-transfections were carried out with three of the most used core systems (HIV, MLV and rVSV) adhering to protocols described in section 4.3.3 utilising JE^{GIII} envelope. If successful, this protocol would be applied to other JEV envelopes. An envelope known to pseudotype well onto each of these cores was included as a positive control in each experiment in order to show that the cores are capable of pseudotyping other heterologous viral envelopes and the issue is with JEV-E specifically rather than the cores. The supernatant from each of these was harvested at 24- (timepoint 1, TP1) and 48- (timepoint 2, TP2)-hours post transfection to determine the optimum time to harvest. The filtered supernatant from each of the three core systems and timepoints was titrated neat–1:3,243 using a 1:3 dilution factor onto BHK-21 and CrFK cells in triplicate to assess the permissiveness of different cell lines to produced JE-PVs. Data was reported in RLU measured on a luminometer. Vero cells were not included in these experiments as there have been several documented previous attempts to pseudotype JEV using these core systems and Vero cells (Mather, 2017; Ruiz-Jimenez et al., 2021). Vero cells are also unsuitable to be used for HIV-capsid based pseudotype systems due to the presence of TRIM5α which restricts retrovirus infection (Lukic & Campbell, 2012).

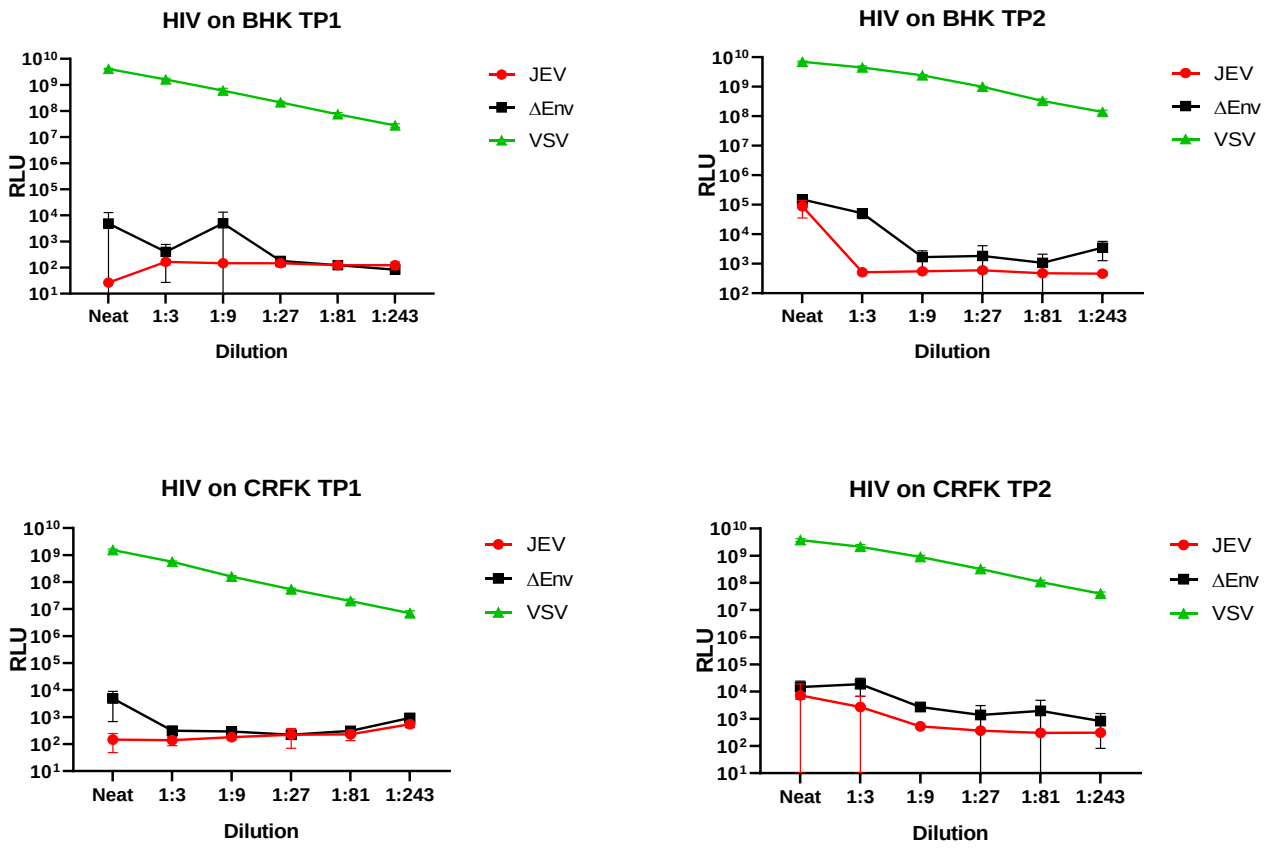

Figure 4.10. HIV-JE PT harvested from BHK and CrFK cells at 24/48hrs p.t.

The HIV core failed to produce viable JE-PVs on BHK and CrFK cells at either time point. Sample harvested from BHK cells 24 hours p.t. resulted in a neat RLU 2-3 log above background ΔE RLU and 2log above background at a 1:9 dilution. Sample harvested at 24 hours p.t from CrFKs also resulted in a neat RLU 2-log above background RLU. No other sample or dilution produced RLU significantly above background RLU. Variability between triplicate data points was large enough for some dilution points to generate error bars greater than the range of results. Other commonly used methodologies including modifying plasmid ratios have been attempted extensively and were not included in this analysis (Mather. 2017).

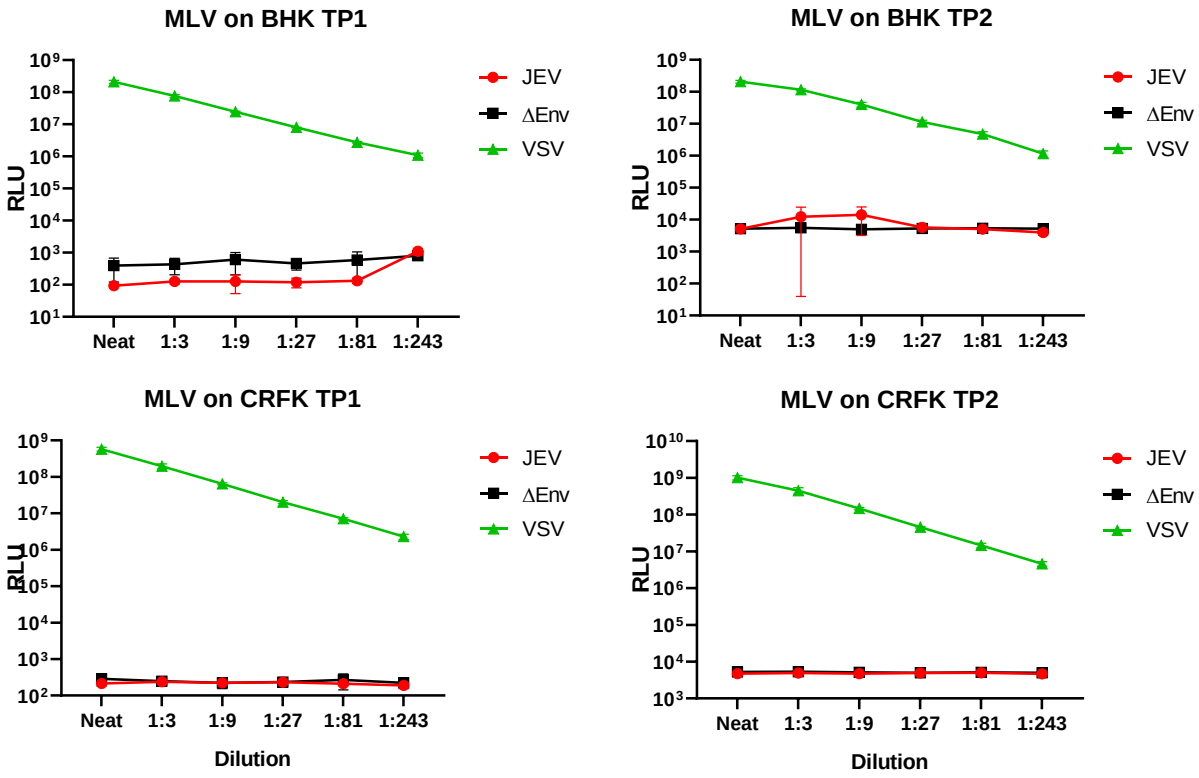

Figure 4.11 JE-PV cannot be produced in BHK or CrFK cells using an MLV capsid at either 24- or 48-hours post transfection

The MLV core failed to produce any JE-PV higher than background levels at either time-point. Background ΔEnv samples correlated almost exactly with transfections where JE-E protein was added. ΔEnv was approximately 1-log higher in both cell lines transduced 48 hours p.t VSV control PV was produced at high titre and able to transduce both BHK and CRFK cells equally.

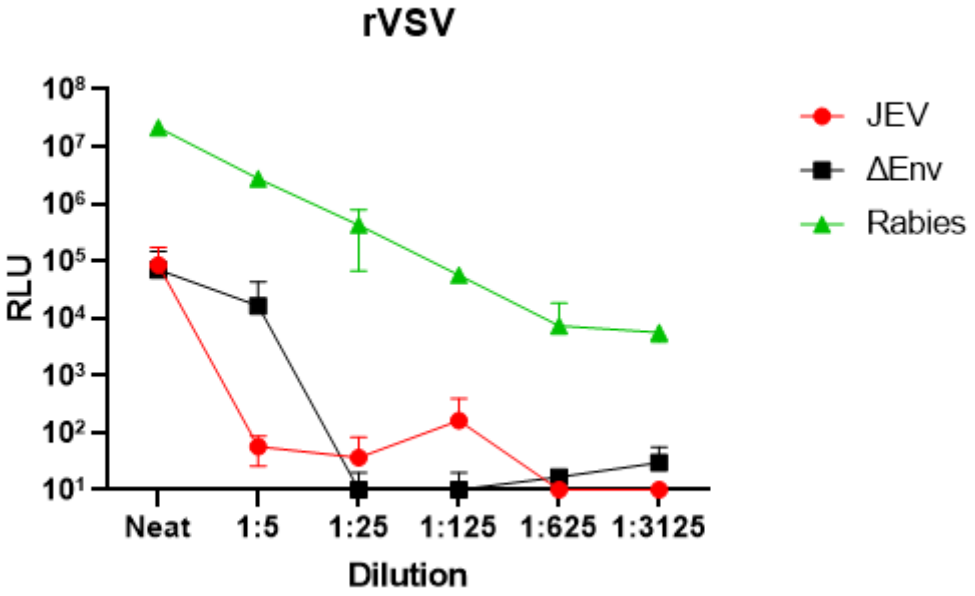

Figure 4.12 rVSV-JE produced in BHK cells and titrated on HEKs do not produce viable pseudotype particles significantly above background ΔE RLU levels.

An envelope free negative control produced a luminescence which was equivalent to the signal produced by the JE-E transfected sample. At a 1:5 dilution the ΔE sample emitted an approximately 3-log higher luminescence than the JE sample, however in all subsequent dilutions the JEV samples were less than or within half a log of the ΔE control. Recombinant VSV pseudotyped with rabies envelope produced a high luminescent signal which titrated in a linear fashion as the dilution increased, up until 1:625 where the signal began to plateau.

4.4.3 HIV Nef does not affect integration of HIV capsid with JE prME.

Some constitutive expression of *nef* occurs in the absence of $ZnCl_2$ (Figure 4.13). This low-level expression appeared to slightly increase the amount of JE-PV produced. Unfortunately, this was not to a useful titre. The amount produced was at maximum, 2-log above the background luminescence as determined by the envelope-free control and reduced to background levels within a single 1:10 dilution. Both other concentrations of $ZnCl_2$ used produced noticeable cytotoxic effects to the HEK producer cells and did not result in an RLU greater than background.

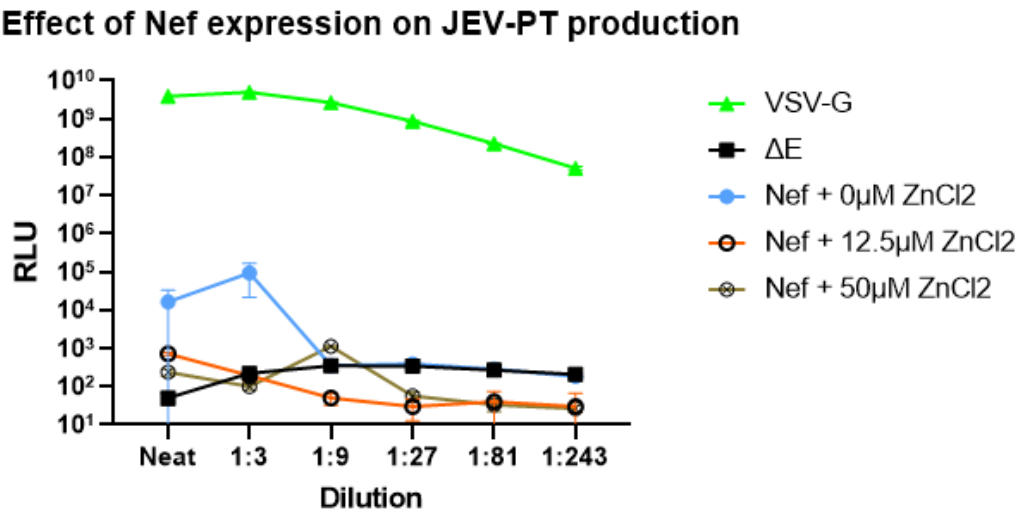

Figure 4.13 Effect of NEF on JEV PV production in HEK293T cells

4.4.4 Signal peptides fail to release a significant amount of JEV-E to the cell surface.

Two signal peptide mutations were generated in order to test the hypothesis that JE-E was being manufactured in the producer cell line and that a strong ER-retention signal peptide located within several of the trans-membrane domains of the envelope protein were preventing assembly of the complete PV particle. The changes were introduced within these trans membrane domains in order to disrupt their function, theoretically reducing retention of the PrME complex within the ER lumen.

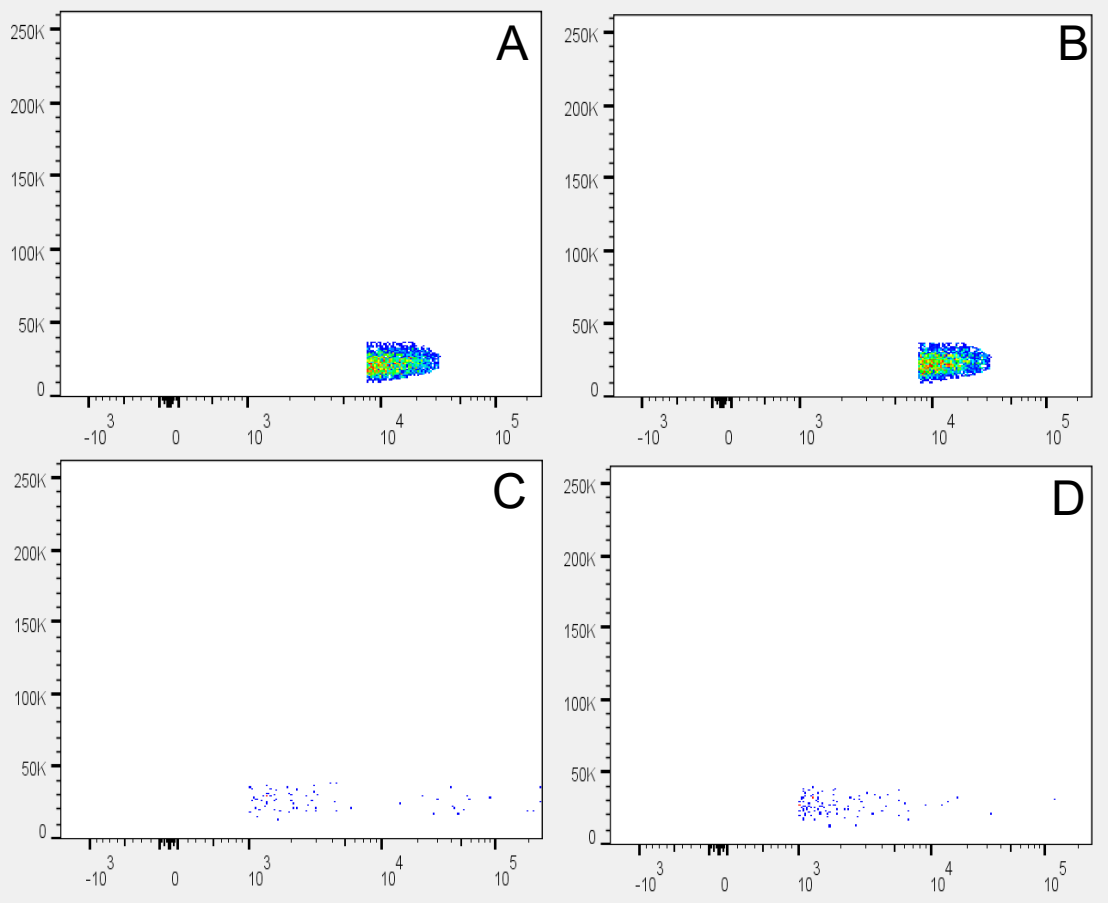

Figure 4.14. Investigation into the intracellular location of JEV-E when modified with altered signal peptides. A: External staining for JEV-E, SP15. B: External staining for JEV-E, SP24. C: Internal staining for JEV-E, SP15. D: External staining for JEV-E, SP24. Data reported as FITC fluorescence against side scatter.

The addition of either signal peptide SP15 or SP24 failed to increase the proportion of JEV-E migrating to the cell surface. Panels A and B which both highlight internal staining contain a far higher proportion of positively stained cells. Panels C and D which represent internal staining are very sparsely stained, implying that these signal peptides did not increase transport of envelope protein.

4.4.5 Dengue replicon system can be used to produce JE-PVs

PrME from the GIII strain of JEV was cloned into a pCAGGS transfer vector and transfected into HEK293T cells. After 3 days, the supernatant was harvested and titrated neat–1:243 using a 3 times dilution factor. The results from this transfection produced RLU far higher than previous experiments when compared to all other pseudotyping systems. The 4-log difference between the test sample and

background RLU as well as the linear reduction in RLU as the dilution increases show that the DenVR1 system is capable of pseudotyping JEV.

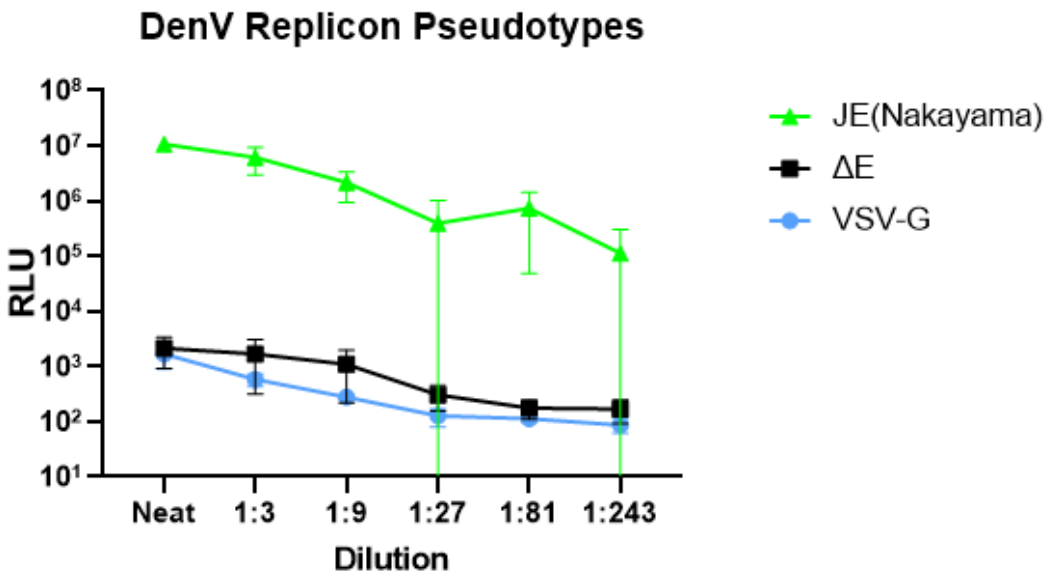

Figure 4.15. Titration of JE-PV (Nakayama) produced using the DenVR1 pseudotyping system transfected onto HEK-293T cells. JE-PV transduction results in an RLU above background envelope free control and VSV-G transduction indicating successful pseudotyping of the JE (Nakayama) envelope protein.

4.4.6 Vero cells are permissive to JE-PV

To investigate which cell line to select as a reporter for downstream neutralisation assays, a range of mammalian cell lines which are frequently used in flavivirus research were profiled to assess their permissiveness with a batch of JEV-PV produced using the DENVR1 system. A wash condition 3 days post-infection (p.i) on the Vero cells was also tested as there had been some evidence that accumulation of cellular debris could interfere with the accuracy of downstream titrations. Permissiveness was measured 3 days p.i and subsequent lysis of cells using a NanoGlo® substrate and read in relative luminescent units (RLU) using a luminometer. Huh7 cells were the least permissive of the cell lines tested, producing an RLU almost 2-log lower than the next closest value. Vero cells that had not been washed prior to lysis produced the highest RLU from a neat PV infection of $5x10^6$ RLU. Washing the Vero cells 3 days p.t. reduced RLU by around half compared to the unwashed cells.

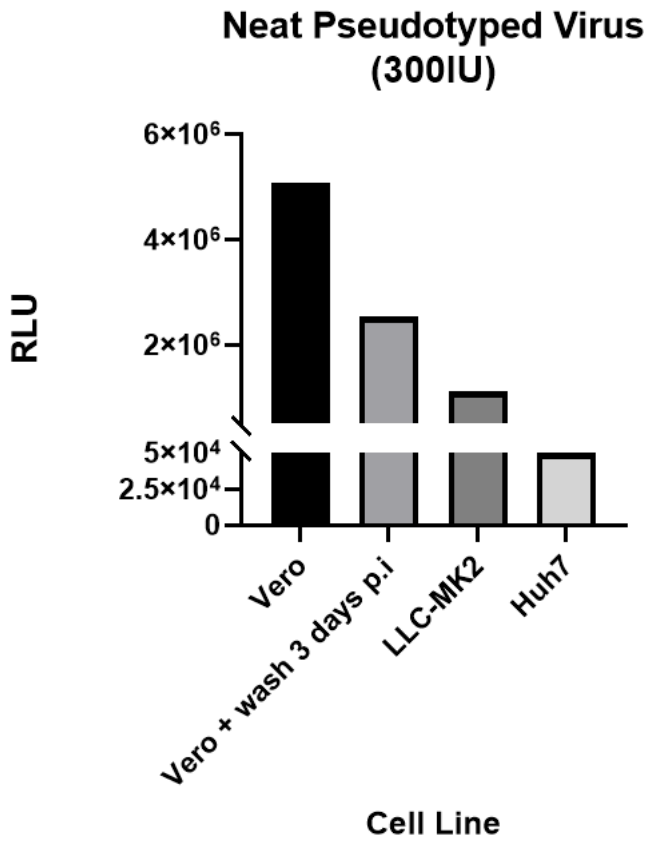

Figure 4.16. Permissiveness of Vero, LLC-MK2 and huh7 cells to JE^{GIII}-PV produced using DENVR1.

4.4.7 Short-term thermal stability study of JE^{GIII}-PVs produced using DENVR1.

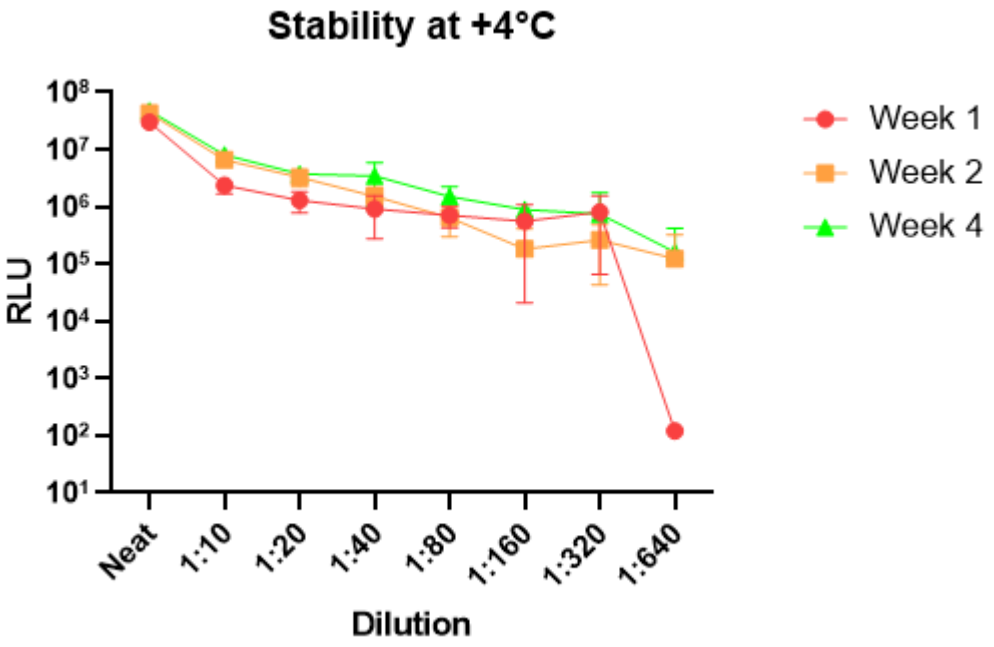

Figure 4.17 Stability of JE^{GIII}-PV over 1 month when stored at +4˚C and later transduced onto Vero cells. Triplicate values for each dilution were used to generate error bars representing standard deviation from the mean.

A sample of JE-PV (Nakayama) titrated at 1-, 2- and 4-week intervals showed no observable degradation in infectivity measured by RLU emission in Vero cells. Averaged neat values between the three timepoints were within 0.2 log and the largest difference between the timepoints tested was at 1:640 dilution. JE-PVs produced using the DenVR1 system are stable at +4˚C for up to 4 weeks.

4.4.8 JE-PV transfection time can be reduced from 4 hours to 90 minutes.

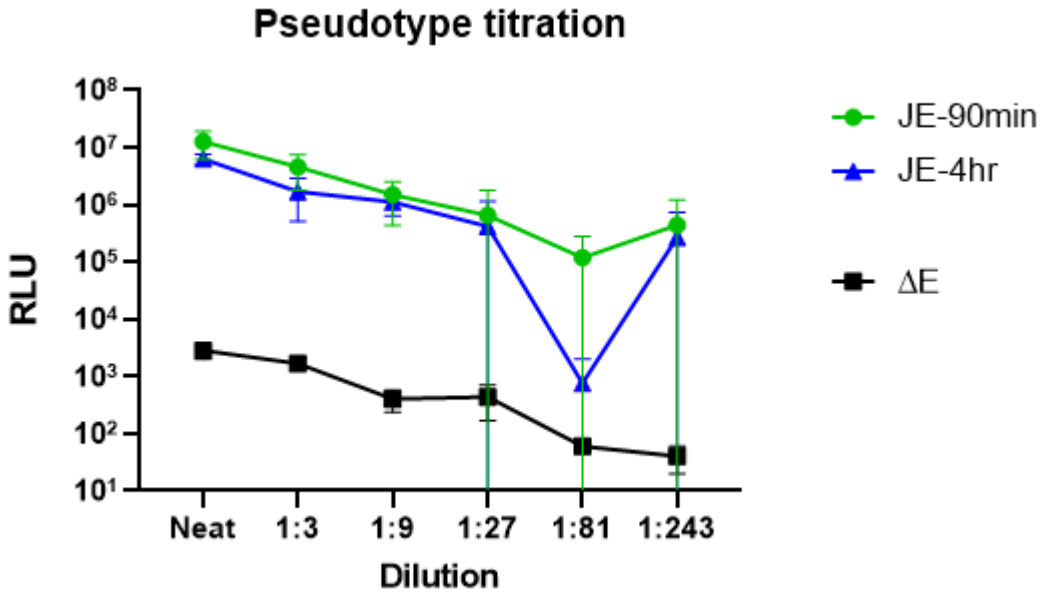

Figure 4.18. Effects of reducing transfection time using DenVR1 PV system and PEI transfection reagent, an envelope free control (ΔE) was used as a negative control. Triplicate values for each dilution were used to generate error bars representing standard deviation from the mean.

While utilising the DenVR1 system it was possible when required to reduce the transfection time from 4–5 hours to 90 minutes. This had no detrimental effect on downstream titre of the produced PVs.

4.4.9 HEK293T produce JE-envelope proteins detected by western blot after transfection with pCAGGS_JE^{GIII}.

To confirm that JE-E had been produced, a commercially available monoclonal antibody (Abcam, UK. Ab41671) was used in a western blot to probe lysate of HEK-293Ts after transfection with pCAGGS_JE^{GIII}.

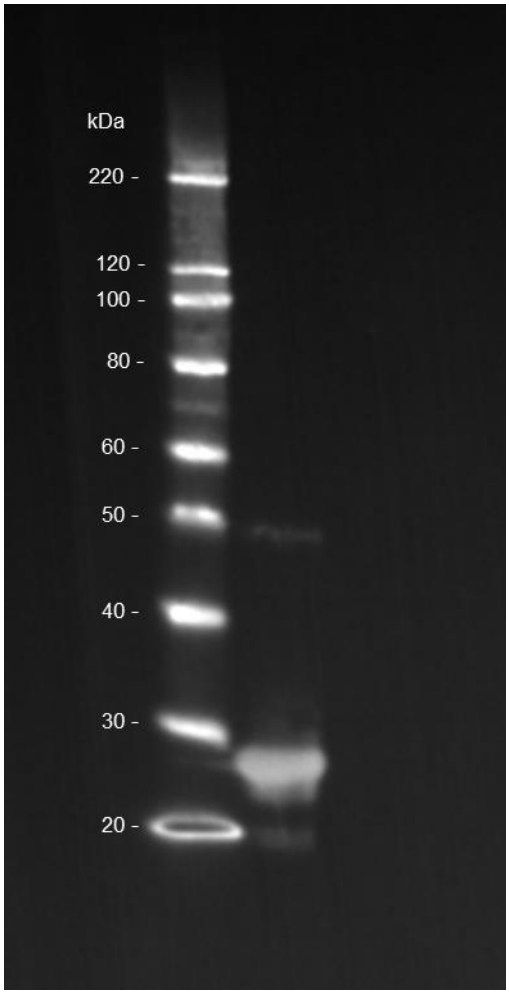

Figure 4.19 JE^{GIII}-PVs express JE envelope protein at the correct molecular weight of 20-30 kDa. Also shown is a smaller band approximately half the size representing a single envelope subunit. Detected using a monoclonal anti JE-E protein antibody (ab41671) and HRP-conjugated secondary.

A band of approximately the correct size for JE-E protein (20-30 kDa) was detected on the western blot. A faint 20 kDa band was also detected and may represent an envelope protein monomer in solution.

4.4.10 Electron microscopy of JE-PV (Nakayama strain) confirms correct morphology of PV particles.

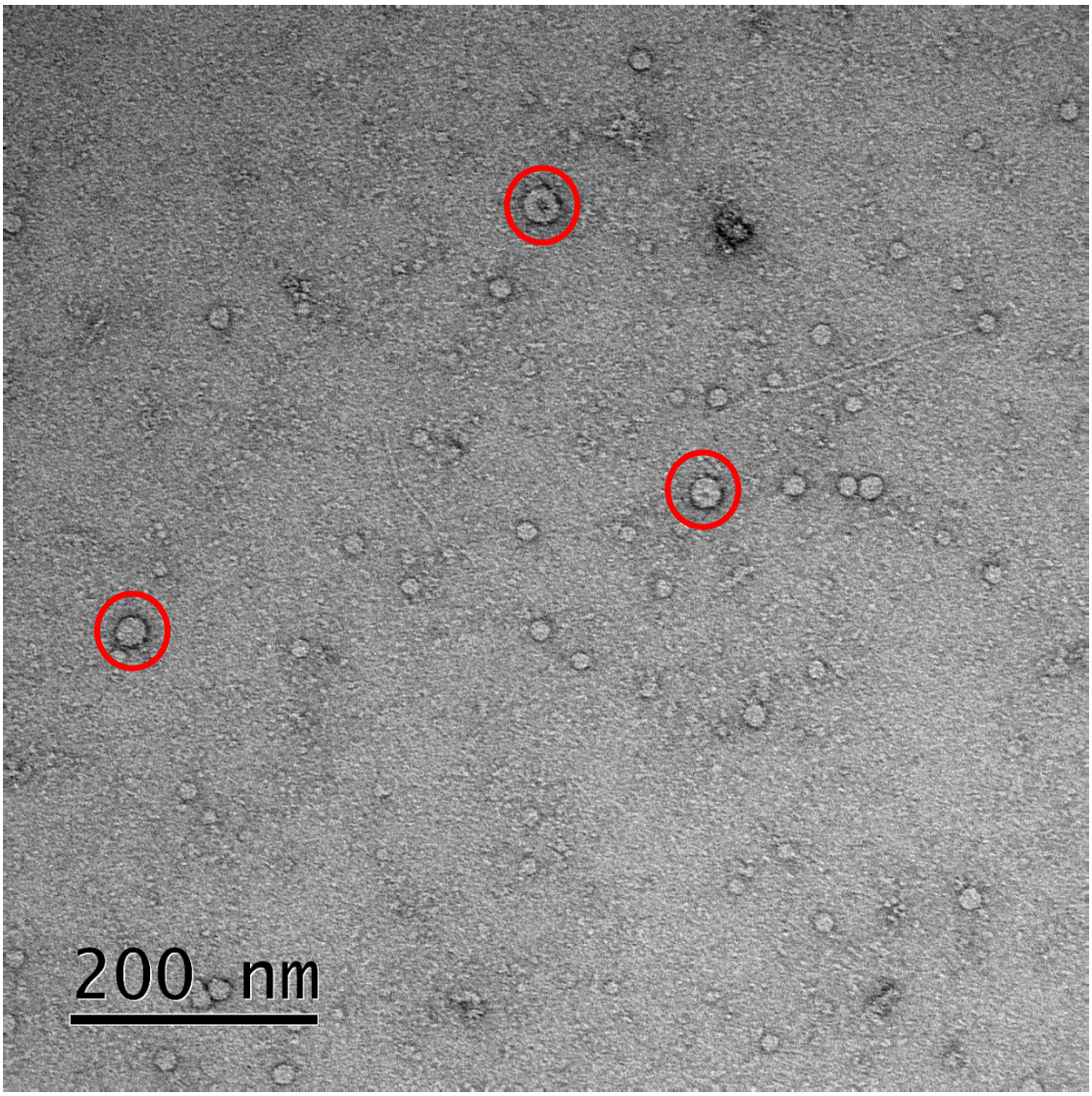

Figure 4.20. Electron micrograph of JEV-PV particles (examples circled) displaying a variation in diameter of 20–50 nm. JE-PV was applied to plasma-cleaned, carbon formvar EM grids for one minute, before two, one-minute washes with 50 µl droplets of dH_2O and then one-minute staining with 2% aqueous uranyl acetate was performed. Excess stain was removed then grids were allowed to airdry. Grids were imaged in a JEM2100 transmission electron microscope using a Gatan ultrascan 4K camera. Images were taken at 50,000 times magnification.

Electron microscopy was performed on JE-PVs (Nakayama strain) in order to assess the morphological characteristics compared to WT-JEV. The images taken confirm that the PVs produced are the approximate size and shape of WT-JEV, with the production of smaller subviral particles that is also seen in nature. WT-JEV exhibits

an icosahedral shape of 40–50 nm in size. The particles imaged in Figure 4.20. Electron micrograph of JEV-PV particles (examples circled) displaying a variation in diameter of 20–50 range from 20–50 nm in diameter.

4.5 Discussion

Initial attempts to pseudotype JEV began by performing a set of experiments utilising the most common cores used to pseudotype other viruses. These were retroviral (HIV), lentiviral (MLV) and rVSV. These experiments aimed to establish how suitable these systems were for flavivirus pseudotypes as some positive results had previously been published (de Wispelaere, Ricklin, et al., 2015; Lee et al., 2014). A variety of different cell lines, harvest times and other conditions were tried. However, these cores did not result in a high enough titre of pseudotype virus to be used in downstream assays. In some experiments, pseudotype JEV was produced at a titre slightly above background, but this would not have been functionally useful in any downstream applications and was considered a negative result based on this criterion. Any pseudotyped JEV must be produced to a titre that will provide a titrating reduction in RLU readout above the background ΔE level. It is worth noting the oversight to fail to include confirmation of Nef protein expression (by western blot) leaves the results open to criticism that the mild increase in JEV-PV^{GIII} production when transfected with a Nef plasmid is an artefact. In hindsight this data should have been included at the time.

Flow cytometry results confirmed that a prominent issue with generating JEV pseudotypes is a lack of envelope protein reaching the cell surface where the HIV, MLV and rVSV cores bud resulting in a reduced/ absent assembly of the pseudotype virus. As well as the potential mismatch in assembly locations of the retroviral and rhabdoviral capsid and JE envelope, the differences between the structures of these virus families is also likely a contributing factor to the difficulty in using them as pseudotype cores. As discussed, JEV envelope is assembled as densely packed antiparallel homodimers in a sphere. HIV, MLV and VSV capsids are pleomorphic without a spherical structure.

At 24-hours post transfection 50% of the population of producer cells expressed JEV envelope protein, however less than 1% of this protein was reaching the cell surface. This trend is repeated when the producer cells are harvested at 48 hours and with

the use of either the SP15 or SP24 signal peptide. A modification to this experiment by including unmodified JEV-E protein would provide further information of the reason for the difficulty in making JE-PVs using existing pseudotyping methods.

Based on these results it was decided that future experiments should seek to address the assembly mismatch between the core and envelope. After thorough searching of the most recent literature, the dengue replicon system was found and after contacting the group responsible for the original work a sample of the system was sent to NIBSC. After PCR amplification to create working and master stocks of the replicon plasmid itself, transfection with DenVR1, D1C and JE-PrME quickly yielded pseudotype at titres 4–5 log higher than an envelope-deficient negative control.

A short stability study was then performed to assess the optimum storage conditions for the JE PVs. It was determined that PVs produced from the dengue replicon system were stable in the fridge for up to 4 weeks. This greatly improves the ease of use of these pseudotypes and highlights their potential as diagnostic tools.

The next phase of this work was to develop and optimise a PV-neutralisation assay utilising vaccinee serum sample held available for use at NIBSC.

5 Development of a pseudotype neutralisation test

5.1 Aim

Utilise JE-PVs generated using the DENVR core system to develop a pseudotype virus neutralisation test (PVNT) for evaluating the neutralising potential of antisera.

5.2 Introduction

A key question which remains regarding the genotype shift JEV has undergone in recent years is the impact it may have on vaccine efficacy. The highly successful vaccines currently in use for protection against JEV result in a strong neutralising antibody response and this is the primary correlate of protection (Y. Van Gessel et al., 2011). Therefore, it is important to understand the potential differing capacity of neutralising antibodies derived from a JEV vaccine to adequately neutralise the different JEV genotypes.

Rapid diagnostic tests such as qPCR and lateral flow tests have greatly improved the capacity to detect and quickly respond to viral pandemics, this was essential during the recent COVID-19 worldwide pandemic. However, neutralisation tests remain the gold standard for quantifying the presence and affinity of neutralising antibodies to a target antigen. Pseudotype virus neutralisation tests (PVNT) are becoming more widely used as surrogates for live viral neutralisation tests. During the COVID-19 pandemic, pseudotyped SARS-CoV-2 was used by numerous labs and enabled them to contribute to the wider research effort (Li et al., 2022; L. Mukhopadhyay, Gupta, Yadav, & Aggarwal, 2022). As previously mentioned, pseudotype viruses are not subject to the same biological containment restrictions that many viruses which cause human and animal disease are. In addition to this, pseudotype viruses can be generated and quantified in around two weeks, this is often several weeks faster than some wild-type viruses which can take upwards of a month (or more) to achieve suitable titres for use in downstream tests.

Neutralisation tests rely on the coincubation of an antisera or neutralising antibody with an infectious agent for a given amount of time. This incubation allows the neutralising agent to bind to the infectious agent and prevent or reduce infection when it is added to a host system (often a healthy monolayer of cells). Infected (or transduced) cells are then left for a defined time depending on the rate of entry of the infectious agent. Percentage infection can be quantified by comparing strength of the marker signal compared to a non-infected control. A caveat of neutralisation tests is that each test must contain its own suitable infected and non-infected controls meaning that direct comparison between tests is not possible.

The PVs described in the previous chapter (and used for this work) contain a nano-luciferase (nano-luc) reporter gene as a reporter. Nano-luciferase is a smaller, rationally designed recombinant protein version of the widely used luciferase protein, it is measured in the same manner as luciferase but is much brighter and better suited to more sensitive applications. The pseudotype system used in this work produces PVs at a relatively low titre, these would be difficult to detect using traditional fluorescent or luminescent markers. Another benefit of nano-luciferase is that because of it being a shorter length protein, the gene encoding for it is likewise much shorter making it easier to clone into various pseudotype systems or other tests which may benefit from a sensitive, luminescent signal. Nano-luc is more expensive to purchase than luciferase so this reporter may not be suitable for all applications particularly in well-established PV systems where high titres of PVs are produced, removing the need for a particularly sensitive reporter system.

Quantification of a virus for use in a neutralisation test is usually done using a TCID50, the infectious dose required to infect 50% of viable cells. This can be used for PVNTs where the “infection” is the percentage of cells which express the reporter signal. Reported luminescent or fluorescent signal measurement can be drastically different between different operators and measurement equipment for a myriad of reasons including training level of the operator, calibration state of equipment and quality of research reagents. Efforts have been made to standardise the amount of PV to add into a neutralisation test (Ferrara & Temperton, 2018) , these suggestions rely on a defined measurement of RLU which can be useful when different groups are working with the same PV system, however this is not always possible when a new system is introduced. A large portion of work in this chapter describes the

challenges faced when transferring a new PV system to a new laboratory and adapting existing protocols.

5.3 Methods

5.3.1 Test reagents

NIBSC contains a large bank of biological reference and standards materials. Within this bank are samples of human sera pre and post vaccination with the US licensed BIKEN vaccine (Ferguson, Johnes, Li, Heath, & Barrett, 2008). The BIKEN vaccine consists of heat inactivated Nakayama strain of JEV replicated in suckling mice brains. Whole blood donations were obtained from six US vaccinees all of which were tested for antibodies to HIV 1+2, HCV and HBV as well as HCV RNA and found to be negative for these markers. Whole blood was pooled and processed to obtain serum, which was freeze dried. In total, 1270 ampoules of pre-vaccine sera and 1400 ampoules of post vaccine sera were stored at NIBSC under the catalogue code 02/184.

As well as the pre-vaccination sera, a commercial alternative naïve serum was sourced from Sigma Aldrich and used in the development of this test (see 5.3.5).

5.3.2 Pseudotyped Virus Neutralisation Test

On day 0, $1x10^4$ Vero cells were seeded into a 96-well Nunc™ plate (ThermoFisher, UK. 168055) and were incubated overnight at 37°C with 5% CO_2.The next day, anti-JE and negative control sera were thawed and diluted 1:10–1:2560, starting with neat sera (as described in 5.3.4). JE-PV was added at a predetermined quantity (as specified in 5.3.5). The sera and JE-PV were incubated at a predetermined temperature and time (as outlined in 5.3.5). The spent media was removed from the cells. 100 µl of the sera/JE-PV mixture was added to the cells, and they were incubated at a predetermined temperature and time (as indicated in 5.3.5).

Four days after the initial infection the plates were ready to be analysed the nano-luciferase buffer was thawed (Promega, UK). Nano-luc reagent was added to the buffer at a 1:50 dilution based on a 100 µl volume per well (*e.g.*, 10 ml per 96-well plate, resulting in 200 µl of nano-luc reagent plus 9.8 ml of nano-luc buffer). Media was removed from the cells. The nano-luc reagent/buffer mixture was added directly

to the cells, and they were allowed to lyse for 3 minutes. The lysed cell mixtures were transferred to a white-bottomed 96-well plate and RLU was subsequently measured using a luminometer.

5.3.3 Plate layout

Triplicate wells for each dilution were plated for both the antisera and naïve sera conditions. Within each neutralisation plate, 6 wells were transduced with JEV-PV only as well as 6 wells with cells only. The luminescence reported from these wells when the test reached endpoint (3 days p.i) was used to calculate the percentage neutralisation values.

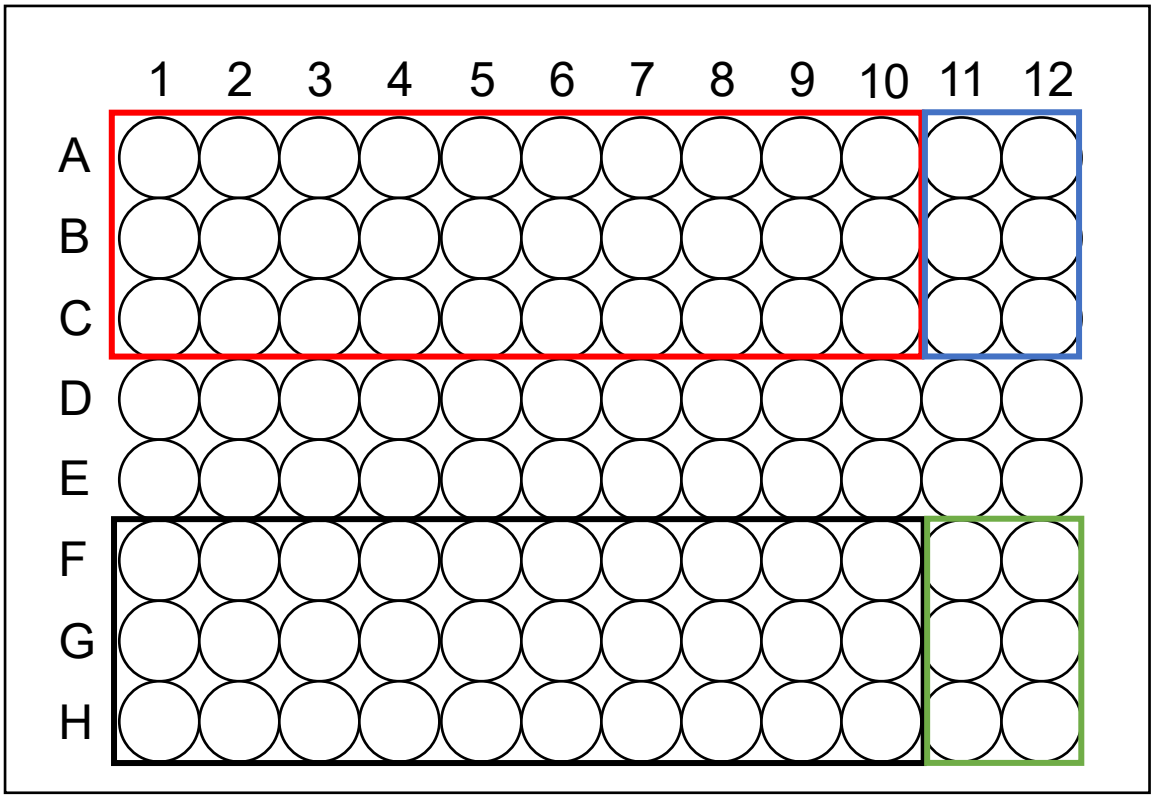

Figure 5.1. Plate layout for a JE-PVNT showing areas where PV + antisera (red), PV + naïve sera (black), JE^{GIII}-PV only (blue) and cells only (green) are located.

5.3.4 Dilution series

Diluent was taken from column one and the amount described in Table 5.1. Dilution series used for 3 wells PV neutralisation test. was aliquoted to the next column. A dilution series of PV from neat to 1:2560 was created in this way before being applied to a confluent cell monolayer.

Table 5.1. Dilution series used for 3 wells PV neutralisation test.

Plate column	PV volume (µl)	M0 volume (µl)	Serial dilution (µl)	Dilution
1	400	0	-	Neat
2	-	585	65	1:10
3	-	325	325	1:20
4	-	325	325	1:40
5	-	325	325	1:80
6	-	325	325	1:160
7	-	325	325	1:320
8	-	325	325	1:640
9	-	325	325	1:1280
10	-	325	325	1:2560

5.3.5 Test variables

A number of variables corresponding to various parts of this test were tested and optimised throughout its development.

5.3.5.1 Incubation conditions

The DENV replicon had previously been used in pseudotype flavivirus neutralisation tests using ZIKV, published test conditions called for coincubation of sera and PV at 4°C overnight followed by a 37°C, 1 hour incubation of the sera/PV mixture on Vero cells. Adjustments to these parameters are described in Table 5.2.

Table 5.2. Matrix of PV coating and PV sera/ antisera coincubation conditions tested.

PV-sera/anti sera coincubation time/ temperature	PV-sera/anti sera cell incubation time/ temperature	Figure
4°C overnight	90 minutes, 37°C	Figure 5.2
4°C overnight	3 hours, 37°C	
37°C, 1 hour	90 minutes, 37°C	
37°C, 1 hour	3 hours, 37°C	
RT, 2 hours	90 minutes, 37°C	
RT, 2 hours	3 hours, 37°C	

5.3.5.2 Determining IU/well to add

Previously published data of a neutralisation test for ZIKV-PV based on the DENVR core system describe using 50–100 IU of PV per well (Matsuda et al., 2018).

One batch of JE^{GIII}-PV was selected and diluted to 50, 100, 250 and 300 IU/well to determine what the optimum quantity of PV was for this test. The undiluted PV had an RLU of $3.42x10^7$/ml. The TCID50/ml was calculated using the Spearman-Karber method as described in Hierholzer and Killington (1996). Finally, the infectious units were derived from TCID50/ml by multiplying by 0.69. This number is based on the Poisson distribution which estimates the number of random events (viral particles) that are likely to occur in a fixed area (volume of media) at a known rate (viral titre). This value may be slightly different depending on viral particle size, viscosity of media used and many other factors. However, a 0.69 factor is sufficient to provide a reliable and standardised metric for describing the quantification of virus. This calculation was performed after each new batch of JE-PV was titrated for each subsequent neutralisation test.

Table 5.3. IU calculations required for one PVNT.

PV name	RLU at neat	TCID50/ml	IU/ml	PV / well
JE^{GIII}-PV	$3.42x10^7$	6410	4422	11µl (50IU)
				22 µl (100IU)
				45 µl (200IU)
				68 µl (300IU)

5.3.5.3 Comparison of heat-inactivation of sera

Standard protocols for neutralisation tests typically include a heat inactivation step for the sera/ antisera prior to mixing with the antigen. This is done to inactivate any complement present in the sera which may kill the reporter cells. An experiment was designed to compare the neutralising potential of sera with and without heat inactivation at 56°C for 30 minutes

.

5.4 Results

Note: Where shown, error bars represent standard deviation.

5.4.1 Screening of incubation times and conditions

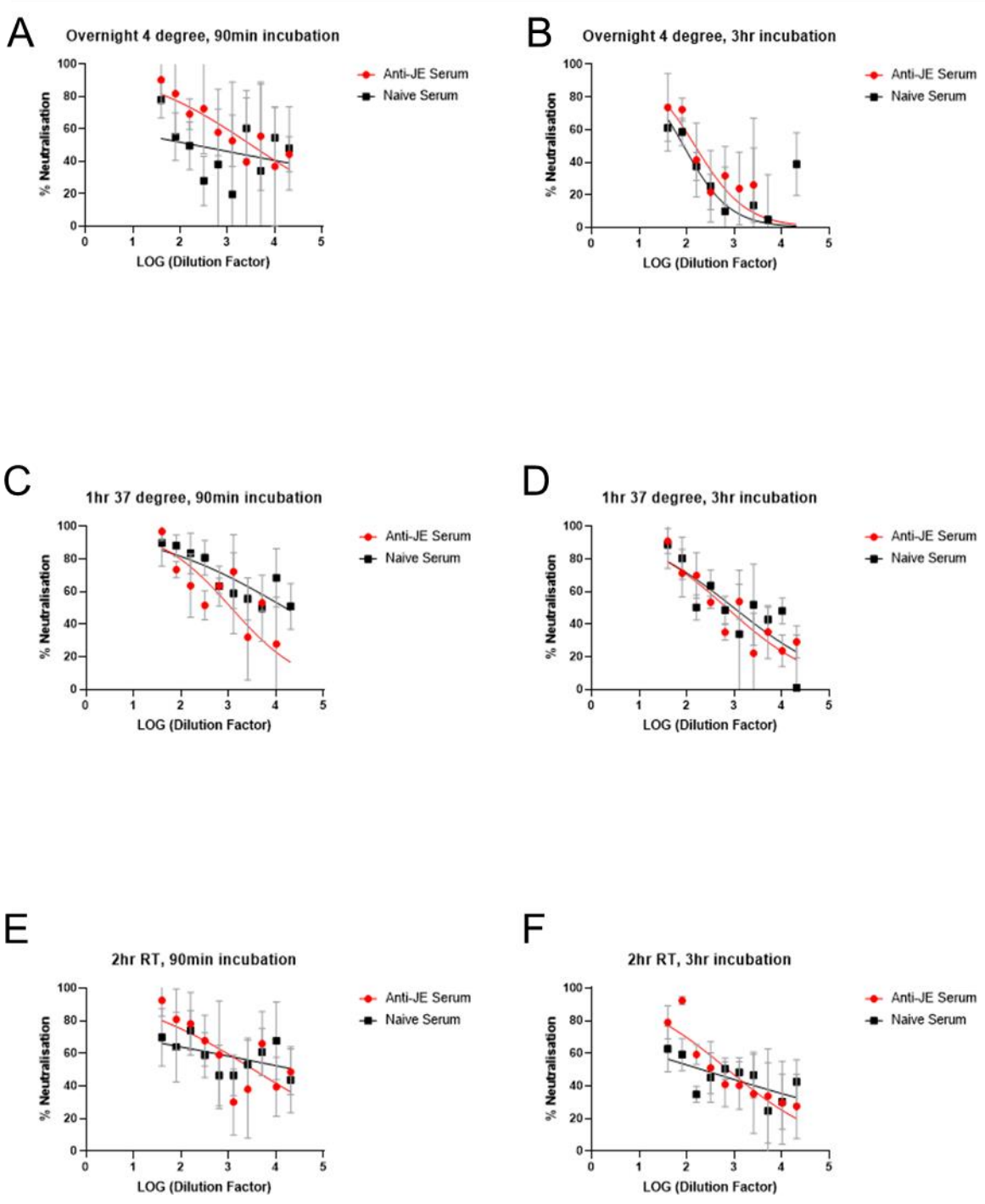

Figure 5.2. Matrix of sera/antisera: PV incubation times and conditions. Panels A and B display that an overnight coincubation of sera and JE-PV at 4°C and then a 3-hour exposure of this mixture to

host cells improved neutralisation dynamics when compared to a 90-minute exposure. Panels C and D display the effect of a 1-hour coincubation of sera/JE-PV at 37°C followed by exposure to host cells for either 90 minutes or 3 hours. Neither variable produced a significantly improved neutralisation. Figures E and F. Standard deviation of results from the mean is displayed on all graphs as error bars.

5.4.2 Quantity of PV used in test has a significant effect on neutralisation dynamics.

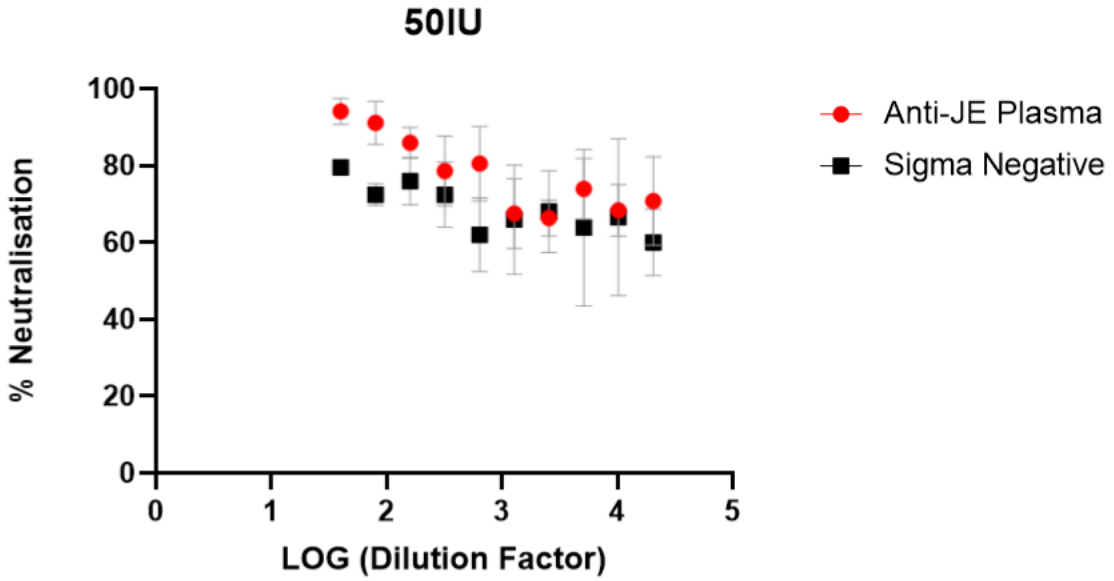

Figure 5.3. 50IU of JE^{GIII}-PV was added to a 2-fold dilution series of anti-JE serum and a negative control serum. This was insufficient to produce a measurable response in a neutralisation test.

At 50 IU of JE^{GIII}-PV is insufficient to transduce enough host cells to produce a measurable neutralising effect. Anti-JE and naive sera samples neutralised most available JEV^{GIII}-PV equally. It is likely that an excess of sera (which was heat inactivated) to PV resulted in any available PV being quickly neutralised.

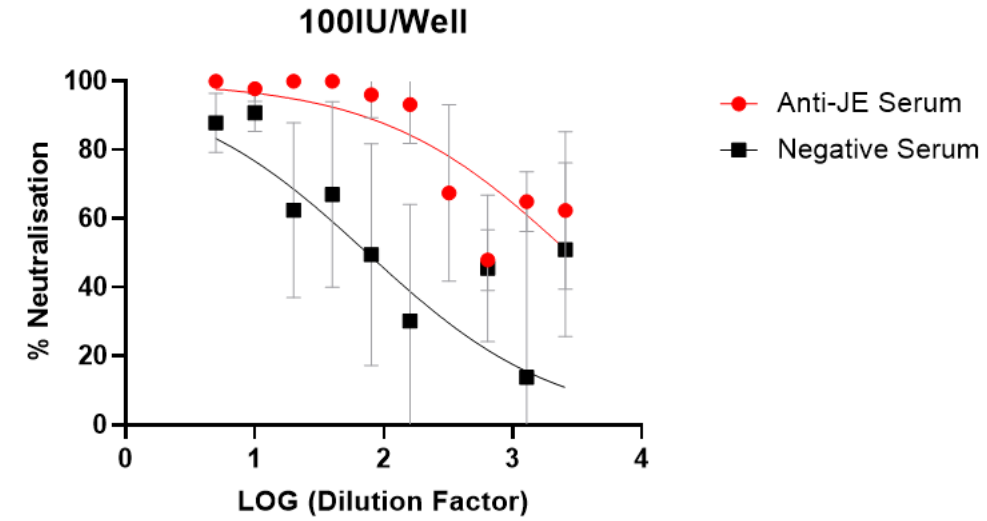

Figure 5.4. 100IU of JE^{GIII}-PV was added to a 2-fold dilution series of anti-JE serum and a negative control serum. 100IU of JE^{GIII}-PV is broadly neutralised in a dose-dependent manner by both vaccinee sera and naïve sera.

At 100 IU of JEV^{GIII}-PV was strongly neutralised in a dose-dependent manner by both anti-JE and naïve human sera. Anti-JE serum resulted in a 24% reduction of luminescent signal from the first to the last dilution point (99% of maximum signal to 75%), naïve serum produced an identical neutralising response (96% of maximum signal to 72%).

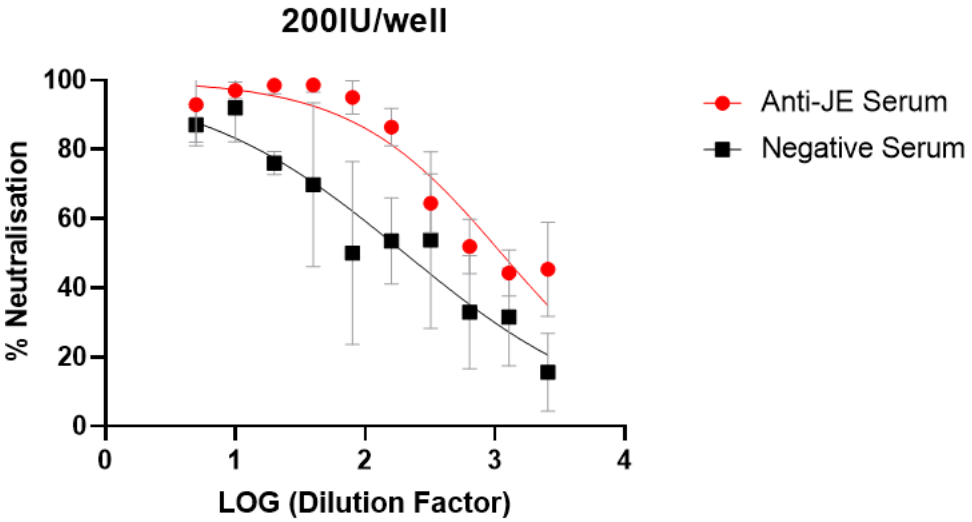

Figure 5.5. 200IU of JE^{GIII}-PV was added to a 2-fold dilution series of anti-JE serum and a negative control serum and is strongly neutralised by vaccinee sera. Naïve serum appears to also possess some neutralising potential in a linear manner.

At 200 IU of JE^{GIII}-PV, a neutralisation curve is beginning to form for both anti-JEV and naïve sera conditions. Overall neutralisation between the first and last dilution points was 30% reduction for JEV antiserum and 58% for naïve serum.

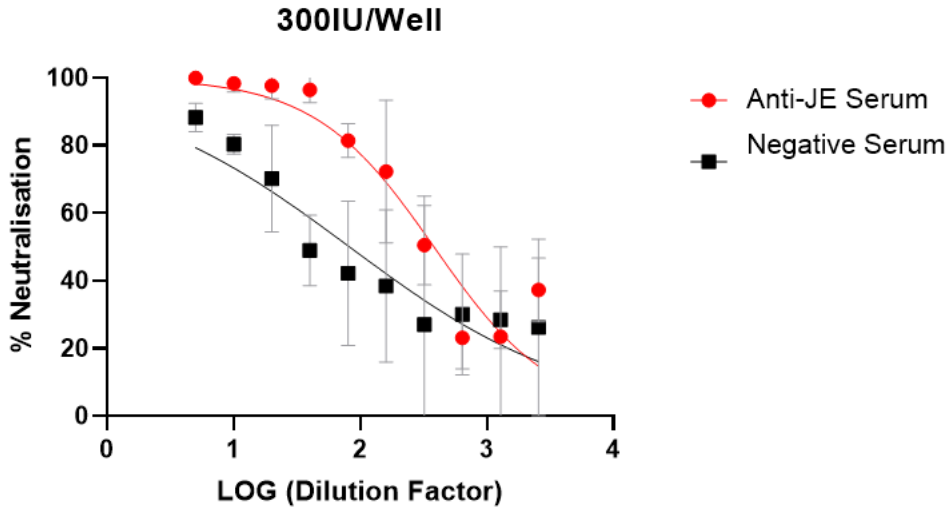

Figure 5.6. 300IU of JE^{GIII}-PV was added to a 2-fold dilution series of anti-JE serum and a negative control serum and is neutralised in a dose dependent manner by vaccinee sera. Pre-vaccinee sera neutralises in a linear manner.

At 300IU/well of JE^{GIII}-PV is neutralised in a dose dependent manner by vaccinee sera. Naïve serum appears to neutralise in a linear manner albeit less strongly.

5.4.3 Heat-inactivation has no effect on the neutralising ability of antisera to JE^{GIII}-PV

Throughout early development of this test naïve serum neutralised JE^{GIII}-PV at higher-than-expected levels. This neutralisation often decreased in a dose dependent manner; naive sera was heat inactivated at 56°C for 30 minutes prior to use in the test as is standard protocol for neutralisation tests. A condition of non-prior heat inactivation was performed to investigate the effects this might have on any

nonspecific neutralisation that may not be being completely abrogated by standard heat inactivation.

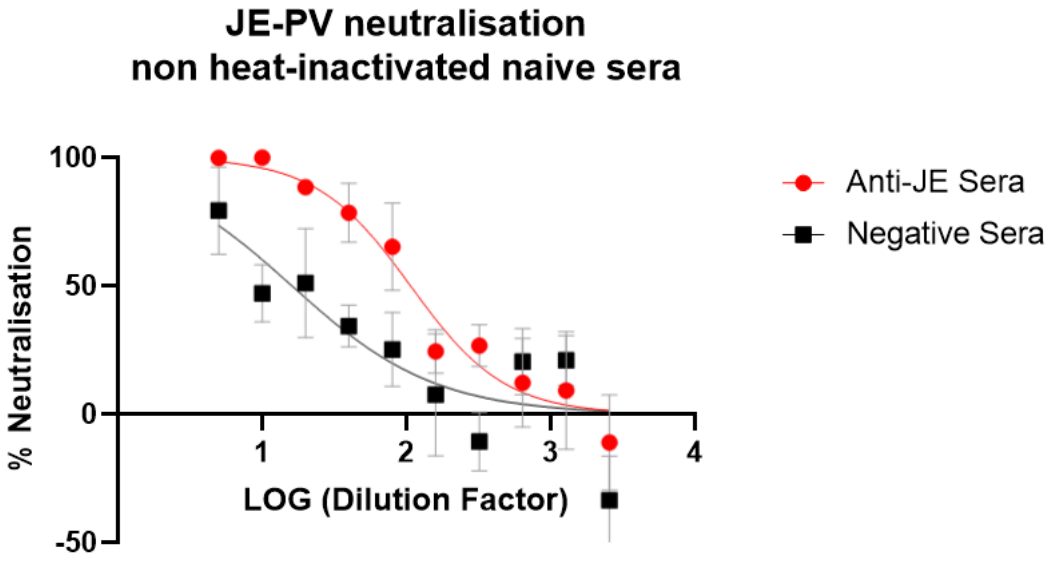

Figure 5.7. 300IU of JE^{GIII}-PV was added to anti-JE sera and negative serum which had been heat inactivated at 56°C for 30 minutes. This did not reduce the linear neutralising capacity of the naïve serum. Heat inactivation is not the cause of non-specific neutralisation of JE^{GIII}-PV by naïve sera.

5.4.4 Comparison of commercially sourced and pre vaccination serum

Commercially available naïve human serum was purchased from Sigma (UK) and a neutralisation test was repeated using the same conditions performed for the 300 IU experiment to determine if the higher-than-expected neutralisation values were due to an issue with the conformation of the JE-PVs or if the pre-vaccination serum

contained pre-existing antibodies to JEV or a related flavivirus.

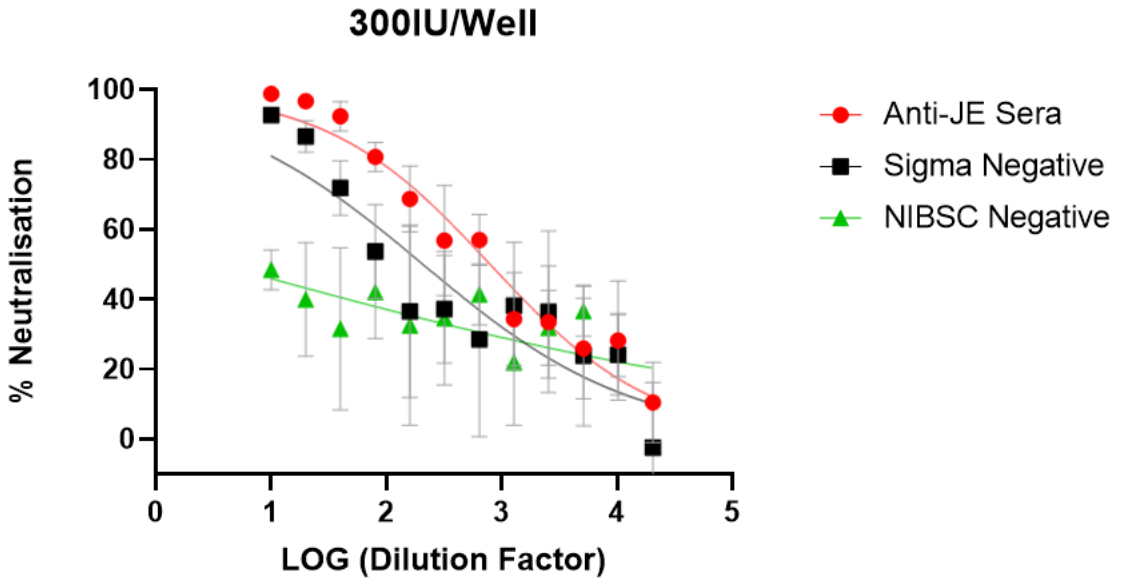

Figure 5.8. 300IU/well JE^{GIII}-PV was added to vaccine derived anti-JE, pre-vaccination naïve serum and a commercially sourced naïve serum obtained from Sigma (UK). Commercially available serum did not neutralise JEGIII-PV to the same extent as the pre vaccine naïve serum. Future experiments utilised this product as a negative control for neutralisation assays going forward.

The commercially sourced naïve human sera did not neutralise JE^{GIII}-PV to the same extent as the sera obtained before vaccination with the BIKEN vaccine. From this experiment onward the commercially sourced naïve sera from Sigma were used.

5.4.5 JE^{GV}-PV is neutralised by BIKEN vaccinee sera.

JE^{GV}-PV was developed alongside PVs for GI and GIII. This was tested against the BIKEN vaccine serum pool and found to be adequately neutralised by antisera. This adds further support to this test as a suitable way to compare neutralising potential of antibodies to emerging variants of JEV and adds support to the argument that GV in its current form can be contained with current generation vaccines.

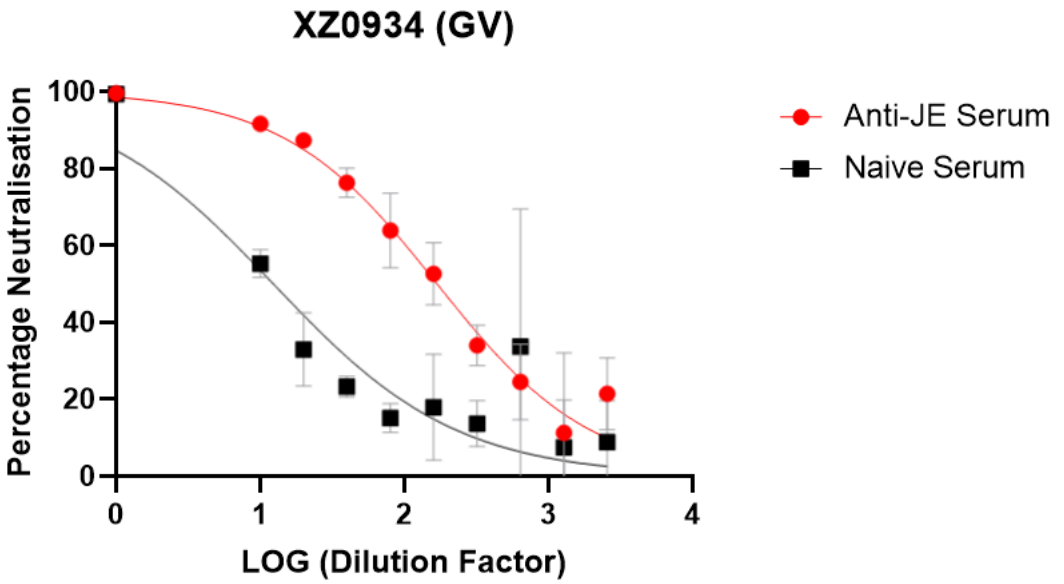

Figure 5.9. 300IU JE^{GV}-PV was added to anti JE-serum obtained from recipients of the JE^{GIII} derived BIKEN vaccine as well as a commercially sourced negative control naïve serum. JE^{GV}-PV was neutralised by sera obtained from BIKEN vaccinees. Naïve serum neutralised JEGV-PV approximately 50% at a neat concentration, this sharply dropped to dropped to 30% neutralisation after a single 1:10 dilution.

5.5 Discussion

When performing live viral neutralisation tests for JEV, neutralisation of 50% at a 1:10 serum dilution is indicative of a protective neutralising response (Markoff, 2000; Yvonne Van Gessel et al., 2011). One issue which remained present throughout much of the test development was that the naïve sera obtained prior to vaccination with the BIKEN vaccine neutralised JE^{GIII}-PV more potently than was expected, this did not reduce when different dilution series or heat inactivation conditions were applied. Eventually this issue was resolved when a commercial alternative naïve serum was obtained. Serum was heat inactivated before use removing complement as a potential cause for the high neutralising capacity. Other reasons for this could include non-specific binding to other components of the serum such as albumin (Williams et al., 2010). The JE-PV preparations whilst filtered, where not purified through a sucrose gradient. This would have removed any other potential neutralising factors present within the harvest supernatant.

Future work in this area could also test the JE vaccinee sera (pre and post) in the earlier experiments performed with other pseudotype core systems, such as VSV-G. This would establish whether there was a component of the serum pool which was causing the neutralisation or if it was an issue with the JE-PVs produced using the Dengue replicon system.

There are several possible explanations for why the pre vaccination sera had and unexpectedly high neutralisation of JE^{GIII}-PV. The pool was generated using serum from only 6 people, therefore even if only one of them had pre-existing flavivirus antibodies, there would not have been much of a dilution effect. Individual aliquots from each of the donor individuals were not available to determine if they varied in their neutralising capacity. The identities of the donors were anonymised so no information was available that might indicate exposure to flaviviruses such as history of travel to a JEV-endemic region or vaccination against yellow fever virus. Furthermore, WNV is endemic, and dengue can occur occasionally, as well as the recent incursions of Zika virus into some southern US states. The DENVR core system has been used to generate PVs to other related flaviviruses including yellow fever and dengue (Matsuda et al., 2018). PVNTs using these PVs and the JE vaccinee sera would resolve the question of cross neutralisation and is certainly an area of future work which should be explored.

As previously mentioned, the reporter gene used within the DENVR pseudotyping system is NanoGlo, this protein has been modified to be brighter than both wild-type firefly and jellyfish luciferase (England, Ehlerding, & Cai, 2016). It is designed for sensitive applications such as detecting low-output PV. The downside of using such a bright reporter is that small variations in the titre of produced PV result in large differences in measured RLU. This was a consistent problem throughout the development of this test and required numerous optimisations of the protocol to achieve a repeatable result.

Sucrose gradient purification of PVs was considered as a method to concentrate multiple batches of PV in order to alleviate the issues related to the low harvest titre, however after some thought it was realised this would have required tens of batches of PV in order to generate sufficient volume to dilute to a working concentration for

downstream neutralisation assays. This was not a practical solution given the time constraints on the project at the time of development.

A particularly unusual aspect of the PVNTs performed by the original authors of the DENVR system was an overnight incubation of PVs and serum/antiserum at 4°C overnight (Suzuki et al., 2014). This was replicated in the experiments displayed by Figure 5.2 and a lower incubation temperature did appear to have a positive impact on neutralisation dynamics. This effect did not appear to be caused by a longer coincubation of the PVs and antiserum alone as it was not replicated among the other incubation time conditions. One possible explanation for this effect is a reduction in the rate of on/off binding performed by the antibodies within the antisera. This condition was not utilised in the finalised PVNT as it was decided this was too far removed from physiological conditions.

An important component of the PVNT development was elucidating the required quantity of PV to add into the test. Four different amounts of PV were trialled, 50, 100, 200 and 300 IU/well of PV. A clear steepening of the neutralisation curve was measured as the quantity of PV increased and 300 IU/well of PV was determined as the required amount to add for a successful PVNT. The JE-PV was made in 10 cm dishes and harvested into a volume of 12–13 ml. One PVNT plate requiring 300 IU PV/well could use up to 6 ml PV per plate (if all wells were utilised). This volume quickly eclipsed the scale JE-PV can be generated in. This meant having to produce multiple batches of PV in advance to have the minimum required amount in advance of performing a PVNT. The original test conditions used for a ZIKV-PVNT are described in 5.3.5.1, these utilised Vero cells also as the target cell line. Other cell lines were not investigated in this work due to the negative results obtained in Chapter 4.

As discussed in Chapter 4, whilst the method used to produce JE-PV was successful, it was also not always consistent, with large variations in PV titre and occasional failure to produce any PV for no apparent reason. Whilst the work in this chapter represents the successful development of a JE-PVNT which certainly has utility to determine vaccine derived antibody efficacy or to determine the capacity for GV to escape vaccine mediated protection, further optimisation in the PV production

process will improve the robustness of this test such that large-scale experiments can be performed further increasing the tests usefulness.

5.6 Conclusion

A PVNT utilising JE-PVs was developed using JE^{GIII}-PV as the model genotype with antisera obtained from BIKEN vaccine recipients. The methods optimised using the JE^{GIII}-PV where also tested on JE^{GV}-PV and results indicate it is easily transferrable to other JE genotypes. This test will be incorporated into a phage screening effort aimed at investigating the potential differences in neutralising epitopes between the genotypes.

The difficulties faced and subsequent optimisations required to develop this test highlight the complexities of technology transfer and strengthen the argument for greater standardisation (where possible) of reagents and protocols.

6 Utilising nanobody phage display to identify shared and unique epitopes on the JEV E protein across genotypes.

6.1 Aim

To utilise a nanobody phage display library to identify shared and unique neutralising epitopes on the JEV-E protein between genotypes I, III and V utilising a pseudotype virus.

6.2 Introduction

6.2.1 Origins of phage display

Phage display was first described in 1985 when the ability of certain bacteriophages to present short peptides on their minor coat protein (PIII) was discovered (Smith, 1985). This technique is now widely used as a means to select for specific binding ligands, including antibodies (Bazan, Calkosinski, & Gamian, 2012). The key principle behind phage display technology is that genotype and phenotype are intrinsically linked, this means that the binding properties of the protein displayed on the phage surface (phenotype) can be precisely determined by the sequence of the corresponding gene packaged within the same virion (genotype).

Phage display is performed using filamentous phage. These are single stranded DNA viruses which infect bacteria using the F pilus on *E. coli*. M13, fd and f1 are the most used filamentous phage and all infect *E. coli*. These phages share 98% gene homology, to the extent that their proteins are interchangeable. Because of this they are often referred collectively as Ff phage.

Filamentous phage have a cylindrical morphology and express five different proteins that constitute the coat: PIII, VI, VII, VIII and IX. These proteins are presented at different levels on the phage surface. There are several

thousand copies of the major coat protein PVIII, and usually five copies of the minor coat protein PIII (Figure 42) located at the distal end of the phage filament (Hay & Lithgow, 2019) . Both the major and minor coat proteins can be utilised for phage display with the major protein being able to display more copies of peptides and PIII being able to incorporate larger proteins, including full length antibodies (L. Zhang et al., 2021), toxins (Angkeow et al., 2022) and functional enzymes (Fernandez-Gacio, Uguen, & Fastrez, 2003).

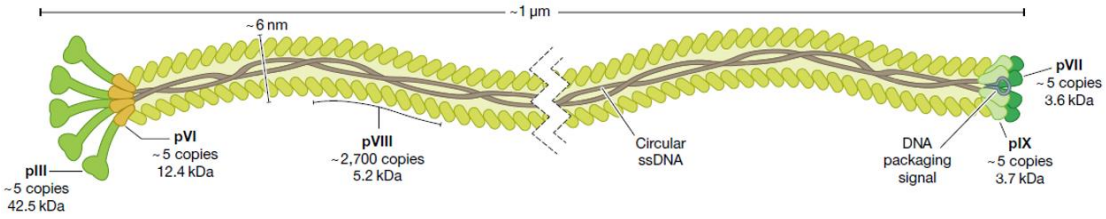

Figure 6.1. Structure of filamentous M13 phage. Adapted from Hay and Lithgow. 2019

When foreign DNA is inserted between the signal sequence and protein coding gene III of a filamentous phage, a fusion protein is generated with the foreign protein incorporated onto the N-terminal of the polypeptide.
With the advent of more sophisticated cloning methods, it has become possible to construct very high diversity phage display antibody libraries representing antibodies with highly diverse complementarity determining regions (CDR) from either naïve or immunised donors or by using antibody scaffolds and introducing synthetic diversity into the CDRs. Diversity for immune libraries is usually around 1 million unique sequences, and for naïve or synthetic libraries is often over 1 billion different antibodies (Almagro, Pedraza-Escalona, Arrieta, & Perez-Tapia, 2019; Tsoumpeli et al., 2022). These libraries can then undergo affinity selection when exposed to antigens of interest. Phage which present antibodies which bind strongly to the antigen of interest can be enriched more than 1000 times compared to non-binders and wild type phage (Smith, 1985). This technique of exposing a phage library to an antigen and selecting for positive binders is known as panning, or bio-panning. The result of several iterative rounds of panning is an enriched library containing in varying quantities, phage displaying an antibody which binds strongly to the antigen of interest.

Ff phage are non-lytic and do not form classical viral plaques, this feature is particularly useful in terms of using phage as a means of protein production as the phage are able to replicate to very high titres within the infected cell and can be recovered efficiently from the host bacteria.

6.2.2 Helper phage

As discussed previously, the two coat proteins (PIII and PVIII) have limitations for the size of fusion protein they can present before stearic hinderance of the protein inhibits the essential functions, for instance PIII interaction with the bacterial *f* pilus required for infection of a bacterial cell, and for both PIII and PVIII, phage assembly. To circumvent this issue, the fusion protein gene can be carried on a phagemid (a plasmid which contains both a phage and bacterial origin of replication) which can express a ligand-coat protein fusion protein. This system then requires a helper phage to provide all other phage proteins to successfully assemble phage displaying the fusion proteins alongside the equivalent wild-type coat protein. The helper phage contains all the genes necessary for packaging, infection, and replication of the resulting phage. As well as this, the helper phage is packaging inefficiently meaning the phage plasmid is preferentially packaged into the new phage particles, reinforcing the link between phenotype and genotype.

The inclusion of wild type PIII coat protein genes on the helper phage and fusion PIII coat protein genes on the phagemid allows a greater size fusion protein to be presented on the phage capsid whilst retaining wild type phage functions. However, this system shows preferential expression of the wild type version and also preferential degradation of the fusion protein within the bacterial periplasmic space (Baek, Suk, Kim, & Cha, 2002). This results in poor levels of the modified surface protein being displayed which can result in low success rates for selecting strongly positive binders. Baek et al. (2002) developed a modified helper phage to help alleviate this. Their helper phage (described as ex-phage) is a mutant M13K07 phage and contains a pIII gene which only produces functional pIII in suppressor strains of bacteria such as TG1. This was achieved via the addition of two amber stop codons, in suppressor strains these codons are often read as a Gln amino acid codon but can also produce a stop in translation. Overall, this results in lower levels

of expression of genes containing an amber stop codon. In ex-phage the amber stop codons replace Glu residues at the 5′ region of the pIII gene. *E. coli* containing a phagemid carrying the pIII fusion protein, when superinfected with ex-phage will produce phage expressing less wild type pIII and have enhanced ligand-coat protein fusion display by up to 100-fold.

6.2.3 Lac operon

The phagemid utilised in these experiments also contained a lacZ promoter upstream of the PIII-fusion coat protein gene sequence. Expression is therefore controlled by the presence/ absence of glucose in the growth medium. An amber stop codon is present between the genes for the displayed protein (in this case a nanobody) and the phage coat protein. This permits fusion of the display protein to the coat protein in strains of *E. coli* which suppress amber stop codons, such as TG1 cells. Glucose in the growth medium will suppress the lacZ promoter thereby preventing display protein-coat protein fusion reducing library bias and toxicity to the producer TG1 cells. During superinfection of TG1 cells with helper phage the glucose is removed from the medium and phage production can commence incorporating the pIII-fusion protein.

The helper phage contains kanamycin resistance but not ampicillin. Therefore, TG1 which contain phagemid only are ampicillin resistant only. Once superinfection occurs the TG1 become bother kanamycin and ampicillin resistant. Resuspending TG1 cells in kanamycin and ampicillin media will select for superinfected cells only.

Panning is performed via either surface tethering of an antigen to a fixed surface (such as a Maxisorp plate), or via recombinant expression of the antigen to the surface of a cell (Panagides et al., 2022). Targets can also be naturally occurring on cell surfaces. These strategies have benefits and drawbacks depending on the end goal of the panning. For this work these approaches were combined, the virus-surface display of the target antigen (JEV-E protein) was used, as this protein can be fully incorporated as the envelope of a pseudotype virus. The pseudotype virus was then immobilised on Maxisorb plates. This allows investigation of binding sites which are as close as possible to the wild-type envelope protein without the containment

requirements of the live virus, and by immobilisation on plates, thorough wash steps can be applied.

Within the different panning systems, panning is generally performed in similar ways. The antigen is presented to the library and time is given to allow binders to attach to the corresponding antigen, several cycles of washing and re-exposure of library to antigen is performed to enrich the library for binders. The phage are then eluted from the antigen (usually by a pH shift) and amplified in bacteria to reach sufficient titre for subsequent rounds of panning. This is usually performed 3-5 times and then several hundred of the output phage are analysed in an immunoassay to determine if individual phage bind to the target antigen. Positive clones are then sequenced, revealing the amino acid sequence of any successful binding protein. This method was applied in the current study but with the addition of subtractive binding stage. The rationale for this work was to select for unique binders for each of the genotypes of JEV studied (GI, III and V). To remove cross-binding phage, after each round of selection where the library was exposed to its homologous antigen (GV-GV), the library was subsequently expose to the heterologous antigen and the non-binding supernatant taken forward. This sub-library of phage was then propagated and used in another round of enrichment panning. In this way, cross-binding phage were removed from the phage library.

6.2.4 Nanobodies

The binding ligands that were used in the present study were nanobodies (or single-domain VHH). These are derived from camelid IgG heavy-chain only antibodies. In 1993, Hamers-Casterman et al. discovered that camels possess some IgG which are devoid of light chains. These molecules consist of heavy-chain dimers and are much smaller than classical immunoglobulins. The research and clinical potential of this feature was quickly realised. Due to their small size and simple structure, nanobodies are more stable in extreme environments than heavy + light chain antibodies (Jin, Odongo, Radwanska, & Magez, 2023) .

Camelids are not the only species which have light-chain deficient immunoglobulins. Sharks also produce these unique antibodies (named immunoglobulin new antigen receptors or IgNARs), however there are some differences between the two species, and this impacts their usefulness as research tools and drugs. Like mammalian IgG camelid heavy chain antibodies contain two fc regions on each chain (four on the whole molecule). Shark IgG has four fc regions per chain (8 in total). The number of loops in the CDR region is also different, camelids share three loops like mammals however shark IgG only contains two (Pothin, Lesuisse, & Lafaye, 2020). These differences mean that shark IgNARs are actually slightly smaller than camelid VHHs.

Nanobodies are ideally suited for use in phage display. They are coded for by relatively small genes which are easily cloned into the filamentous phage (or phagemid) genome, are tolerated well by many cell lines and have a high affinity for their target. As well as this, due to their small size they can access cryptic epitopes which may remain elusive to larger immunoglobulins. Nanobodies are also easy to produce and have a higher bioavailability. In 2018 the first nanobody based drug was released whilst others are still in development.

6.3 Methods

6.3.1 pSD3-VHH library and helper phage

Phagemid pSD3-VHH containing the VHH library were provided by Dr Alison Gray (University of Nottingham).

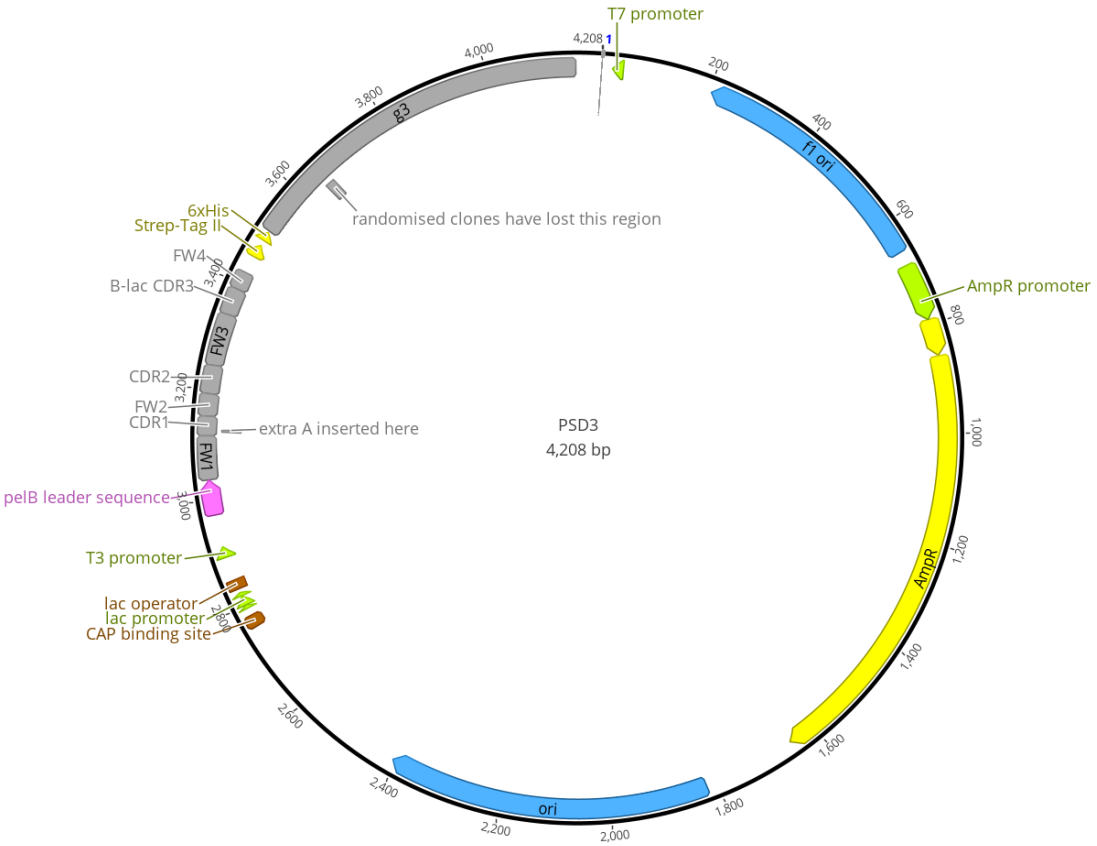

Figure 6.2. Plasmid map of the phagemid pSD3 containing the VHH gene (highlighted in grey). Diversity was introduced into the variable CDR3 domain.

The phagemid pSD3-VHH library was developed via a whole plasmid inverse PCR method whereby $1x10^9$ 12-mer, 16-mer or 21-mer random peptide codons were introduced into the CDR3 region in the phagemid vector pSD3 (Tsoumpeli et al., 2022). As well as the variable CDR3 region the fusion gene contained a 6xHis-tag for protein identification via immunostaining and the phagemid vector contained an ampicillin resistance gene.

This library was validated both computationally by next generation sequencing and experimentally by isolation of ligands to target antigens by biopanning. Aliquots of exphage stock were provided by Dr. Janet Daly's group (University of Nottingham), a genome map was not available. Full details of library generation can be found in the Tsoumpeli et al. 2021 paper.

6.3.2 TG1 stock production

An aliquot of TG1 cells was provided by Dr. Janet Daly (University of Nottingham) and grown on minimal agar for 2-3 days then one colony was

picked and grown in 10ml 2YT media overnight, 210rpm, 37°C. The next day, the sample was centrifuge at 3000xg, 10 minutes and the supernatant discarded. The pellet was resuspended in 25% glycerol and store in 1ml aliquots at ≤-80°C. When required, an aliquot was thawed and grown on minimal agar media overnight to present the F pilus ready for phage infection.

6.3.3 Exphage production

Competent TG1 cells were grown in 10ml 2YT media (2.1.2) overnight at 180rpm, 37°C and then inoculated into 2 litres of 2YT media and left to grow at 180rpm, 37°C until an optical density (OD) of 0.4 was reached (approximately 3 hours). Exphage phage was added at an MOI of 10 (equates to $4x10^8$ helper phage).

The culture was left, static, for 30 minutes and then gently shaken for 30 minutes at 30°C, 220rpm. After time had elapsed, 500ml 2YT was added to the culture then the total volume was split across four 2L flasks and Kanamycin was added to a final concentration of 50µg/ml. This was grown overnight at 30°C, 200rpm. The next day the culture was centrifuged at 12,000xg for 20 minutes, 4°C and the supernatant was collected, and the pellet was discarded.

6.3.4 PEG precipitation of helper phage

To precipitate helper phage with polyethylene glycol (PEG), 250ml, 20% w/v PEG-8000/2.5M NaCl was added to each litre of helper phage supernatant then placed on ice for 1 hour. The phage/PEG mixture was then centrifuged at 8000xg for 20 minutes the supernatant was discarded. Centrifugation and supernatant discard was repeated twice more for 1 minute to remove all residual PEG. The phage pellet was resuspended by adding 30ml PBS/ 1L of initial supernatant and left static to dissolve pellet for 5–10 minutes at RT.

For storage at ≤-80°C, 15% glycerol w/v was added. Helper phage was them aliquoted into 1ml aliquots for long term storage.

6.3.5 Helper phage titration

Before titration, 2YT agar plates were poured and 10ml TG1 was grown in 2YT media to an OD of 0.2.

An aliquot of helper phage was thawed and used to create a dilution series $1:10^3$–10^{14} in PBS, 20 µl of each dilution was added to 180 µl of TG1 cells then spread across the 2YT agar plates and grown overnight at 37°C.

To ensure TG1 stocks remain uncontaminated with phage a 2YT agar plate was prepared in advance with 50ug/ml kanamycin to grow a sample of TG1 cells.

6.3.6 Target antigen selection

Pseudotype JEV produced using the DENVR core system was used as the target antigen for these experiments. A mixture of JE^{GI} and JE^{GIII} PVs, or JE^{GV}-PV were used to pan the VHH library. A mixture of GI and GIII was chosen as these are the two most prevalent genotypes causing human infection worldwide and well-protected against by current vaccines (1.10). In contrast GV is the most divergent genotype with a reduced homology to GI/III within the E protein. Therefore, it was determined that unique neutralising epitopes on the GV E protein would prove the most useful for the future control of JEV should a genotype shift towards GV prevalence occur in the future.

6.3.7 Input and output phage titration

Before and after each round of panning the titre of the input/output phage was determined via titration in PBS and subsequent infection of a known quantity of TG1 cells. This was performed as 5 x 1:100-fold serial dilutions for the input phage followed by a final 1:10 dilution for each via the addition of TG1 cells; and 4 x 1:10 dilutions starting at neat for the output phage with a final 1:10 dilution for each, again via the addition of TG1 cells. All TG1 cells used in phage titration was grown to an OD of between 0.4-0.6 before use.

6.3.8 PV coating volume

To determine the optimal PV coating volume for use as a positive control, 50 or 100µl JE-^{GI}, ^{III} and ^{V}-PV (RLU 10^8) were added with equal volumes bicarbonate coating buffer to 8 wells of a Maxisorp plate and incubated at 4°C

overnight then detected using an anti-JE HRP conjugated antibody (ab41671) following the ELISA. Absorbance was measured in a spectrophotometric plate reader at 450nm after addition of TMB for 30 minutes.

6.3.9 Panning regimen

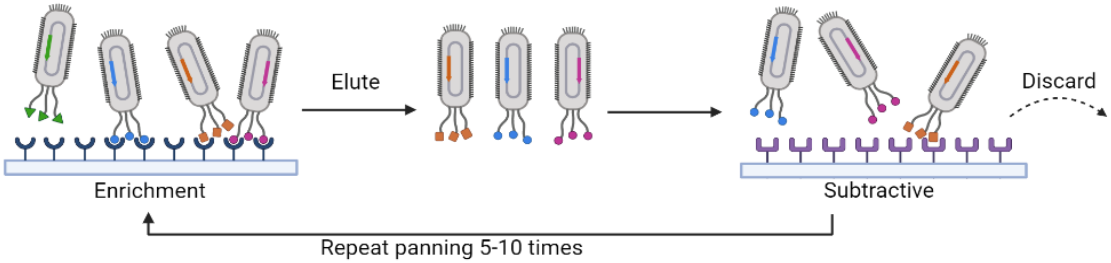

Figure 6.3. Graphic illustration of panning regimen including a subtractive panning step. Pseudovirus particles are bound to a solid surface using a bicarbonate buffer and exposed to the phage library. Non-bound phage is removed through several stages of washing, bound phage is then eluted from the pseudovirus, and a fraction diluted to determine titre. A subtractive panning step utilising capsid only PV as the bound antigen was performed after each round of enrichment panning.

Two colonies of TG1 cells were picked into 10ml 2YT and incubated at 37°C, 300rpm until an OD of 0.5 had been reached. Maxisorp plates which had been pre-coated with 100µl of the relevant antigen ($JE^{GI/GIII}$ or ^{GV}-PV) and incubated overnight at 4°C were washed once with 1xPBS then blocked with 3% milk powder in 1xPBS for 1 hour at RT. The phage was blocked with 200µl 18% milk powder in 6xPBS per ml of phage for 30 minutes to 1 hour at RT.

The blocked Maxisorp plate was then rinsed 3 times with 1xPBS and 100µl of the blocked phage was added per well to the plate and left at RT for 1-3 hours. After this time had elapsed the plate was washed 10 times with PBST (0.1% tween) followed by 10 times with 1xPBS (in the first round of panning this was reduced to 5 washes each). The remaining bound phage was then eluted using 100µl, 0.1M glycine (adjusted to pH2) and left for 10 minutes at RT. Eluted phage were then neutralised with 100µl 1M (pH 7.4) tris and pooled for subsequent panning rounds and titration to determine output titre. As described in Figure 6.3 a subtractive panning step was introduced to remove phage binding to capsid only.

Storage medium was prepared using 2YT, 25% glycerol and 2% glucose with 150µg/ml ampicillin and 250µl of output phage was aliquoted for long-term storage.
Output phage was diluted 1:10, 4 times in PBS to achieve a final serial dilution of neat, 1:10, 100, 1000 and subsequently plated onto 2YT agar with 150µg/ml ampicillin, 2% glucose. A negative control plate was also added each titration which consisted of TG1 cells only without phage. The TG1 cells on this plate should not grow unless cells were contaminated with phage.
The remaining eluted phage was added to 10ml TG1 and incubated at 37°C, static for 30 minutes and then pelleted at 3000xg for 10 minutes. The supernatant was discarded, and the pellet was resuspended in 1ml 2YT and plated out onto a bioassay plate and incubated at 37°C overnight.
The next day the bioassay plate was scraped into 5ml 2YT storage media (2.5). This stock was used as the input phage for the subsequent panning round.

6.3.10 Polyclonal ELISA

After all panning rounds were complete a polyclonal ELISA was performed to determine that the library had been enriched. A 96-well Maxisorp plate was coated with 100µl antigen in bicarbonate coating buffer and stored at +4°C overnight. The next day the plate was washed three times with 400µl 3xPBS. The coated plate was then blocked with 400µl of 3% milk powder in 1xPBS and left at RT for 1 hour. The phage supernatant (1ml) was blocked for 30 minutes in 200µl 18% milk powder in 6xPBS. After the required time had elapsed the blocking media was aspirated from the plate (taking care not to touch the bottom of the wells) and 100µl of blocked phage was added per well and incubated at RT for 1-3 hours. Meanwhile, Rabbit anti-M13 antibody (Abcam, ab235228) and goat anti-rabbit-HRP conjugated antibody (Abcam, ab205718) were blocked with 3% milk powder in 1xPBS for 1 hour. After 1-3 hours the Maxisorp plate was washed 5x with 1xPBST (0.1% tween) then 5x with 1xPBS. 100µl of the blocked anti-M13 antibody was added per well and left at RT, static for 1 hour. This was then washed as before and 100µl of the goat anti-rabbit HRP conjugated antibody was added per well and left at RT,

static for 1 hour then washed as before. 100µl of ECL substrate was added per well, left for 30 minutes at RT then neutralised with 50µl H_2SO_4 followed by reading at 420nm on a spectrophotometer.

6.3.11 Clonal selection

Infected TG1 stocks containing phagemid were titrated and plated on 2YT-amp-glucose agar plates to achieve sufficient density for individual clone picks.

After growing overnight at 37°C, 50 individual clones were picked into 2ml deep-well plates containing 200µl 2YT with 150ug/ml ampicillin, 2% glucose and grown overnight at 300rpm, 37°C.

The next day 200µl 2YT/150µg/ml ampicillin/2% glucose was added to 50 wells of a 96-deep well plate and inoculated with 10µl of overnight culture per well.

Exphage was added at 10^9 to each well (3 µl exphage to 3ml 2YT then 20 µl to each well) and left static for 30 min then placed in a 37°C incubator and shaken for 30 min, 300rpm. The deep well plate was then centrifuged for 30 min, 1800xg for 10 minutes and the medium was aspirated being careful not to disturb the pellet. The pellet was resuspended in 200 µl 2YT, 50 µg/ml kanamycin, 150 µg/ml ampicillin and placed in a shaking incubator overnight at 30°C, 300rpm.

Glycerol stocks can be made by adding 15% glycerol to the first plate followed by subsequence storage at ≦-80°C (Freeze media is 15ml 2YT, 1.6ml glucose, 5ml glycerol)

The next day the deep well plate was centrifuge for 10 min, 1800xg, 4°C. Use 100µl supernatant in monoclonal phage ELISA.

6.3.12 Monoclonal ELISA

The polyclonal ELISA informed which round contained the peak diversity of each enriched library fraction. This was round 3 for panning against GI/GIII and round 4 for GV. Output phage from these rounds was selected and amplified as described in 6.3.9 and used as the test material in an ELISA (as

in 6.3.10) with either the homologous or heterologous antigen for the clones being tested.

6.3.13 Homologous versus heterologous binding of panned phage

In order to isolate VHH which bind uniquely to epitopes on their respective antigen, a comparative monoclonal ELISA was performed. Two plates were coated with each antigen ($G^{I/III}$ and G^{V}) and the monoclonal ELISA was performed on both plates for the respective round of clones picked. The results were overlayed to highlight if any of the selected clones had higher binding signal to a specific antigen. The clones with the largest difference in binding between their homologous antigen and the heterologous antigen were selected for sequencing so that the CDR3 could be determined.

6.3.14 Sequencing of positive clones

Positive clones were selected based on the greatest difference in ELISA signals between the homologous and heterologous antigen. These clones were then grown overnight at 37°C, 250rpm in 5ml 2YT, the next day the phagemid DNA was extracted via miniprep (2.2.5) and shipped to Eurofins Genomics (Wolverhampton, UK). CDR3 sequences were probed with the shared forward and reverse primers 5′ GCT GCA AAT GAA CAA TTT GAA GCC G 3′ and 5′ ATC AGT TTC TGT TCA GCA CCC AC 3′ respectively. These primers bind to the upstream FW3 and downstream multiple cloning site either side of the variable CDR3 gene region resulting in a 168bp sequencing read.

6.4 Results

6.4.1 Coating volume of PV for panning

Two batches each of genotypes I (Ishikawa), III (Nakayama) and V (XZ0934) were selected for their matched titre and coated at either 50 or 100µl with equal volumes bicarbonate buffer. The higher volume of PVs resulted in approximately 50% greater absorbance when compared to the reduced volume of PV. There was also less variation within the 100µl coat condition

therefore it was decided this volume of PVs would be used as the bound antigen for panning. All assay conditions were identical between the two plates aside from the varied PV coating volume.

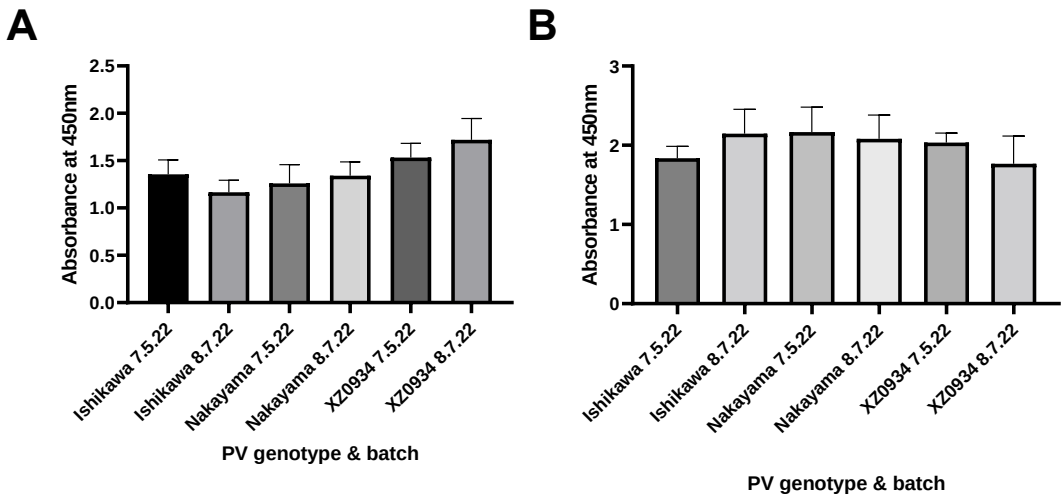

Figure 6.4. Determination of optimal coating concentration of PV. Absorbance measured from anti-JE antibody ab41671 on 100µl of three genotypes of JE-PV coated onto a Maxisorp plate. A: 50µl of JE-PV coated to a Maxisorp plate using bicarbonate buffer for 1 hour at 37°C. B: 100µl of JE-PV coated to a Maxisorp plate using a bicarbonate buffer for 1 hour at 37°C.

6.4.2 Polyclonal ELISA

Three antigens were used for panning. JE-PVs presenting envelope protein from genotypes I and III or representing V. Genotypes I and III were combined in equal titres and were panned against together. After 7 rounds of panning, the pooled output phage from every round for each of the antigens was used for a polyclonal ELISA to determine whether panning had been successful. Enrichment was show within all three panning experiments to the target antigen. The library panned against GV-PV showed the weakest enrichment compared to the other two antigens however at round 3 this represented a 3.5-fold increase in overall binding compared to binding at round 1. Round 3 was deemed the peak point of enrichment for the panning against each antigen and pooled samples from this round were taken forward for clone selection. Only $JE^{GI/III}$-PV and JE^{GV}-PV were taken forward for

clonal selection as JE-Ag was no longer required as a control.

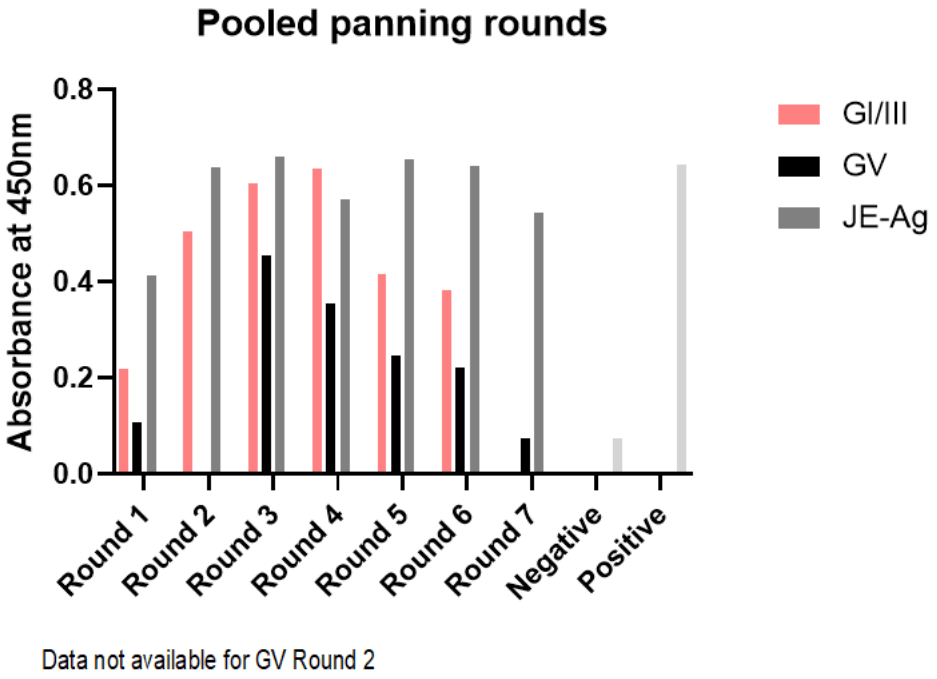

Figure 6.5. Polyclonal ELISAs of pooled output phage for each of the three antigens over seven rounds of panning showed enrichment for the target peaking at round 3 for GV-E and round 4 for GI//III E when compared to a blank (no antigen) negative control. A commercially supplied JE-E protein was used as a positive control. Data for JE^{GV}-PV round 2 were lost and therefore unavailable.

6.4.3 Homologous versus heterologous binding of panned phage

Fifty clones were picked from round 3 of the phage library panned against JE$^{GI/III}$-PV and used in a monoclonal ELISA against both the homologous and heterologous antigen. A negative cutoff value of 3SD above a blank well (no antigen but all other ELISA steps followed) was used and based on this 21/50 clones reported absorbances above this value. All positive clones except one were within 0.1OD of both antigens. Clone number 28 had a marginally higher signal for its homologous antigen GI/III than GV. All positive clones were taken forward for sequencing of the CDR3 region.

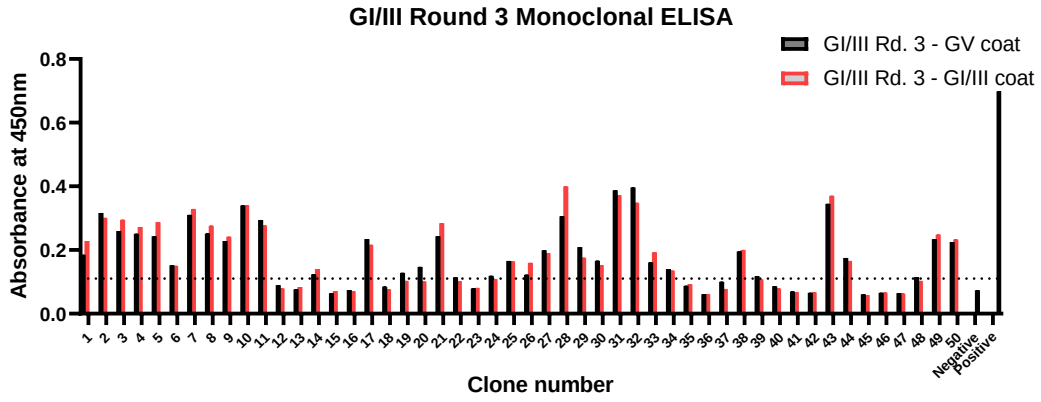

Figure 6.6. Monoclonal ELISA performed using 50 clones selected from round 3 of panning against JE$^{GI/III}$-PV. Two plates were coated with either JE$^{GI/III}$-PV or JE^{GV}-PV and individual clones tested for binding affinity to target antigen. Affinity measured as absorbance at 450nm and compared to an average triplicate blank antigen well and anti-JE-E HRP conjugated antibody used as a positive control. Cutoff value of 3SD negative control displayed as dotted line.

Fifty clones were selected from round 3 output phage panned against JE^{GV}-PV and used in a monoclonal ELISA against the homologous and heterologous antigen. Of the 50 clones picked 8 reported an OD above the negative cutoff value of 0.1. Clone 3 reported the largest difference in signal between the GV coated plate and GI/III coated plate. All 7 positive clones were selected for sequencing of the variable CDR3 region.

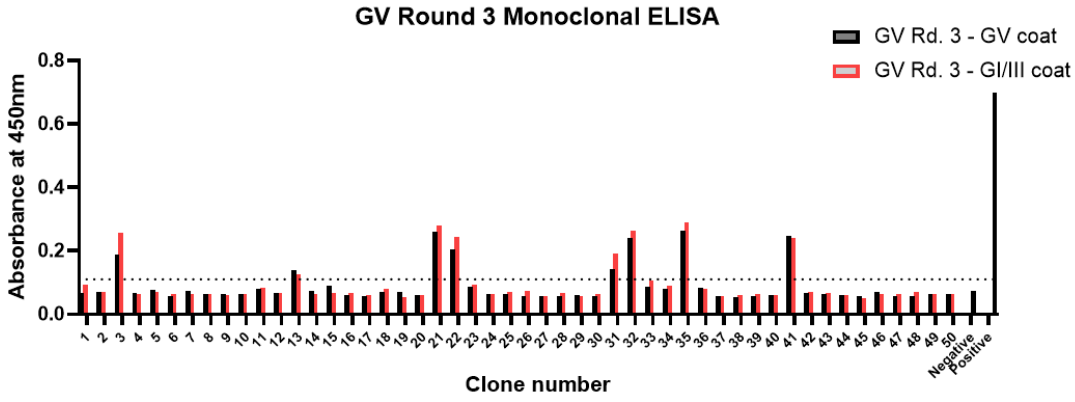

Figure 6.7. Monoclonal ELISA using 50 clones selected from round 3 of panning against JE^{GV}-PV. Two plates coated with either JE^{GV}-PV or JE$^{GI/III}$-PV. Affinity measured as absorbance at 450nm and compared to an average triplicate blank antigen well and anti-JE-E HRP conjugated antibody used as a positive control. Cutoff value of 3SD negative control displayed as dotted line.

6.4.4 Sequences of homologous VHH

Extracted DNA from the 38 binding clones from both pooled libraries were Sanger sequenced. Eight, JE^{GV}-PV panned phage all shared a common Phenylalanine at position 14 (Figure 50), the same sequence was isolated twice in clones 3 and 21, further indicating significant enrichment for true binders to the target antigen.

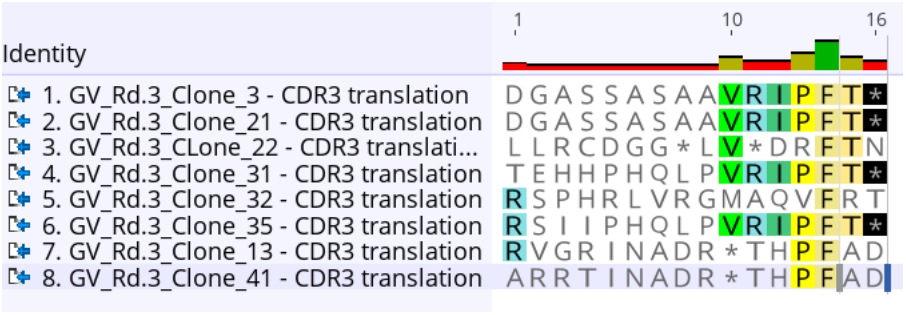

Figure 6.8. Translated CDR3 region from within 8 positive clones panned against JE^{GV}-PV. Shared amino acids are highlighted across the 8 sequences. A "PF" motif is present in 6/8 of the sequences as well as a shared Phenylalanine at position 14 in each positive sequence. Stop codon translations are marked with an asterisk, these are amber stops and, are translated into Q-Glutamine in amber-suppressor strains.

Thirty clones panned against the JE$^{GI/GIII}$-PV antigens were sequenced. A high number of partially and fully shared sequences were returned indicating strong enrichment of true binder to the target antigen. The same phenylalanine at, position 14 present in the library panned against GV was also present in this library. Further, the PF motif present in some GV clones was also present in 17/ 30 clones sequenced. Identical sequences are a positive indicator that enrichment has been successful to the target.

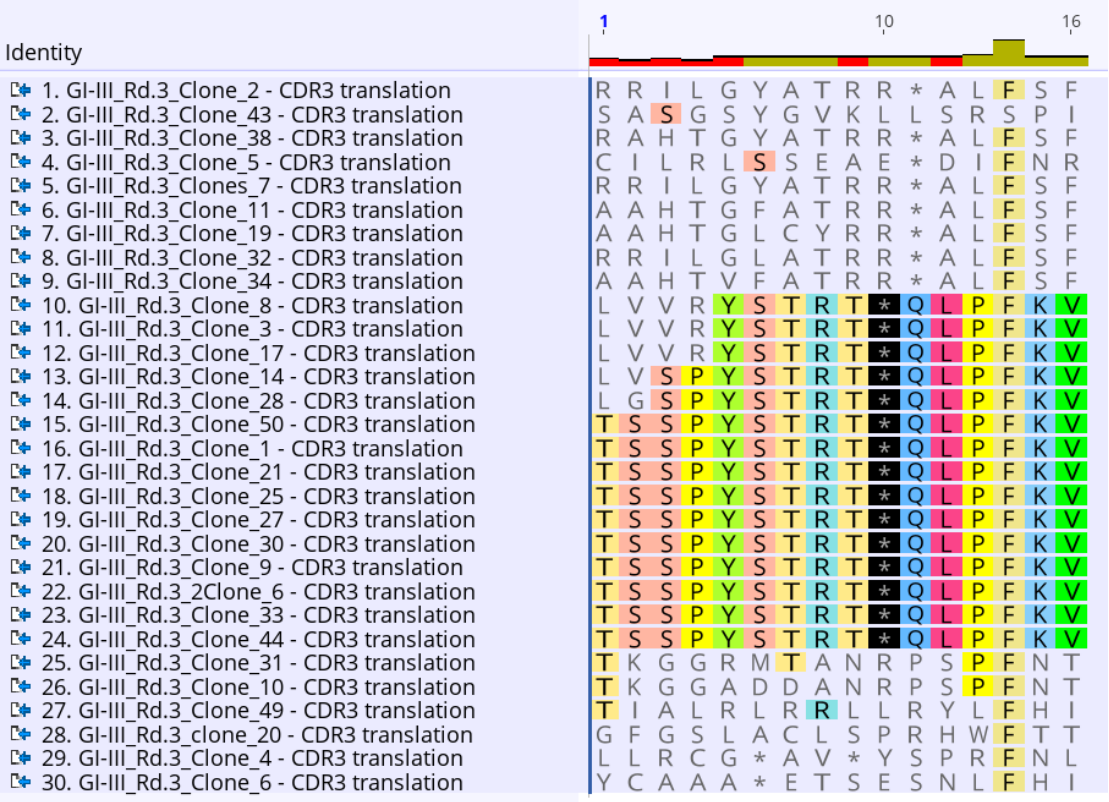

Figure 6.9. Translated CDR3 region from within 30 positive clones panned against JE$^{GI/III}$-PV. 10/30 clones shared identical CDR3 regions. All clones except clone 43 possess a Phenylalanine at position 14. A "PF" motif is the most shared amino acid pairing across the 30 positive clones, present in 17/30 sequences.

6.5 Discussion

The nanobody phage library used in this chapter is classed as a synthetic library, meaning that the diversity is generated via random DNA synthesis by utilising trimer-phosphoramidite-oligonucleotides. This method has the relative advantage of being quick to produce and resulting in a high diversity of CDR3 sequences to screen for positive binders to a target antigen, a further advantage also being that differing length CDRs can be used. The library used in these experiments contained a 16-mer CDR3, other commonly used lengths are 12 and 15. The 16-mer is closest in structure to the native antibody CDR3 however small lengths can recognise epitopes inaccessible to larger length CDRs and are useful for certain applications (Valdés-Tresanco, Molina-Zapata, Pose, & Moreno, 2022). Immune libraries are an alternative type of phage library, these are produced when an original donor animal(s) is prior immunised with a target antigen. There are relative advantages to

both methods however the synthetic library was selected for use in this research as the target epitope on the envelope protein was not known. Immune libraries are also costly and time consuming to fully construct. However, the immunisation process does produce highly specific nanobodies and can greatly reduce the number of rounds of biopanning required to select positive binders to the target antigen.

As well as the GI/III and GV panned libraries, a commercially sourced whole-inactivated JE antigen was sourced from Venture technologies, Malaysia and used as a third library antigen. This was done in order to provide a control for panning in the event that the JE-PV was unable to adequately enrich the library as a result of its low titre (See 4.5).

Polyclonal ELISA results showed enrichment of the VHH library to the three target antigens indicating that panning had successfully selected binders to these targets. The library panned against JE^{GV}-PV appeared to be the least enriched towards its target however at round 3 this represented a 3-fold increase compared to round 1. However enrichment by round 3 is often 10-100 times that of round 1 (Sidhu & Geyer, 2015). Despite this modest enrichment, selection of 50 clones from each library was performed and monoclonal ELISAs for each target antigen were carried out, these showed a strong cross-binding between most positive clones and the heterologous antigen despite the subtractive panning which had been performed at every round. For the clones panned against $JE^{GI/III}$-PV clone number 28 and for clones panned against JE^{GV}-PV, clone number 3 displayed a higher signal to their homologous target. Sequencing of the CDR3 of all clones which bound to either target antigen above the background OD cutoff was carried out. Results from this sequencing showed a mixed population of shared and unique CDR3s with a strong conservation of specific motifs. Multiple copies of the same CDR3 sequence and the selection of motifs across distinct clones strongly suggest the panning and enrichment was successful as it would be statistically improbable to randomly select for the same CDR motif from distinct clones from such a highly diverse library. Overall, 38 clones from both libraries were sequenced, of these 38, 37 possess a phenylalanine at position 14 and 23/38 possess a “PF” motif at positions 13-14. These results paired with the results obtained from the monoclonal ELISAs performed with both antigens suggest that these shared amino acid sequences have

bind to a shared epitope on the JE-E protein. This would explain the cross-binding reported in *Figure 6.6* and *Figure 6.7*.

There are other possible explanations for the cross binding reported, however. Affinity for extraneous proteins or components of the media the PVs were grown in or an affinity for the plastic the assays are performed in could be considered as alternative explanations. Binding to media components is unlikely to be the source of the cross-binding, subtractive panning was performed at every round of panning in which any phage binding to these agents were selected against. However, to confirm this assumption, an ELISA utilising these components as fixed antigens would demonstrate the affinity of the phage clones to bind to these targets and represents an element of future work.

One aspect of the work performed in this chapter which could be changed if repeated would be a more stringent purification process of JE-PVs prior to baiting the synthetic phage library, PVs were passed through a 0.45μm filter however this could have been improved by sucrose gradient purification and quantification of a standardised amount of PV to be coated onto each plate. The PV preparations used in this work were likely not entirely homogenous which contributed to the variation within results.

Another consideration is that the phage panned against each antigen are binding to shared elements of the dengue capsid of which the pseudotype is based. It has been reported previously that the density of the envelope of a PV is not always that of the wild-type virus, indeed the PVs generated in this work are difficult to detect via western blot but can be titrated via transduction of a target cell line. This may suggest that there are fewer copies of the JE-E protein incorporated around the dengue capsid than is thought. This issue would be compounded by the small nature of VHH, which as discussed previously are able to access cryptic epitopes or areas of a PV particle which are inaccessible to larger immunoglobulins. To address this, as well as PVs, a dengue capsid only condition could be included which would establish if the VHH are binding to an exposed region of capsid rather than the envelope protein and would also be suitable to test for binding to media components. The question of binding to exposed regions of the dengue capsid as the source of this could also be further explored via expression and purification of the individual VHH and measurement of their neutralisation potential in a suitable assay.

Re-cloning of the CDR3 sequences identified from positive binders to GV-E protein could be easily performed to insert this (Ministro, Manuel, & Goncalves, 2020; J. H. Zhang, Shan, Liang, Du, & Li, 2022) region into a mammalian expression vector for Fc-fusion expression in a suitable mammalian cell line (such as CHO). After Fc fusion had been achieved, a simple protein purification with protein A or G columns would then be sufficient to isolate the pure nanobodies from cell culture where they could then be tested at varying concentrations in the pseudotype virus neutralisation assay as described in the previous chapter.

6.6 Conclusion

Understanding if there are unique neutralising epitopes which exist on the GV E protein would be crucial to the design of future GV-specific vaccines should another genotype shift occur withing JEV. Nanobody phage display utilising pseudotype JEV^{GV} is an ideal methodology to investigate this.

Pseudotype JEV representing genotypes I, III and V were used to enrich a nanobody phage library and subtract cross-reactive binders from each of the phage populations. These enriched libraries were then tested for homologous and heterologous target antigen binding capacity and binders were taken forward for sequencing. Unfortunately, the neutralising potential of these nanobodies was not determined, however, in a preliminary experiment it was determined that they are produced and secreted from mammalian cells without a preceding IL2 signal sequence. To our knowledge this represents a new way in which nanobodies of this type can be produced, reducing the number of steps required for their large-scale production.

7 Discussion

In Chapter 1 it was discussed that the five genotypes of JEV represent the continuing evolution and adaption of this virus to its geographic spread. Originally evolving in Indonesia (T. Solomon et al., 2003) and spreading to its current endemic range encompassing all of southeast Asia, China and islands in the Torres strait. with a recent incursion into northern Australia (Hanna et al., 1999; van den Hurk, Pyke, Mackenzie, Hall-Mendelin, & Ritchie, 2019). The development of a highly successful inactivated virus vaccine grown in suckling mouse brains (JE-VAX) led to a drastic reduction in cases from its introduction in the 1930s. Modern versions of this vaccine have improved safety and tolerance as well as reduced cost and enhanced availability of the vaccine and has further reduced cases, particularly serious infections. However, all vaccines from the first developed to modern versions are based on genotype 3. The question has arisen as a result of the changing geographic spread of the five genotypes whether this vaccine is still suitable in the changing landscape we now face. It is well documented that since the early 2000s there has been a major shift in the predominant genotype isolated both from wild sources and human infections. Genotype I is now the most common genotype of JEV. As well as this, the once very rare genotype V is becoming more frequently isolated 3.4.1.

I initially undertook a comprehensive analysis of JEV E gene sequencing data and reconfirmed these facts, that the predominant genotype of JEV is now genotype I and that genotype V is indeed increasing in prevalence. As well as the changing genotypic landscape, other work has shown that recombinant flaviviruses are possible to generate under artificial conditions (Taucher et al., 2010). The question then arises whether this has happened already in a natural environment and if this poses a future threat to vaccine mediated protection. To address this question, I first genotyped all available JEV E gene sequences via homology within the envelope protein gene to pre-existing reference sequences for each genotype. I then performed a sliding window analysis on this dataset and identified 4 recombinants. Of these 4 recombinants, all included one genotype III parent. This was unsurprising given its prevalence in nature. However, the presence of these recombinants across

disparate time periods may suggest that recombination is not a one-off event and can occur more regularly in nature than previously thought.

Recombination analysis of this type is not without criticisms, however. The historical nature of many of these gene sequences leaves the analysis open to weaknesses caused by sequencing errors, mistakes in concatamerization of the fragments and even mislabelling of samples. The scale of the analysis presented in this work should reduce the impact of any potential bias or errors caused by the aforementioned reasons. The presence of four recombinants identified in the data spread across a wide chronological gap, matching the shift in genotype prominence supported by my own analysis makes the case that these are true recombinants and that JEV has recombined at least four times in nature. This does appear to be a rare occurrence however, and therefore the risk of recombination with live viral vaccines is negligible and should not reduce confidence in their widespread use in endemic regions.

In chapter 4, JEV-PVs representing genotype III was successfully generated using a dengue replicon system created by Matsuda et al. (2015). This three-plasmid system utilises a structural-gene deficient dengue virus genome which also contains a nano-luciferase reporter gene. The gene encoding for the capsid is present on the second plasmid as well as a selection marker conferring carbenicillin resistance. The envelope genes for the virus to be pseudotyped are included on a third plasmid.

It was established that this system is capable of generating JEV-PV in sufficient titres to be used for the development of a pseudotype neutralisation assay. Pseudotypes produced using the DENVR system are conformationally correct as determined by electron microscopy and are neutralised by JE-E protein specific antibodies. Pseudotype particles are also stable for periods up to a month at +4˚C. The methods used to produce these PVs are reliable, robust, and repeatable. These characteristics make these PVs an excellent tool for research.

Existing systems are unable to produce JE-PVs despite numerous, extensive efforts to do so (Ruiz-Jimenez et al., 2021). Methods employed to attempt this have included recombinant and chimeric glycoproteins, differing lentiviral and retroviral cores. The difficulty in producing not only JE-PVs but those from other member of the flavivirus family have been discussed at length. The prevailing view is a combination of a mismatch in the assembly location between the pseudotype system

being used and the envelope to be pseudotyped is the primary reason for either failure to pseudotype or low yield of PVs making them unusable for most applications.

JE-PVs produced with the DenVR1 system are produced at a relatively low yield, however due to the extremely bright nano-luciferase reporter, it is possible to quantify them within serological assays. This does not eliminate some of the challenges associated with their use, due to the low yield a slight reduction in batch-to-batch titre will produce a large variance in RLU measured in downstream assays. This was seen multiple times throughout development in this thesis and was the cause of many of the time-consuming optimisations required. Further improvements are required for this system to be truly repeatable and scalable however currently this is the only pseudotype system capable of producing JE-PVs.

After it was demonstrated that JE-PVs representing genotypes I, III and V could be pseudotyped using the DenVR1 system, a neutralisation assay was developed. This required the optimisation of several assay parameters including but not limited to, incubation time and temperature of antisera and pseudotype virus, concentration of all individual components, dilution series to be used, blocking step times and agents. This was a particularly time-consuming portion of the work described in this thesis, however the final assay conditions were eventually determined and confirmed that the JE-PVs were neutralised in the same way that WT-JEV is neutralised by vaccinee sera.

Vaccinee sera obtained from recipients of the BIKEN vaccine successfully neutralised JE-PVs representing genotypes I, III and V at a cutoff value of 50% neutralisation at a 1:10 serum dilution. This is indicative of a protective response (Markoff, 2000). Naïve serum did not achieve this. These data further support the idea that current generation vaccines are sufficient to continue to control JEV in the event of increased prevalence of genotype V.

Antibodies raised against the different species of flavivirus are notoriously cross reactive, leading to great difficulty in accurate diagnosis of infection given the heavy reliance on serology as the primary method of doing so. A sensitive and specific neutralisation assay utilising flavivirus pseudotype virus would greatly aid the understanding of a virus spread. There are important questions to be answered

relating to this such as whether a suspected outbreak is the result of waning immunity/ ineffective vaccination or a new flavivirus spreading into a previously unaffected area.

With a pseudotype JEV and neutralisation assay developed it was then possible to attempt to identify shared and unique epitopes across the envelope protein. This was attempted by utilising nanobody phage display. This technique has been used by other groups to achieve similar goals (Gaiotto et al., 2021). This involved several rounds of panning using JE-PVs against a naïve library. Subtractive rounds of panning were performed between each antigen binding round to try and eliminate phage binding to other parts of the PV particle as well as non-specific media components or plastic. After several rounds of panning, I performed a polyclonal ELISA and confirmed that positive selection of phage binding to the antigen of interest had occurred, shown by an increase in binding across the 7 rounds of panning. After this, the output phage from the third round was selected to be probed for monoclonal selection. Fifty clones were isolated and their ability to bind to JE-PV was tested in an ELISA.

The results from these experiments were weaker than expected, however the strongest binders were selected and amplified then subsequently extracted via miniprep and the variable CDR3 domain was sequenced. This revealed that of the 38 positive binders (across both antigen targets), a “PF” motif was present in 23 of them. This was true for both phage panned against $JE^{GI/GIII}$-PV and JE^{GV}-PV. This strongly suggest binding to a shared epitope of the envelope protein. These CDR3 sequences were subsequently cloned into a mammalian expression vector with the intention of isolating the nanobody itself and generating dimers for neutralisation tests however due to time constraints this was not possible. The testing of these sequences for their neutralisation potential should certainly be the immediate focus of any future work. Elucidating the shared and unique epitopes across the different genotypes of JEV would aid development of pan-neutralising vaccines, providing insurance against future genotypic replacement in nature and possibly reducing the impact of possible recombination events between genotypes.

8 Conclusion

The use of pseudotyping as a tool to investigate viral entry mechanics and characterise immune responses to infection is a growing field of study. These replication deficient chimeras are safe, easy to handle and relatively quick to produce, even to new infections as seen during the COVID-19 pandemic and the speed of development of SARS-CoV-2-PVs by numerous groups around the world. However not all viruses pseudotype easily, and flaviviruses are one of these groups. A large portion of this work involved the development of protocols to create and use JEV-PVs. The successful development of JEV-PVs representing genotypes I, III and V will allow for better characterisation of the differences and similarities between the envelope proteins. These methodologies will certainly be of use to future researchers wanting to investigate JEV infection and control.

Completion of the work started in this thesis relating to the isolation of the candidate VHH binders should be the primary focus of any future work, and in the longer term, production of a wider range of JEV pseudotypes eventually encompassing different flavivirus species. This would aid the development of truly specific neutralisation assays for the flaviviruses of concern to human health.

There are many questions left unanswered within flavivirus research and knowledge of JEV infection and spread. As the climate warms and populations continue to live in closer proximity to viral vectors, the incidences of JEV (and other flaviviruses) infection will continue to rise. It is therefore crucial to continue to study along with other related viruses, which can result in life changing consequences for surviving victims.

Fortunately, vaccine control of JEV is remarkably effective and data presented within this thesis suggests that this will remain the case in the near future. Long term surveillance and control efforts will be greatly aided by the continued development of better pseudotype systems and assays which utilise them to better study the entry mechanics and antibody binding efficiencies of current vaccines as well as to produce the theoretical products of numerous hypothetical recombination events to assess if this poses any significant threat to the continued vaccine control of JEV.

9 References

Alcon-LePoder, S., Drouet, M. T., Roux, P., Frenkiel, M. P., Arborio, M., Durand-Schneider, A. M., . . . Flamand, M. (2005). The secreted form of dengue virus nonstructural protein NS1 is endocytosed by hepatocytes and accumulates in late endosomes: implications for viral infectivity. *J Virol, 79*(17), 11403-11411. doi:10.1128/JVI.79.17.11403-11411.2005

Almagro, J. C., Pedraza-Escalona, M., Arrieta, H. I., & Perez-Tapia, S. M. (2019). Phage Display Libraries for Antibody Therapeutic Discovery and Development. *Antibodies (Basel), 8*(3). doi:10.3390/antib8030044

Angkeow, J. W., Monaco, D. R., Chen, A., Venkataraman, T., Jayaraman, S., Valencia, C., . . . Larman, H. B. (2022). Phage display of environmental protein toxins and virulence factors reveals the prevalence, persistence, and genetics of antibody responses. *Immunity, 55*(6), 1051-1066 e1054. doi:10.1016/j.immuni.2022.05.002

Baek, H., Suk, K.-h., Kim, Y.-h., & Cha, S. (2002). An improved helper phage system for efficient isolation of specific antibody molecules in phage display. *Nucleic acids research, 30*(5), e18-e18.

Bazan, J., Calkosinski, I., & Gamian, A. (2012). Phage display--a powerful technique for immunotherapy: 1. Introduction and potential of therapeutic applications. *Hum Vaccin Immunother, 8*(12), 1817-1828. doi:10.4161/hv.21703

Blazevic, J., Rouha, H., Bradt, V., Heinz, F. X., & Stiasny, K. (2016). Membrane Anchors of the Structural Flavivirus Proteins and Their Role in Virus Assembly. *J Virol, 90*(14), 6365-6378. doi:10.1128/JVI.00447-16

Brien, J. D., Austin, S. K., Sukupolvi-Petty, S., O'Brien, K. M., Johnson, S., Fremont, D. H., & Diamond, M. S. (2010). Genotype-specific neutralization and protection by antibodies against dengue virus type 3. *Journal of Virology, 84*(20), 10630-10643.

Campbell, G. L., Hills, S. L., Fischer, M., Jacobson, J. A., Hoke, C. H., Hombach, J. M., . . . Ginsburg, A. S. (2011). Estimated global incidence of Japanese encephalitis: a systematic review. *Bull World Health Organ, 89*(10), 766-774, 774A-774E. doi:10.2471/BLT.10.085233

Cao, L., Fu, S., Gao, X., Li, M., Cui, S., Li, X., . . . Liang, G. (2016). Low Protective Efficacy of the Current Japanese Encephalitis Vaccine against the Emerging Genotype 5 Japanese Encephalitis Virus. *PLoS Negl Trop Dis, 10*(5), e0004686. doi:10.1371/journal.pntd.0004686

Carney, J., Daly, J. M., Nisalak, A., & Solomon, T. (2012). Recombination and positive selection identified in complete genome sequences of Japanese encephalitis virus. *Arch Virol, 157*(1), 75-83. doi:10.1007/s00705-011-1143-4

Cha, G. W., Lee, E. J., Lim, E. J., Sin, K. S., Park, W. W., Jeon, D. Y., . . . Jeong, Y. E. (2015). A novel immunochromatographic test applied to a serological survey of Japanese encephalitis virus on pig farms in Korea. *PLoS One, 10*(5), e0127313. doi:10.1371/journal.pone.0127313

Chambers, T. J. H., C.S.; Galler, R.; Rice, C.M. (1990). Flavivirus genome organisation, expression and replication. *Annual Reviews in Microbiology*(44), 649-688.

Chang, Y.-S., Liao, C.-L., Tsao, C.-H., Chen, M.-C., Liu, C.-I., Chen, L.-K., & Lin, Y.-L. (1999). Membrane permeabilization by small hydrophobic nonstructural proteins of Japanese encephalitis virus. *Journal of Virology, 73*(8), 6257-6264.

Ciczora, Y., Callens, N., Seron, K., Rouille, Y., & Dubuisson, J. (2010). Identification of a dominant endoplasmic reticulum-retention signal in yellow fever virus pre-membrane protein. *J Gen Virol, 91*(Pt 2), 404-414. doi:10.1099/vir.0.015339-0

Cooke, S. J., Coates, K., Barton, C. H., Biggs, T. E., Barrett, S. J., Cochrane, A., . . . Mann, D. A. (1997). Regulated expression vectors demonstrate cell-type-specific sensitivity to human immunodeficiency virus type 1 Nef-induced cytostasis. *Journal of General Virology, 78*(2), 381-392.

de Wispelaere, M., Frenkiel, M. P., & Despres, P. (2015). A Japanese encephalitis virus genotype 5 molecular clone is highly neuropathogenic in a mouse model: impact of the structural protein region on virulence. *J Virol, 89*(11), 5862-5875. doi:10.1128/JVI.00358-15

de Wispelaere, M., Ricklin, M., Souque, P., Frenkiel, M. P., Paulous, S., Garcia-Nicolas, O., . . . Despres, P. (2015). A Lentiviral Vector Expressing Japanese Encephalitis Virus-like Particles Elicits Broad Neutralizing Antibody Response in Pigs. *PLoS Negl Trop Dis, 9*(10), e0004081. doi:10.1371/journal.pntd.0004081

Dermendjieva, M., Donald, C., Kohl, A., & Evans, D. (2020). Recombination between African and Asian lineages of Zika virus in vitro and its consequences for viral phenotype. *Access Microbiology, 2*(7A), 790.

Dermendjieva, M., Donald, C., Kohl, A., & Evans, D. (2022). Recombination, and Then What? How Zika Virus Hybrids Improve Their Fitness: Microbiology Society.

Diallo, A. O. I., Chevalier, V., Cappelle, J., Duong, V., Fontenille, D., & Duboz, R. (2018). How much does direct transmission between pigs contribute to Japanese Encephalitis virus circulation? A modelling approach in Cambodia. *PLoS One, 13*(8), e0201209. doi:10.1371/journal.pone.0201209

Do, L. P., Bui, T. M., Hasebe, F., Morita, K., & Phan, N. T. (2015). Molecular epidemiology of Japanese encephalitis in northern Vietnam, 1964-2011: genotype replacement. *Virol J, 12*, 51. doi:10.1186/s12985-015-0278-4

Do, L. P., Bui, T. M., & Phan, N. T. (2016). Mechanism of Japanese encephalitis virus genotypes replacement based on human, porcine and mosquito-originated cell lines model. *Asian Pac J Trop Med, 9*(4), 333-336. doi:10.1016/j.apjtm.2016.03.007

Dowd, K. A., DeMaso, C. R., Pelc, R. S., Speer, S. D., Smith, A. R. Y., Goo, L., . . . Pierson, T. C. (2016). Broadly Neutralizing Activity of Zika Virus-Immune Sera Identifies a Single Viral Serotype. *Cell Rep, 16*(6), 1485-1491. doi:10.1016/j.celrep.2016.07.049

Dumoulin, F. L., von dem Bussche, A., Li, J., Khamzina, L., Wands, J. R., Sauerbruch, T., & Spengler, U. (2003). Hepatitis C virus NS2 protein inhibits gene expression from different cellular and viral promoters in hepatic and nonhepatic cell lines. *Virology, 305*(2), 260-266. doi:10.1006/viro.2002.1701

England, C. G., Ehlerding, E. B., & Cai, W. (2016). NanoLuc: A Small Luciferase Is Brightening Up the Field of Bioluminescence. *Bioconjug Chem, 27*(5), 1175-1187. doi:10.1021/acs.bioconjchem.6b00112

Erlanger, T. E., Weiss, S., Keiser, J., Utzinger, J., & Wiedenmayer, K. (2009). Past, present, and future of Japanese encephalitis. *Emerg Infect Dis, 15*(1), 1-7. doi:10.3201/eid1501.080311

Ferguson, M., Johnes, S., Li, L., Heath, A., & Barrett, A. (2008). Effect of genomic variation in the challenge virus on the neutralization titres of recipients of inactivated JE vaccines--report of a collaborative study on PRNT50 assays for Japanese encephalitis virus (JE) antibodies. *Biologicals, 36*(2), 111-116. doi:10.1016/j.biologicals.2007.07.002

Fernandez-Gacio, A., Uguen, M., & Fastrez, J. (2003). Phage display as a tool for the directed evolution of enzymes. *Trends Biotechnol, 21*(9), 408-414. doi:10.1016/S0167-7799(03)00194-X

Fernandez, E., Kose, N., Edeling, M. A., Adhikari, J., Sapparapu, G., Lazarte, S. M., . . . Diamond, M. S. (2018). Mouse and Human Monoclonal Antibodies Protect against Infection by Multiple Genotypes of Japanese Encephalitis Virus. *mBio, 9*(1). doi:10.1128/mBio.00008-18

Ferrara, F., & Temperton, N. (2018). Pseudotype Neutralization Assays: From Laboratory Bench to Data Analysis. *Methods Protoc, 1*(1). doi:10.3390/mps1010008

Floridis, J., McGuinness, S. L., Kurucz, N., Burrow, J. N., Baird, R., & Francis, J. R. (2018). Murray Valley Encephalitis Virus: An Ongoing Cause of Encephalitis in Australia's North. *Trop Med Infect Dis, 3*(2). doi:10.3390/tropicalmed3020049

Fritz, R., Blazevic, J., Taucher, C., Pangerl, K., Heinz, F. X., & Stiasny, K. (2011). The unique transmembrane hairpin of flavivirus fusion protein E is essential for membrane fusion. *J Virol, 85*(9), 4377-4385. doi:10.1128/JVI.02458-10

Gaiotto, T., Ramage, W., Ball, C., Risley, P., Carnell, G. W., Temperton, N., . . . Hufton, S. E. (2021). Nanobodies mapped to cross-reactive and divergent epitopes on A(H7N9) influenza hemagglutinin using yeast display. *Sci Rep, 11*(1), 3126. doi:10.1038/s41598-021-82356-4

Gallichotte, E. N., Baric, T. J., Nivarthi, U., Delacruz, M. J., Graham, R., Widman, D. G., . . . de Silva, A. M. (2018). Genetic variation between dengue virus type 4 strains impacts human antibody binding and neutralization. *Cell reports, 25*(5), 1214-1224.

Gao, X., Liu, H., Li, X., Fu, S., Cao, L., Shao, N., . . . Liang, G. (2019). Changing Geographic Distribution of Japanese Encephalitis Virus Genotypes, 1935-2017. *Vector Borne Zoonotic Dis, 19*(1), 35-44. doi:10.1089/vbz.2018.2291

Gerold, G., Bruening, J., Weigel, B., & Pietschmann, T. (2017). Protein interactions during the flavivirus and hepacivirus life cycle. *Molecular & Cellular Proteomics, 16*(4 suppl 1), S75-S91.

Gould, E. A., & Solomon, T. (2008). Pathogenic flaviviruses. *The Lancet, 371*(9611), 500-509. doi:10.1016/s0140-6736(08)60238-x

Gromowski, G. D., Firestone, C. Y., & Whitehead, S. S. (2015). Genetic Determinants of Japanese Encephalitis Virus Vaccine Strain SA14-14-2 That Govern Attenuation of Virulence in Mice. *J Virol, 89*(12), 6328-6337. doi:10.1128/JVI.00219-15

Hahn, C. S., Hahn, Y. S., Rice, C. M., Lee, E., Dalgarno, L., Strauss, E. G., & Strauss, J. H. (1987). Conserved elements in the 3′ untranslated region of flavivirus RNAs and potential cyclization sequences. *Journal of molecular biology, 198*(1), 33-41.

Hahn, C. S., Lustig, S., Strauss, E. G., & Strauss, J. H. (1988). Western equine encephalitis virus is a recombinant virus. *Proceedings of the National Academy of Sciences, 85*(16), 5997-6001.

Hameed, M., Wahaab, A., Nawaz, M., Khan, S., Nazir, J., Liu, K., . . . Ma, Z. (2021). Potential Role of Birds in Japanese Encephalitis Virus Zoonotic Transmission and Genotype Shift. *Viruses, 13*(3). doi:10.3390/v13030357

Han, N., Adams, J., Chen, P., Guo, Z. Y., Zhong, X. F., Fang, W., . . . Rayner, S. (2014). Comparison of genotypes I and III in Japanese encephalitis virus reveals distinct differences in their genetic and host diversity. *J Virol, 88*(19), 11469-11479. doi:10.1128/JVI.02050-14

Han, N., Adams, J., Fang, W., Liu, S. Q., & Rayner, S. (2015). Investigation of the genotype III to genotype I shift in Japanese encephalitis virus and the impact on human cases. *Virol Sin, 30*(4), 277-289. doi:10.1007/s12250-015-3621-4

Hanna, J. N., Ritchie, S. A., Phillips, D. A., Lee, J. M., Hills, S. L., Van der Hurk, A. F., . . . Mackenzie, J. S. (1999). Japanese encephalitis in north Queensland, Australia, 1998. *Medical Journal of Australia, 170*.

Hay, I. D., & Lithgow, T. (2019). Filamentous phages: masters of a microbial sharing economy. *EMBO Rep, 20*(6). doi:10.15252/embr.201847427

Hierholzer, J., & Killington, R. (1996). Virus isolation and quantitation *Virology methods manual* (pp. 25-46): Elsevier.

Honjo, S., Masuda, M., & Ishikawa, T. (2019). Effects of the Japanese Encephalitis Virus Genotype V-Derived Sub-Viral Particles on the Immunogenicity of the Vaccine Characterized by a Novel Virus-Like Particle-Based Assay. *Vaccines (Basel), 7*(3). doi:10.3390/vaccines7030081

Jin, B. K., Odongo, S., Radwanska, M., & Magez, S. (2023). Nanobodies: A Review of Generation, Diagnostics and Therapeutics. *Int J Mol Sci, 24*(6). doi:10.3390/ijms24065994

Kalia, M., Chandra, V., Rahman, S. A., Sehgal, D., & Jameel, S. (2009). Heparan sulfate proteoglycans are required for cellular binding of the hepatitis E virus ORF2 capsid protein and for viral infection. *J Virol, 83*(24), 12714-12724. doi:10.1128/JVI.00717-09

Karna, A. K., & Bowen, R. A. (2019). Experimental Evaluation of the Role of Ecologically-Relevant Hosts and Vectors in Japanese Encephalitis Virus Genotype Displacement. *Viruses, 11*(1). doi:10.3390/v11010032

Kell, A. M., Wargo, A. R., & Kurath, G. (2014). Viral fitness does not correlate with three genotype displacement events involving infectious hematopoietic necrosis virus. *Virology, 464-465*, 146-155. doi:10.1016/j.virol.2014.07.003

Khromykh, A. A., Meka, H., Guyatt, K. J., & Westaway, E. G. (2001). Essential role of cyclization sequences in flavivirus RNA replication. *J Virol, 75*(14), 6719-6728. doi:10.1128/JVI.75.14.6719-6728.2001

Kilpatrick, A. M., Meola, M. A., Moudy, R. M., & Kramer, L. D. (2008). Temperature, viral genetics, and the transmission of West Nile virus by Culex pipiens mosquitoes. *PLoS Pathog, 4*(6), e1000092. doi:10.1371/journal.ppat.1000092

Kim, J. M., Yun, S. I., Song, B. H., Hahn, Y. S., Lee, C. H., Oh, H. W., & Lee, Y. M. (2008). A single N-linked glycosylation site in the Japanese encephalitis virus prM protein is critical for cell type-specific prM protein biogenesis, virus particle release, and pathogenicity in mice. *J Virol, 82*(16), 7846-7862. doi:10.1128/JVI.00789-08

King, B., Temperton, N. J., Grehan, K., Scott, S. D., Wright, E., Tarr, A. W., & Daly, J. M. (2016). Technical considerations for the generation of novel pseudotyped viruses. *Future Virology, 11*(1), 47-59. doi:10.2217/fvl.15.106

Kretschmer, M., Kadlubowska, P., Hoffmann, D., Schwalbe, B., Auerswald, H., & Schreiber, M. (2020). Zikavirus prME Envelope Pseudotyped Human Immunodeficiency Virus Type-1 as a Novel Tool for Glioblastoma-Directed Virotherapy. *Cancers, 12*(4), 1000. doi:10.3390/cancers12041000

Lee, H. J., Min, K. I., Lee, J., Kang, S. H., Jeon, W., Nam, J. H., . . . Kim, Y. B. (2009). The prM-independent packaging of pseudotyped Japanese encephalitis virus. *Virol J, 6*, 115. doi:10.1186/1743-422X-6-115

Lee, H. J., Min, K. I., Park, K. H., Choi, H. J., Kim, M. K., Ahn, C. Y., . . . Kim, Y. B. (2014). Comparison of JEV neutralization assay using pseudotyped JEV with the conventional plaque-reduction neutralization test. *J Microbiol, 52*(5), 435-440. doi:10.1007/s12275-014-3529-y

Li, Y., Wang, M., Wu, H., Zhao, H., Dong, L., Li, Y., . . . Kang, X. (2022). Development of a rapid neutralizing antibody test for SARS-CoV-2 and its application for neutralizing antibody screening and vaccinated serum testing. *Infectious Medicine, 1*(2), 95-102. doi:10.1016/j.imj.2022.04.003

Lin, Y.-J., & Wu, S.-C. (2005). Histidine at Residue 99 and the Transmembrane Region of the Precursor Membrane prM Protein Are Important for the prM-E Heterodimeric Complex Formation of Japanese Encephalitis Virus. *Journal of Virology, 79*(13), 8535-8544. doi:10.1128/jvi.79.13.8535-8544.2005

Liu, H., Wu, R., Yuan, L., Tian, G., Huang, X., Wen, Y., . . . Wen, X. (2017). Introducing a cleavable signal peptide enhances the packaging efficiency of lentiviral vectors pseudotyped with Japanese encephalitis virus envelope proteins. *Virus Res, 229*, 9-16. doi:10.1016/j.virusres.2016.12.007

Liu, H., Zhang, J., Niu, Y., & Liang, G. (2021). The 5' and 3' Untranslated Regions of the Japanese Encephalitis Virus (JEV): Molecular Genetics and Higher Order Structures. *Front Microbiol, 12*, 730045. doi:10.3389/fmicb.2021.730045

Luca, V. C., AbiMansour, J., Nelson, C. A., & Fremont, D. H. (2012). Crystal structure of the Japanese encephalitis virus envelope protein. *J Virol, 86*(4), 2337-2346. doi:10.1128/JVI.06072-11

Lukic, Z., & Campbell, E. M. (2012). The cell biology of TRIM5α. *Curr HIV/AIDS Rep, 9*(1), 73-80. doi:10.1007/s11904-011-0102-8

Mandl, C. W., Heinz, F. X., & Kunz, C. (1988). Sequence of the structural proteins of tick-borne encephalitis virus (western subtype) and comparative analysis with other flaviviruses. *Virology, 166*(1), 197-205.

Markoff, L. (2000). Points to consider in the development of a surrogate for efficacy of novel Japanese encephalitis virus vaccines. *Vaccine, 18*, 26-32.

Mather, S. T. (2017). *Development of pseudotyped virus assays for the serological study of Japanese encephalitis flavivirus*: University of Kent (United Kingdom).
Matsuda, M., Yamanaka, A., Yato, K., Yoshii, K., Watashi, K., Aizaki, H., . . . Suzuki, R. (2018). High-throughput neutralization assay for multiple flaviviruses based on single-round infectious particles using dengue virus type 1 reporter replicon. *Sci Rep, 8*(1), 16624. doi:10.1038/s41598-018-34865-y
Mercier-Delarue, S., Durier, C., Colin de Verdiere, N., Poveda, J. D., Meiffredy, V., Fernandez Garcia, M. D., . . . Simon, F. (2017). Screening test for neutralizing antibodies against yellow fever virus, based on a flavivirus pseudotype. *PLoS One, 12*(5), e0177882. doi:10.1371/journal.pone.0177882
Ministro, J., Manuel, A. M., & Goncalves, J. (2020). Therapeutic Antibody Engineering and Selection Strategies. In A. C. Silva, J. N. Moreira, J. M. S. Lobo, & H. Almeida (Eds.), *Current Applications of Pharmaceutical Biotechnology* (pp. 55-86). Cham: Springer International Publishing.
Mohammed, M. A., Galbraith, S. E., Radford, A. D., Dove, W., Takasaki, T., Kurane, I., & Solomon, T. (2011). Molecular phylogenetic and evolutionary analyses of Muar strain of Japanese encephalitis virus reveal it is the missing fifth genotype. *Infect Genet Evol, 11*(5), 855-862. doi:10.1016/j.meegid.2011.01.020
Mukhopadhyay, L., Gupta, N., Yadav, P. D., & Aggarwal, N. (2022). Neutralization assays for SARS-CoV-2: Implications for assessment of protective efficacy of COVID-19 vaccines. *Indian J Med Res, 155*(1), 105-122. doi:10.4103/ijmr.ijmr_2544_21
Mukhopadhyay, S., Kuhn, R. J., & Rossmann, M. G. (2005). A structural perspective of the flavivirus life cycle. *Nat Rev Microbiol, 3*(1), 13-22. doi:10.1038/nrmicro1067
Nabeshima, T., Loan, H. T. K., Inoue, S., Sumiyoshi, M., Haruta, Y., Nga, P. T., . . . Morita, K. (2009). Evidence of frequent introductions of Japanese encephalitis virus from south-east Asia and continental east Asia to Japan. *J Gen Virol, 90*(Pt 4), 827-832. doi:10.1099/vir.0.007617-0
Ng, W. C., Soto-Acosta, R., Bradrick, S. S., Garcia-Blanco, M. A., & Ooi, E. E. (2017). The 5' and 3' Untranslated Regions of the Flaviviral Genome. *Viruses, 9*(6). doi:10.3390/v9060137
Nitatpattana, N., Dubot-Peres, A., Gouilh, M. A., Souris, M., Barbazan, P., Yoksan, S., . . . Gonzalez, J. P. (2008). Change in Japanese encephalitis virus distribution, Thailand. *Emerg Infect Dis, 14*(11), 1762-1765. doi:10.3201/eid1411.080542
Niu, J., Jiang, Y., Xu, H., Zhao, C., Zhou, G., Chen, P., & Cao, R. (2018). TIM-1 Promotes Japanese Encephalitis Virus Entry and Infection. *Viruses, 10*(11). doi:10.3390/v10110630
Nowak, T., & Wengler, G. (1987). Analysis of disulfides present in the membrane proteins of the West Nile flavivirus. *Virology, 156*(1), 127-137.
O'Donnell, C. D., & Shukla, D. (2008). The Importance of Heparan Sulfate in Herpesvirus Infection. *Virol Sin, 23*(6), 383-393. doi:10.1007/s12250-008-2992-1
Pacca, C. C., Severino, A. A., Mondini, A., Rahal, P., D'Avila S, G., Cordeiro, J. A., . . . Nogueira, M. L. (2009). RNA interference inhibits yellow fever virus replication in vitro and in vivo. *Virus genes, 38*(2), 224-231. doi:10.1007/s11262-009-0328-3
Pan, X. L., Liu, H., Wang, H. Y., Fu, S. H., Liu, H. Z., Zhang, H. L., . . . Liang, G. D. (2011). Emergence of genotype I of Japanese encephalitis virus as the dominant genotype in Asia. *J Virol, 85*(19), 9847-9853. doi:10.1128/JVI.00825-11
Panagides, N., Zacchi, L. F., De Souza, M. J., Morales, R. A. V., Karnowski, A., Liddament, M. T., . . . Fercher, C. (2022). Evaluation of Phage Display Biopanning Strategies for the Selection of Anti-Cell Surface Receptor Antibodies. *Int J Mol Sci, 23*(15). doi:10.3390/ijms23158470
Panda, K., Alagarasu, K., & Parashar, D. (2021). Oligonucleotide-Based Approaches to Inhibit Dengue Virus Replication. *Molecules, 26*(4), 956.
Partridge, J., Ghimire, P., Sedai, T., Bista, M. B., & Banerjee, M. (2007). Endemic Japanese encephalitis in the Kathmandu valley, Nepal. *The American journal of tropical medicine and hygiene, 77*(6), 1146-1149.

Plourde, A. R., & Bloch, E. M. (2016). A Literature Review of Zika Virus. *Emerg Infect Dis, 22*(7), 1185-1192. doi:10.3201/eid2207.151990
Poonsiri, T., Wright, G. S. A., Solomon, T., & Antonyuk, S. V. (2019). Crystal Structure of the Japanese Encephalitis Virus Capsid Protein. *Viruses, 11*(7). doi:10.3390/v11070623
Pothin, E., Lesuisse, D., & Lafaye, P. (2020). Brain Delivery of Single-Domain Antibodies: A Focus on VHH and VNAR. *Pharmaceutics, 12*(10). doi:10.3390/pharmaceutics12100937
Rajaiah, P., & Kumar, A. (2022). Japanese encephalitis virus in India: An update on virus genotypes. *Indian J Med Res, 156*(4&5), 588-597. doi:10.4103/ijmr.IJMR_2606_19
Rey, F. A., Heinz, F. X., Mandl, C., Kunz, C., & Harrison, S. C. (1995). The envelope glycoprotein from tick-borne encephalitis virus at 2 Å resolution. *Nature, 375*(6529), 291-298.
Ruiz-Jimenez, F., Perez-Olais, J. H., Raymond, C., King, B. J., McClure, C. P., Urbanowicz, R. A., & Ball, J. K. (2021). Challenges on the development of a pseudotyping assay for Zika glycoproteins. *J Med Microbiol, 70*(9). doi:10.1099/jmm.0.001413
Saito, M., Taira, K., Itokazu, K., & Mori, N. (2007). Recent change of the antigenicity and genotype of Japanese encephalitis viruses distributed on Okinawa Island, Japan. *The American journal of tropical medicine and hygiene, 77*(4), 737-746.
Salminen, M. O., Carr, J. K., Burke, D. S., & McCUTCHAN, F. E. (1995). Identification of breakpoints in intergenotypic recombinants of HIV type 1 by bootscanning. *AIDS research and human retroviruses, 11*(11), 1423-1425.
Schmidt, O., & Teis, D. (2012). The ESCRT machinery. *Curr Biol, 22*(4), R116-120. doi:10.1016/j.cub.2012.01.028
Schuh, A. J., Guzman, H., Tesh, R. B., & Barrett, A. D. (2013). Genetic diversity of Japanese encephalitis virus isolates obtained from the Indonesian archipelago between 1974 and 1987. *Vector Borne Zoonotic Dis, 13*(7), 479-488. doi:10.1089/vbz.2011.0870
Schuh, A. J., Ward, M. J., Brown, A. J. L., & Barrett, A. D. (2014). Dynamics of the emergence and establishment of a newly dominant genotype of Japanese encephalitis virus throughout Asia. *Journal of Virology, 88*(8), 4522-4532.
Sidhu, S. S., & Geyer, C. R. (2015). *Phage display in biotechnology and drug discovery*: CRC Press.
Smit, J. M., Moesker, B., Rodenhuis-Zybert, I., & Wilschut, J. (2011). Flavivirus cell entry and membrane fusion. *Viruses, 3*(2), 160-171. doi:10.3390/v3020160
Smith, G. P. (1985). Filamentous fusion phage: novel expression vectors that display cloned antigens on the virion surface. *Science, 228*(4705), 1315-1317.
Solomon, T., Ni, H., Beasley, D. W., Ekkelenkamp, M., Cardosa, M. J., & Barrett, A. D. (2003). Origin and evolution of Japanese encephalitis virus in southeast Asia. *J Virol, 77*(5), 3091-3098. doi:10.1128/jvi.77.5.3091-3098.2003
Solomon, T. M. D., N.; Kneen, R.; Gainsborough, M.; Vaughn, D.W; & Thi Khanh, V. (2000). Japanese Encephalitis. *Journal of Neurology, Neurosurgery and Psychiatry*(68), 405-415.
Suzuki, R., Ishikawa, T., Konishi, E., Matsuda, M., Watashi, K., Aizaki, H., . . . Wakita, T. (2014). Production of single-round infectious chimeric flaviviruses with DNA-based Japanese encephalitis virus replicon. *J Gen Virol, 95*(Pt 1), 60-65. doi:10.1099/vir.0.058008-0
Tajima, S., Shibasaki, K. I., Taniguchi, S., Nakayama, E., Maeki, T., Lim, C. K., & Saijo, M. (2019). E and prM proteins of genotype V Japanese encephalitis virus are required for its increased virulence in mice. *Heliyon, 5*(11), e02882. doi:10.1016/j.heliyon.2019.e02882
Takhampunya, R., Kim, H. C., Tippayachai, B., Kengluecha, A., Klein, T. A., Lee, W. J., . . . Evans, B. P. (2011). Emergence of Japanese encephalitis virus genotype V in the Republic of Korea. *Virology Journal, 8*(449).
Tang, W. F., Ogawa, M., Eshita, Y., Aono, H., & Makino, Y. (2010). Molecular evolution of Japanese encephalitis virus isolates from swine in Oita, Japan during 1980-2009. *Infect Genet Evol, 10*(2), 329-336. doi:10.1016/j.meegid.2009.12.005

Tani, H., Morikawa, S., & Matsuura, Y. (2011). Development and Applications of VSV Vectors Based on Cell Tropism. *Front Microbiol, 2*, 272. doi:10.3389/fmicb.2011.00272
Tani, H., Shiokawa, M., Kaname, Y., Kambara, H., Mori, Y., Abe, T., . . . Matsuura, Y. (2010). Involvement of ceramide in the propagation of Japanese encephalitis virus. *J Virol, 84*(6), 2798-2807. doi:10.1128/JVI.02499-09
Taucher, C., Berger, A., & Mandl, C. W. (2010). A trans-complementing recombination trap demonstrates a low propensity of flaviviruses for intermolecular recombination. *J Virol, 84*(1), 599-611. doi:10.1128/JVI.01063-09
Tijani, M., Munis, A. M., Perry, C., Sanber, K., Ferraresso, M., Mukhopadhyay, T., . . . Takeuchi, Y. (2018). Lentivector Producer Cell Lines with Stably Expressed Vesiculovirus Envelopes. *Mol Ther Methods Clin Dev, 10*, 303-312. doi:10.1016/j.omtm.2018.07.013
Tsai, T. F. (1993). Inactivated Japanese encephalitis virus vaccine; recommendations of the Advisory Committee on Immunization Practices (ACIP).
Tsarev, S., Sanders, M., Vaughn, D., & Innis, B. (2000). Phylogenetic analysis suggests only one serotype of Japanese encephalitis virus. *Vaccine, 18*, 36-43.
Tsoumpeli, M. T., Gray, A., Parsons, A. L., Spiliotopoulos, A., Owen, J. P., Bishop, K., . . . Gough, K. C. (2022). A Simple Whole-Plasmid PCR Method to Construct High-Diversity Synthetic Phage Display Libraries. *Mol Biotechnol, 64*(7), 791-803. doi:10.1007/s12033-021-00442-4
Twiddy, S. S., & Holmes, E. C. (2003). The extent of homologous recombination in members of the genus Flavivirus. *J Gen Virol, 84*(Pt 2), 429-440. doi:10.1099/vir.0.18660-0
Usami, Y., Wu, Y., & Gottlinger, H. G. (2015). SERINC3 and SERINC5 restrict HIV-1 infectivity and are counteracted by Nef. *Nature, 526*(7572), 218-223. doi:10.1038/nature15400
Usami, Y., Wu, Y., & Göttlinger, H. G. (2015). SERINC3 and SERINC5 restrict HIV-1 infectivity and are counteracted by Nef. *Nature, 526*(7572), 218-223.
Valdés-Tresanco, M. S., Molina-Zapata, A., Pose, A. G., & Moreno, E. (2022). Structural Insights into the Design of Synthetic Nanobody Libraries. *Molecules, 27*(7). doi:10.3390/molecules27072198
van den Hurk, A. F., Pyke, A. T., Mackenzie, J. S., Hall-Mendelin, S., & Ritchie, S. A. (2019). Japanese Encephalitis Virus in Australia: From Known Known to Known Unknown. *Trop Med Infect Dis, 4*(1). doi:10.3390/tropicalmed4010038
Van Gessel, Y., Klade, C. S., Putnak, R., Formica, A., Krasaesub, S., Spruth, M., . . . Dewasthaly, S. (2011). Correlation of protection against Japanese encephalitis virus and JE vaccine (IXIARO((R))) induced neutralizing antibody titers. *Vaccine, 29*(35), 5925-5931. doi:10.1016/j.vaccine.2011.06.062
Van Gessel, Y., Klade, C. S., Putnak, R., Formica, A., Krasaesub, S., Spruth, M., . . . Dewasthaly, S. (2011). Correlation of protection against Japanese encephalitis virus and JE vaccine (IXIARO®) induced neutralizing antibody titers. *Vaccine, 29*(35), 5925-5931.
Villordo, S. M., Alvarez, D. E., & Gamarnik, A. V. (2010). A balance between circular and linear forms of the dengue virus genome is crucial for viral replication. *RNA, 16*(12), 2325-2335. doi:10.1261/rna.2120410
Villordo, S. M., & Gamarnik, A. V. (2009). Genome cyclization as strategy for flavivirus RNA replication. *Virus Res, 139*(2), 230-239. doi:10.1016/j.virusres.2008.07.016
Wahala, W. M., Donaldson, E. F., de Alwis, R., Accavitti-Loper, M. A., Baric, R. S., & de Silva, A. M. (2010). Natural strain variation and antibody neutralization of dengue serotype 3 viruses. *PLoS pathogens, 6*(3), e1000821.
Wang, H. Y., Takasaki, T., Fu, S. H., Sun, X. H., Zhang, H. L., Wang, Z. X., . . . Liang, G. D. (2007). Molecular epidemiological analysis of Japanese encephalitis virus in China. *J Gen Virol, 88*(Pt 3), 885-894. doi:10.1099/vir.0.82185-0

Wang, Q., Yang, S., Yang, K., Li, X., Dai, Y., Zheng, Y., . . . Wu, R. (2023). CD4 is an important host factor for Japanese encephalitis virus entry and replication in PK-15 cells. *Vet Microbiol, 287*, 109913. doi:10.1016/j.vetmic.2023.109913

Wei, J., Wang, X., Zhang, J., Guo, S., Pang, L., Shi, K., . . . Ma, Z. (2019). Partial cross-protection between Japanese encephalitis virus genotype I and III in mice. *PLoS Negl Trop Dis, 13*(8), e0007601. doi:10.1371/journal.pntd.0007601

Williams, A. J., Curnock, R., Reed, C. R., Easton, P., Rokni, S., & Bingley, P. J. (2010). Anti-BSA antibodies are a major cause of non-specific binding in insulin autoantibody radiobinding assays. *J Immunol Methods, 362*(1-2), 199-203. doi:10.1016/j.jim.2010.09.009

Wu, K. P., Wu, C. W., Tsao, Y. P., Kuo, T. W., Lou, Y. C., Lin, C. W., . . . Cheng, J. W. (2003). Structural basis of a flavivirus recognized by its neutralizing antibody: solution structure of the domain III of the Japanese encephalitis virus envelope protein. *J Biol Chem, 278*(46), 46007-46013. doi:10.1074/jbc.M307776200

Xiao, C., Li, C., Di, D., Cappelle, J., Liu, L., Wang, X., . . . Ma, Z. (2018). Differential replication efficiencies between Japanese encephalitis virus genotype I and III in avian cultured cells and young domestic ducklings. *PLoS Negl Trop Dis, 12*(12), e0007046. doi:10.1371/journal.pntd.0007046

Yamashita, T., Unno, H., Mori, Y., Tani, H., Moriishi, K., Takamizawa, A., . . . Matsuura, Y. (2008). Crystal structure of the catalytic domain of Japanese encephalitis virus NS3 helicase/nucleoside triphosphatase at a resolution of 1.8 A. *Virology, 373*(2), 426-436. doi:10.1016/j.virol.2007.12.018

Yu, I.-M., Holdaway, H. A., Chipman, P. R., Kuhn, R. J., Rossmann, M. G., & Chen, J. (2009). Association of the pr peptides with dengue virus at acidic pH blocks membrane fusion. *Journal of Virology, 83*(23), 12101-12107.

Yu, Y. (2013). Development of Japanese encephalitis attenuated live vaccine virus SA14-14-2 and its characteristics. *Encephalitis. Open Access: InTech*, 181-206.

Yun, S. I., & Lee, Y. M. (2018). Early Events in Japanese Encephalitis Virus Infection: Viral Entry. *Pathogens, 7*(3). doi:10.3390/pathogens7030068

Zhang, D., Wang, X., & Zhou, Z. (2017). Impacts of Small-Scale Industrialized Swine Farming on Local Soil, Water and Crop Qualities in a Hilly Red Soil Region of Subtropical China. *Int J Environ Res Public Health, 14*(12). doi:10.3390/ijerph14121524

Zhang, J. H., Shan, L. L., Liang, F., Du, C. Y., & Li, J. J. (2022). Strategies and Considerations for Improving Recombinant Antibody Production and Quality in Chinese Hamster Ovary Cells. *Front Bioeng Biotechnol, 10*, 856049. doi:10.3389/fbioe.2022.856049

Zhang, L., Cong, Y., Li, H., Chen, L., Li, B., Huang, J. X., & Dong, J. (2021). Construction of a full-length antibody phage display vector. *J Immunol Methods, 494*, 113052. doi:10.1016/j.jim.2021.113052